

# Azimuthal and Single Spin Asymmetries in Hard Scattering Processes

U. D'Alesio, F. Murgia

INFN, Sezione di Cagliari and Dipartimento di Fisica, Università di Cagliari,  
C.P. 170, I-09042 Monserrato (CA), Italy

November 4, 2018

## Abstract

In this article we review the present understanding of azimuthal and single spin asymmetries for inclusive and semi-inclusive particle production in unpolarized and polarized hadronic collisions at high energy and moderately large transverse momentum. After summarizing the experimental information available, we discuss and compare the main theoretical approaches formulated in the framework of perturbative QCD. We then present in some detail a generalization of the parton model with inclusion of spin and intrinsic transverse momentum effects. In this context, we extensively discuss the phenomenology of azimuthal and single spin asymmetries for several processes in different kinematical configurations. A comparison with the predictions of other approaches, when available, is also given. We finally emphasize some relevant open points and challenges for future theoretical and experimental investigation.

# Contents

<b>1</b>	<b>Introduction</b>	<b>3</b>
<b>2</b>	<b>Experimental results on azimuthal and transverse single spin asymmetries</b>	<b>4</b>
2.1	Transverse single spin asymmetries for $p^\uparrow p \rightarrow h + X$ processes . . . . .	5
2.1.1	E704-Fermilab results . . . . .	5
2.1.2	BNL-RHIC results . . . . .	6
2.2	Azimuthal asymmetries in polarized semi-inclusive deeply inelastic scattering . . . . .	7
2.2.1	HERMES results . . . . .	8
2.2.2	COMPASS results . . . . .	9
2.2.3	JLAB-CLAS results . . . . .	10
2.3	Azimuthal asymmetries in unpolarized processes . . . . .	10
2.3.1	SIDIS processes . . . . .	10
2.3.2	Drell-Yan processes . . . . .	11
2.3.3	$e^+e^- \rightarrow \pi\pi + X$ processes . . . . .	12
<b>3</b>	<b>Theoretical approaches to single spin asymmetries</b>	<b>13</b>
3.1	Parton model approaches including intrinsic transverse motion . . . . .	14
3.1.1	QCD developments . . . . .	18
3.1.2	The impact parameter picture . . . . .	20
3.1.3	Models and constraints for TMD distributions . . . . .	21
3.2	Twist-three effects in collinear pQCD . . . . .	23
3.3	A semiclassical model . . . . .	27
<b>4</b>	<b>Spin asymmetries in the generalized parton model</b>	<b>28</b>
4.1	Polarized cross sections and helicity formalism . . . . .	28
4.2	Spin and TMD parton distribution functions at leading twist . . . . .	29
4.3	Spin and TMD fragmentation functions at leading twist . . . . .	32
4.3.1	Quark and gluon fragmentation into an unpolarized hadron . . . . .	33
4.3.2	Quark fragmentation into a spin 1/2 hadron . . . . .	34
4.4	Helicity amplitudes for the elementary process $ab \rightarrow cd$ . . . . .	34
4.5	Kernels for doubly polarized processes . . . . .	36
<b>5</b>	<b>Phenomenology of single spin asymmetries</b>	<b>38</b>
5.1	Unpolarized cross sections and SSA's in $pp \rightarrow C + X$ . . . . .	38
5.1.1	Pion, kaon and heavy meson production . . . . .	39
5.1.2	Prompt photon production . . . . .	47
5.1.3	Transverse $\Lambda$ polarization in unpolarized $pp$ collisions . . . . .	47
5.2	SSA's for double inclusive production in $pp$ collisions . . . . .	49
5.3	Azimuthal asymmetries and SSA's in Drell-Yan processes . . . . .	49
5.4	$e^+e^-$ annihilation in two nearly back-to-back hadrons . . . . .	51
5.5	Semi-inclusive deeply inelastic scattering . . . . .	53
5.5.1	Azimuthal dependence in unpolarized SIDIS . . . . .	54
5.5.2	Transverse SSA's in SIDIS . . . . .	56
5.5.3	Phenomenological extractions of Sivers and Collins functions . . . . .	60
<b>6</b>	<b>Conclusions and outlook</b>	<b>61</b>

# 1 Introduction

Polarization phenomena in hadronic processes deeply challenge high-energy physics theories and perturbative Quantum Chromodynamics (pQCD). It has been known since a long time that experimental results for several polarized processes can hardly be explained by means of available theoretical approaches. Some relevant examples are: *i*) The large spin-spin correlation measured in  $pp$  elastic scattering and its unusual behaviour as a function of the relevant kinematical variables; *ii*) The so-called “spin crisis”, and the fact that quarks only account for a small fraction of the total proton spin; *iii*) The large transverse polarization of hyperons produced in unpolarized hadronic collisions; *iv*) The large transverse single spin asymmetries (SSA) measured in inclusive pion and kaon production in polarized hadronic collisions and in semi-inclusive deeply inelastic scattering (SIDIS). Due to space limitation, in this work we will not cover at all the topics *i*) and *ii*). The rich, low-energy aspects of topics *iii*) and *iv*), which may be confronted only with nonperturbative approaches, will also remain uncovered. A comprehensive overview on these subjects and on related topics can be found in several review papers, addressing both their theoretical and experimental aspects [1, 2, 3, 4, 5, 6, 7, 8, 9, 10, 11, 12, 13, 14, 15, 16, 17]. Here we will focus on the high-energy regime and the treatment in the context of pQCD approaches of transverse SSA’s and, marginally, of the transverse polarization of spin 1/2 particles in unpolarized processes.

The SSA for the inclusive process  $A^\uparrow B \rightarrow C + X$  is defined as

$$A_N = \frac{d\sigma^\uparrow - d\sigma^\downarrow}{d\sigma^\uparrow + d\sigma^\downarrow} = \frac{d\Delta\sigma}{2d\sigma^{\text{ump}}}, \quad (1)$$

where  $d\sigma^{\uparrow(\downarrow)}$  stands for the invariant differential cross section,  $E_C d^3\sigma^{\uparrow(\downarrow)}/d^3\mathbf{p}_C$ , for the production of hadron  $C$ , with 4-momentum  $p_C^\mu = (E_C, \mathbf{p}_T, p_L)$ , in the scattering of a hadron  $A$  off an unpolarized hadron  $B$ , with  $A$  upwards (downwards) transversely polarized w.r.t. the production plane. More precisely, in the  $AB$  center of mass frame, with  $A$  moving along the  $+Z$  direction and  $C$  produced in the  $XZ$  plane, the upwards (downwards) transverse spin directions are respectively along  $\pm Y$ . The SSA, or analyzing power,  $A_N$ , is also denoted as “left-right” asymmetry since, by rotational invariance, the number of left going hadrons  $C$  when  $A$  is downwards polarized,  $d\sigma^\downarrow$ , is the same as the number of right going hadrons  $C$  with  $A$  upwards polarized. Notice that left (right) is defined w.r.t. the plane spanned by the momentum and spin directions of the polarized hadron  $A$  looking downstream its direction of motion.

The transverse polarization measured in the  $AB \rightarrow C^\uparrow + X$  process, where  $C$  is a spin 1/2 hadron, is defined, analogously to  $A_N$  in Eq. (1), as  $P_T = (d\sigma^\uparrow - d\sigma^\downarrow)/d\sigma^{\text{ump}}$ , where now the arrows in  $d\sigma^{\uparrow(\downarrow)}$  stand for the transverse spin directions for the final hadron  $C$ .

Most of these processes show peculiar and unexpected dependences on the relevant kinematical variables: the rapidity,  $y = (1/2) \ln[(E_C + p_L)/(E_C - p_L)]$ , or the pseudorapidity  $\eta = -(1/2) \ln \tan(\theta/2)$ , the Feynman variable,  $x_F = p_L/p_L^{\text{max}}$ , and  $p_T$ , where  $\theta$  and  $p_L$  ( $p_T$ ) are respectively the production angle and the longitudinal (transverse) momentum of the observed particle w.r.t. the direction of the colliding beams. The magnitude and behaviour of these polarized observables are very difficult to account for in pQCD approaches, as well as in nonperturbative models, and have motivated a huge amount of theoretical work. Although significant progress has been done, as it will be illustrated in the rest of this review, much remains to be clarified. Moreover, a new family of second-generation experiments are starting to produce new sets of data with larger statistics, at higher energies and with an enlarged coverage of the kinematical variables. For these reasons, we will try to collect the main ideas on SSA’s and give an account of their present status, both from the experimental and, in more depth, the theoretical side.

The study of SSA’s is strongly related to our understanding of the structure of hadrons and their spin and orbital angular momentum content in terms of partons. This leads naturally to a special attention to the role played by parton distribution and fragmentation functions in pQCD approaches.

In this review we will then present, in some detail, a new class of parton distributions, beyond the usual collinear ones, resulting from the inclusion of spin and intrinsic transverse momentum effects. We will also show how they can help in describing the observed SSA results. In particular, two spin and transverse momentum dependent (TMD) mechanisms, introduced in the early 90s, will play a special role: the Sivers effect, describing the asymmetry in the azimuthal distribution of an unpolarized parton inside a transversely polarized hadron [18, 19]; the Collins effect, describing the azimuthal asymmetry in the fragmentation of a transversely polarized quark into an unpolarized hadron [20, 21].

Among the topics not covered in this review, that are of some relevance in the context of SSA's, we mention the generalized parton distributions (GPD) and the dihadron fragmentation functions (DiFF). GPD's represent another generalization of ordinary parton distributions and indeed could provide a unified parameterization of many different aspects of hadron physics. We refer the interested reader to the following papers [22, 23, 24, 25, 26, 27, 28, 29], which emphasize the different aspects of the physics encoded in these quantities. We also mention their possible connection to the TMD distributions, discussed in Refs. [30, 31, 32, 33, 34, 35]. Concerning DiFF's (describing the probability that a parton hadronizes into two hadrons plus anything else) we recall their role in spin studies, in particular for the extraction of the transversity distribution function in double inclusive processes in  $pp$  collisions and SIDIS [36, 37], and the azimuthal correlations in  $e^+e^-$  annihilations. Some seminal papers on the DiFF's, with their definitions and properties, are [38, 21, 39, 40, 41, 42, 43, 44].

The outline of this review is the following: in section 2 we present an overview of experimental results on SSA's, including also the azimuthal asymmetries observed in unpolarized collisions, that are intimately connected to our main subject. In section 3 we discuss QCD theoretical approaches to SSA's, which represent nowadays the most reliable attempts towards the understanding of the observed results. Their most recent developments are also presented. We will discuss in particular two pQCD approaches: one based on the extension of the collinear factorization theorems, at leading twist, with the inclusion of intrinsic transverse momentum effects; another one based on a twist-three collinear formalism. As a representative example, a short account of a semiclassical model will be also given. In section 4 we will give a detailed description of the first pQCD approach within the helicity formalism. Its phenomenological implications and a comparison with the results of other theoretical approaches are collected in section 5. Finally, perspectives and conclusions are gathered in section 6.

This work is to a great extent based on our longstanding and fruitful collaboration with M. Anselmino, M. Boglione, and E. Leader; without their contribution it would have been impossible. We are also grateful to A. Kotzinian, S. Melis, and A. Prokudin for valuable collaboration in the last years. Many people have contributed with enlightening discussions and clarifying remarks to this work, before and during its completion; in particular it is a pleasure to thank A. Bacchetta, D. Boer, C. Bomhof, L. Gamberg, Y. Koike, A. Metz, P. Mulders, F. Pijlman, P. Schweitzer, W. Vogelsang, F. Yuan, for their theoretical insights; H. Avakian, L. Bland, F. Bradamante, M. Grosse Perdekamp, D. Hasch, S. Heppelmann, J. Lee, A. Martin, L. Nogach, R. Seidl, F. Videbaek, for their kind support on the experimental side and for providing us with preliminary results of their experimental collaborations.

## 2 Experimental results on azimuthal and transverse single spin asymmetries

A comprehensive account of all experimental information available today on polarization phenomena in high-energy hadronic physics is well beyond the scope of this review. Forced by space limitation, in the following pages we will only summarize the most significant results, limiting ourselves to those concerning the main subjects of this paper: transverse single-spin and azimuthal asymmetries. The selection presented somehow reflects our personal perception. We apologize for those papers and topics not included and discussed here. The interested reader may fortunately find complete and comprehensive

accounts on this subject in Refs. [1, 2, 9, 13].

Whenever possible we will refer to published work. For ongoing experiments we will also quote available preliminary results. We will not discuss details concerning experimental setups, detector performances, etc., referring to the quoted papers for all technical aspects. In order to avoid duplicates, we will not show plots of the results in this section, deferring instead to section 5, where a selection of relevant results, and their comparison with theoretical predictions and fits, will be presented.

## 2.1 Transverse single spin asymmetries for $p^\uparrow p \rightarrow h + X$ processes

Starting from the late 70s and during the 80s a number of experimental collaborations presented early results on SSA's for the  $pp \rightarrow h + X$  process. For its impact on the later developments we mention, for instance, the work on the transverse  $\Lambda$  polarization by Bunce *et al.* [45]. SSA's significantly different from zero were found for the  $p^\uparrow p \rightarrow \pi + X$  process in the forward production region (large positive  $x_F$ ), at relatively small transverse momentum,  $p_T$ . These results were in accord with previous extensive measurements performed for similar exclusive channels (e.g.,  $\pi p \rightarrow \pi p$ ) and were interpreted as purely nonperturbative effects. Additional measurements on the  $p_T$  dependence of these results showed interesting behaviours, difficult to understand and explain. All these experiments were fixed-target ones, at relatively low c.m. energies and low  $p_T$  (below 1.0-1.5 GeV/c). Therefore, no serious attempt was made to understand these effects in terms of pQCD involving hard elementary scattering. Moreover, a well-known paper by Kane, Pumplin and Repko [46], reinforced the common wisdom that spin effects should become negligible at high-energy scales.

### 2.1.1 E704-Fermilab results

During the 90s, the E581/E704 Collaborations at Fermilab (henceforth indicated as the E704 Collaboration) set the stage at a different level, because of the larger c.m. energy available ( $\sqrt{s} \simeq 20$  GeV), the improved separation between the  $x_F$  and  $p_T$  kinematical dependence of the SSA's and the small but significant extension of the  $p_T$  range covered. The E704 Collaboration collected SSA data for  $pp$  and  $\bar{p}p$  collisions using (for the first time) polarized secondary  $p, \bar{p}$  beams and for several produced particles (mainly pions, but also photons,  $\Lambda$  and  $\eta$  particles). The experiment covered essentially two different kinematical regions:  $0.2 \leq x_F \leq 0.6$  and  $p_T$  in the range  $0.2 \div 2.0$  GeV/c (the forward production, or beam fragmentation, region);  $|x_F| \leq 0.15$  and  $p_T$  values up to 4.0 GeV/c (the central rapidity region). The main results gathered by the E704 Collaboration can be summarized as follows:

1) Large SSA's (up to 30-40% in magnitude) have been measured for inclusive pion production in the large positive  $x_F$  region, for polarized proton and antiproton beams colliding with an unpolarized hydrogen target [47, 48, 49, 50]. For both neutral and charged pions the SSA was found to be almost zero at low  $x_F$ , up to  $x_F \sim 0.3$ , where it starts raising with increasing  $x_F$ , reaching values of  $\sim 15\%$  and  $30 - 40\%$  in size for  $\pi^0$ 's and  $\pi^\pm$ 's respectively [see Fig. 3, p. 41]. The measured asymmetries are roughly similar in magnitude but opposite in sign for positive and negative pions (and positive in the  $p^\uparrow p \rightarrow \pi^+ + X$  case); for charged pions, they change sign (being somehow reduced in size) when going from polarized proton to polarized antiproton beams. The asymmetry for neutral pions is always positive and almost half of that of the nearest charged pion case, in good agreement with isospin conservation in the fragmentation process. Information gathered on the  $p_T$  dependence of the SSA's was less detailed. In Ref. [50] the  $p_T$  dependence of the SSA for charged pions in the  $\bar{p}^\uparrow p \rightarrow \pi^\pm + X$  process was measured at moderate  $p_T$  ( $0.2 \leq p_T \leq 1.5$  GeV/c) over a wide  $x_F$  range,  $0.2 \leq x_F \leq 0.9$ . A threshold for the onset of the asymmetry was observed around  $p_T \sim 0.5$  GeV/c, below which the SSA was essentially zero and above which it increases in magnitude with  $p_T$ . In general, in all data sets considered, the magnitude of the SSA at large positive  $x_F$  was found to be more pronounced for the largest  $p_T$  values reached. No data on the corresponding unpolarized cross sections were presented.



2) In the central rapidity region,  $|x_F| \leq 0.15$  and  $1.0 < p_T < 4.5$  GeV/ $c$ , the inclusive and semi-inclusive SSA's for neutral pions, using transversely polarized 200 GeV/ $c$  proton and antiproton beams off a hydrogen target were measured [51]. These asymmetries were found to be consistent with zero within the experimental uncertainties over the full  $p_T$  range covered, both for polarized proton and antiproton beams [see, e.g., Fig. 7 (left panel), p. 45]. In this case, measurements of the corresponding invariant unpolarized cross sections were also provided.

3) The SSA for inclusive direct-photon production,  $p^\uparrow p \rightarrow \gamma + X$ , was measured in the central rapidity region at  $2.5 < p_T < 3.1$  GeV/ $c$  [52]. Data on the corresponding unpolarized cross section at  $2.5 < p_T < 3.8$  GeV/ $c$  were also provided. Only two data points were measured for the SSA, that was found to be consistent with zero within (large) experimental uncertainties.

4) Some interesting results are also available for SSA's in inclusive  $\Lambda$  and  $\eta$ -meson production [53, 54], showing non-vanishing, sizable asymmetries in kinematical regions similar to those considered above.

The E704 results triggered renewed interest on SSA's, given the larger c.m. energy available as compared to that of previous experiments and the large, unambiguous effects measured. However, a clear separation between the  $x_F$  and  $p_T$  dependence of the results was not reached and the covered  $p_T$  range was still limited, although the largest SSA's were measured at the highest  $p_T$ . For all the 90s these results were the only ones available at sufficiently high c.m. energies. The advent of new experimental setups started a new stage in the investigation of transverse spin effects in hadronic processes.

Transverse SSA's were also measured, although again at lower total c.m. energies, by experimental collaborations at IHEP (Protvino). In Ref. [55] they have shown the transverse SSA for  $\pi^0$ 's inclusively produced in the collisions of a 40 GeV/ $c$   $\pi^-$  beam off transversely polarized protons and deuterons, in the region  $|x_F| \leq 0.2$  and  $1.6 \leq p_T \leq 3.2$  GeV/ $c$ . The SSA's were found to be approximately equal for the two reactions, compatible with zero or slightly positive for  $1.0 \leq p_T \leq 2.0$  GeV/ $c$ , large in magnitude and negative for  $2.4 \leq p_T \leq 3.2$  GeV/ $c$ . In Ref. [56] SSA's were measured for inclusive hadron production in collisions of a transversely polarized 40 GeV/ $c$  proton beam with an unpolarized liquid hydrogen target. The asymmetries were measured for  $\pi^\pm$ ,  $K^\pm$ , protons and antiprotons, produced in the central region,  $0.02 \leq x_F \leq 0.10$  and  $0.7 \leq p_T \leq 3.4$  GeV/ $c$ . Within experimental errors, the measured asymmetries for  $\pi^\pm$ ,  $K^\pm$  and  $\bar{p}$  show a linear dependence on  $x_T = 2p_T/\sqrt{s}$  and change sign near  $x_T = 0.37$ . For protons, a negative SSA, independent of  $x_T$ , was found.

### 2.1.2 BNL-RHIC results

Starting from the end of the 90s, very interesting results on transverse SSA's and unpolarized cross sections for inclusive single particle production in polarized hadronic collisions came up and are currently collected by the experimental collaborations (STAR, PHENIX, BRAHMS) using the Relativistic Heavy Ion Collider (RHIC) at the Brookhaven National Laboratories (BNL).

For the first time proton-proton collisions, with one (both) beam(s) transversely (longitudinally) polarized, can be studied at c.m. energies as large as 200 GeV, with the possibility to reach  $\sqrt{s} = 500$  GeV in the near future. This represents a significant advancement with respect to all previous (fixed target) experiments. The setups of the three RHIC experiments allow to cover a large kinematical range, including particularly the previously almost unexplored negative  $x_F$  region.

Let us also remind a precursor experiment at the BNL Alternate Gradient Synchrotron (AGS). The E925 Collaboration [57, 58] measured transverse SSA's for charged pions using an incident 22-GeV/ $c$  transversely polarized proton beam on hydrogen and carbon targets, in the range  $0.55 < x_F < 0.75$  and  $0.6 < p_T < 1.2$  GeV/ $c$ . Although still at low energies and  $p_T$ , this experiment gave a first, independent confirmation of the large SSA's measured by the E704 Collaboration.

We now give a summary of the main high-energy RHIC results on SSA's:

1) The STAR collaboration measured the transverse SSA for forward neutral pion production in  $p^\uparrow p$  collisions at  $\sqrt{s} = 200$  GeV, average pseudorapidity  $\langle \eta \rangle = 3.8$  and  $30 < E_\pi \simeq x_F \sqrt{s}/2 < 55$  GeV,

corresponding to  $1.0 < \langle p_T \rangle < 2.4$  GeV/ $c$  [59]. The unpolarized cross section was also measured at  $\langle \eta \rangle = 3.3, 3.8, 4.0$  [59, 60] and found to be consistent with next-to-leading order (NLO) pQCD calculations [17, 61]. In agreement with the E704 results, the SSA is small for  $x_F$  values below about 0.3 and becomes large and positive at higher  $x_F$ . The spin-dependent azimuthal asymmetry for almost back-to-back dijets in  $p^\uparrow p$  collisions at  $\sqrt{s} = 200$  GeV was measured over a wide pseudorapidity range for the two jets and found to be consistent with zero within experimental uncertainties [62].

Preliminary results for  $\pi^0$  SSA's, based on a larger data sample, for both positive and negative  $x_F$  in the range  $0.2 < |x_F| < 0.6$ , collected at two average pseudorapidities,  $\langle \eta \rangle = 3.3$  (corresponding to  $1.6 < \langle p_T \rangle < 3.7$  GeV/ $c$ ) and  $\langle \eta \rangle = 3.7$  (corresponding to  $1.3 < \langle p_T \rangle < 2.8$  GeV/ $c$ ) have been presented [63]. They essentially confirm the previous data published in the positive  $x_F$  region and show a SSA consistent with zero for negative  $x_F$  [see Fig. 4 (right panel), p. 43]. A preliminary study of the  $p_T$  dependence of the neutral pion SSA for  $x_F > 0.4$  and in  $x_F$ -bins for  $0.25 < x_F < 0.56$ , using combined data at  $\langle \eta \rangle = 3.3, 3.7, 4.0$ , in the range  $1 < p_T < 4$  GeV/ $c$  was also performed [63]. Data show a non trivial dependence of the SSA on  $p_T$ , which seems not to behave as a smooth decreasing function of  $p_T$  [see Fig. 6, p. 44]. Other interesting STAR preliminary results concern the differential cross section for inclusive charged pion production at mid-rapidity and for inclusive neutral pion production at forward and mid-rapidity in  $pp$  collisions at  $\sqrt{s} = 200$  GeV [64].

2) The PHENIX Collaboration has measured the unpolarized cross section and the transverse SSA for neutral pions and charged hadrons produced at mid-rapidity ( $|\eta| < 0.35$ ) in  $p^\uparrow p$  collisions at  $\sqrt{s} = 200$  GeV [65, 66, 67]. For neutral pions (charged hadrons) the unpolarized cross section in the range  $0.5 < p_T < 20$  GeV/ $c$  ( $0.5 < p_T < 7.0$  GeV/ $c$ ) was found to be in good agreement, above  $\sim 2$  GeV/ $c$ , with pQCD calculations at NLO accuracy [17, 61]. The SSA for both neutral pions and charged hadrons was found to be consistent with zero within errors in the range  $1.0 < p_T < 5.0$  GeV/ $c$  [66]. These results are in agreement with those found by the E704 Collaboration at lower energy and in similar kinematical conditions [51] [see also Fig. 7 (right panel), p. 45], extending them to larger  $p_T$  values, previously unexplored. The invariant unpolarized cross section for direct-photon production at mid-rapidity was also measured up to  $p_T = 16$  GeV/ $c$  in  $\sqrt{s} = 200$  GeV  $pp$  collisions [68, 69]. Data are well described by NLO theoretical predictions for  $p_T > 5$  GeV/ $c$ ; in addition, the ratio of isolated photons to all nonhadronic decay photons is well described by pQCD for  $p_T > 7$  GeV/ $c$ . Other recent PHENIX preliminary results concern [70]: measurements of the SSA for forward neutrons and mid-rapidity  $J/\psi$ 's at  $\sqrt{s} = 200$  GeV; for the neutron case, large flat asymmetries for positive  $x_F$  and SSA's consistent with zero in the negative  $x_F$  range were observed.

3) The BRAHMS Collaboration has recently presented preliminary results for invariant unpolarized cross sections for charged hadrons,  $\pi^\pm$ ,  $K^\pm$ , proton, antiproton production in  $pp$  collisions at  $\sqrt{s} = 200$  GeV measured at forward rapidities ( $y = 2.95$  and  $3.3$ ) and  $p_T$  up to 4 GeV/ $c$  [71]. Other interesting preliminary results have also been presented [72] concerning: the invariant cross section for  $pp \rightarrow \pi^- + X$  at  $\sqrt{s} = 62.4$  GeV and rapidity  $y \sim 2.7, 3.3$ ; the SSA for  $\pi^\pm$ ,  $K^\pm$  at  $\sqrt{s} = 62.4$  GeV, for both negative and positive  $x_F$  in the range  $0.25 < |x_F| < 0.6$ , and  $p_T$  up to  $\sim 1.5$  GeV/ $c$ ; the SSA for  $\pi^\pm$ ,  $K^\pm$ ,  $p$  and  $\bar{p}$  at  $\sqrt{s} = 200$  GeV,  $0.15 < x_F < 0.3$  and  $0.2 < p_T < 3.5$  GeV/ $c$ . Among the main features of these results we mention: the almost flat  $x_F$ -behaviour of  $A_N$  for  $\pi^\pm$  at 200 GeV and  $\theta = 2.3^\circ$  [see Fig. 5 (left panel), p. 44]; the comparable and sizable  $K^+$  and  $K^-$  SSA's observed at 200 and 62 GeV [see Fig. 8, p. 46]; a large  $A_N$  for antiproton production and an almost vanishing SSA for the proton case.

## 2.2 Azimuthal asymmetries in polarized semi-inclusive deeply inelastic scattering

Starting from the end of the 90s the HERMES Collaboration at DESY, and later the COMPASS Collaboration at CERN and the CLAS Collaboration at Jlab, have performed a series of measurements of beam and target azimuthal asymmetries in semi-inclusive particle production in the deeply inelastic col-

lisions of longitudinally polarized leptons off both longitudinally and transversely polarized proton and deuteron targets. As it will be discussed in detail in the following sections, these azimuthal asymmetries with respect to the virtual photon direction, in the  $\gamma^*$ -target c.m. frame, can give a lot of information. The azimuthal angles under consideration refer e.g. to the transverse component of the observed hadron momentum ( $\phi_h$ ) and of the initial hadron polarization vector ( $\phi_S$ ) w.r.t. the virtual photon direction, measured from the leptonic plane [see Fig. 14, p. 55]. By integrating the polarized cross section or the asymmetries, opportunely multiplied by some circular function of the azimuthal angles, one can disentangle several interesting contributions to single spin asymmetries and other polarized observables. These moments of the azimuthal asymmetries are usually indicated by  $A_{S_B S_T}^{W(\phi)}$ , where  $S_B, S_T = U, L, T$  refer to unpolarized ( $U$ ), longitudinally ( $L$ ) and (for the target) transversely ( $T$ ) polarized beam, target respectively, while  $W(\phi)$  refers to some appropriate  $\phi$ -dependent circular function,  $W = 1, \sin \phi, \cos \phi, \sin 2\phi$ , etc. As a phenomenologically relevant example,  $A_{UT}^{\sin(\phi_h \pm \phi_S)}$  is given as [73]

$$A_{UT}^{\sin(\phi_h \pm \phi_S)} \equiv 2\langle \sin(\phi_h \pm \phi_S) \rangle = \frac{\int d\phi_h d\phi_S \sin(\phi_h \pm \phi_S) [d\sigma(\phi_S) - d\sigma(\phi_S + \pi)]}{\int d\phi_h d\phi_S [d\sigma(\phi_S) + d\sigma(\phi_S + \pi)]}. \quad (2)$$

Notice that in the literature sometimes the factor two in the above equation is not included.

Throughout this section and in the sequel, we will make use of the well-known DIS kinematical variables:  $P, \ell, \ell', q = \ell - \ell'$  are respectively the four-momenta of the target nucleon, the initial and final leptons and the virtual photon exchanged;  $Q^2 = -q^2$ ;  $x_B = Q^2/(2P \cdot q)$  is the Bjorken variable;  $\nu = q \cdot P/M$  is the lepton energy loss in the target nucleon rest frame;  $y = (P \cdot q)/(P \cdot \ell)$  is the so-called inelasticity;  $W$  is the c.m. energy of the virtual photon-target nucleon system. Additionally, we also adopt the usual SIDIS variables:  $P_h$  is the four-momentum of the final observed hadron, and  $\mathbf{P}_{h\perp}$  its transverse component w.r.t. the virtual photon direction of motion, with magnitude  $P_{h\perp} \equiv |\mathbf{P}_{h\perp}|$ ;  $z_h = (P \cdot P_h)/(P \cdot q)$  is the usual hadronic variable.

### 2.2.1 HERMES results

In its first stage, HERMES was equipped with a longitudinally polarized hydrogen target. This gave access to measurements of the quark helicity distributions (in DIS) and to the leading-twist azimuthal asymmetry  $A_{UL}^{\sin 2\phi_h}$ , associated with the transverse momentum dependent (TMD) quark distribution in a longitudinally polarized hadron convoluted with the Collins function. In the virtual photon-target center of mass frame, even a longitudinally polarized (in the Lab. frame) proton target acquires a (kinematically) small ( $\sim 1/Q$ ) transverse spin component. Therefore, early attempts to measure transverse SSA's and some related effects (namely the Sivers and Collins effects) through the azimuthal asymmetry  $A_{UL}^{\sin \phi_h}$  were performed. Even if these transverse-spin contributions mix up with concurrent effects due to subleading-twist quark distribution and fragmentation functions, first indications for interesting physics were found. Concerning SSA's, however, the most interesting HERMES results came out with the advent of a transversely polarized hydrogen target. This allowed to extract the first unambiguous indications of non-vanishing leading-twist transverse SSA's in SIDIS, and to disentangle the possible contributions due to the Sivers and Collins effects.

The kinematical regime covered by the HERMES experiment is approximately the following (some differences are possible for specific measurements; we refer to the original papers for more detail):  $1 < Q^2 < 15$  (GeV/c)<sup>2</sup>;  $0.023 < x_B < 0.4$ ;  $y < 0.85$ ;  $W^2 > 10$  GeV<sup>2</sup>;  $2 < E_h < 15$  GeV,  $0.2 < z_h < 0.7$ ;  $P_{h\perp} > 50$  MeV/c. Notice that in some cases more selective cuts on the last two variables are used.

We now briefly summarize the main results of the HERMES experiment, quoting only those results that are relevant in the context of this review paper (a full account of all HERMES results may be found in the papers quoted in the bibliography):

1) First evidence of azimuthal SSA's for charged [74] and neutral [75] pion production in deeply inelastic scattering of polarized positrons off a longitudinally polarized hydrogen target;  $A_{UL}^{\sin \phi_h}$  was found to be



significant and comparable for  $\pi^+$  and  $\pi^0$  production, and consistent with zero for  $\pi^-$ . Indications of an increasing of this analyzing power with increasing of  $x_B$ , and with  $P_{h\perp}$  up to  $\sim 0.8$  GeV/ $c$ , were also found.  $A_{UL}^{\sin 2\phi_h}$  was found to be consistent with zero for both  $\pi^+$  and  $\pi^-$ .

2) Measurement of azimuthal SSA's in SIDIS production of pions and kaons on a longitudinally polarized deuterium target [76]; the dependences of these asymmetries on  $x_B$ ,  $P_{h\perp}$ , and  $z_h$  were investigated; positive asymmetries for  $\pi^+$  and  $\pi^0$  and an indication of a positive asymmetry for  $\pi^-$  mesons were found; the asymmetry for  $K^+$  was measured to be comparable with that for  $\pi^+$  mesons;

3) Measurement of the azimuthal SSA's  $A_{UT}^{\sin(\phi_h \pm \phi_S)}$  in SIDIS production of charged pions and kaons on a transversely polarized hydrogen target [77, 78]. For the first time two different phenomena, possibly associated with the Sivers and Collins effects, indistinguishable in previous data were disentangled. The  $\langle \sin(\phi_h - \phi_S) \rangle$  moment was measured to be positive and nonzero for  $\pi^+$  and consistent with zero for  $\pi^-$  mesons [see Fig. 16 (left panel), p. 58]. The  $\langle \sin(\phi_h + \phi_S) \rangle$  moment was found to be positive for  $\pi^+$  and negative and comparable in magnitude for  $\pi^-$  mesons [see Fig. 17 (left panel), p. 59]. For charged kaons the measured  $A_{UT}^{\sin(\phi_h - \phi_S)}$  asymmetry came out to be positive, showing large values for  $K^+$ ;  $A_{UT}^{\sin(\phi_h + \phi_S)}$  for  $K^-$ , even if with large error bars, presented large positive values [see Fig. 18, p. 59].

4) Extraction of subleading-twist effects in SSA's in SIDIS production of charged pions on a longitudinally polarized hydrogen target [79]. By combining measurements of azimuthal asymmetries with both longitudinally and transversely polarized hydrogen targets (see previous point) this contribution was found to be significantly positive for  $\pi^+$  mesons, therefore dominating the asymmetries on a longitudinally polarized target (see points 1) and 2) above). The subleading-twist contribution for  $\pi^-$  mesons was found to be small.

5) Measurement of the subleading-twist beam spin asymmetry  $A_{LU}^{\sin \phi_h}$  in the azimuthal distribution of pions produced in SIDIS [80].  $A_{LU}^{\sin \phi_h}$  for  $\pi^+$ 's was found to be consistent with zero for low  $z_h$  and rising with  $z_h$  up to about 0.02; for  $\pi^-$ 's,  $A_{LU}^{\sin \phi_h}$  was found to be consistent with zero within the statistical accuracy; for neutral pions, the asymmetry was found to be roughly constant and of the order of 0.03, decreasing to zero only in the lowest/highest  $z_h$  regions.

6) Interesting preliminary results on azimuthal SSA's in SIDIS production of charged kaons on a transversely polarized hydrogen target have been also presented (see, e.g., Ref. [81]).

## 2.2.2 COMPASS results

The COMPASS Collaboration at CERN has performed measurements of transverse azimuthal asymmetries for charged hadrons produced in deeply inelastic scattering of the CERN-SPS 160 GeV/ $c$  muon beam off a transversely polarized deuteron target. The high-energy lepton beam allows to reach large values of  $Q^2$  and a very large coverage of  $W$ . This can be very helpful in disentangling genuine TMD effects from perturbatively generated contributions. The large  $x_B$  region covered, well below the valence region, allows to better estimate the first moments of the TMD distributions and test related sum rules. Moreover the use of a transversely polarized (isospin scalar) deuteron target well complements with HERMES results, in particular concerning flavour separation of the TMD distributions and fragmentation functions. COMPASS also plans to perform measurements with a transversely polarized proton target in the near future.

The asymmetries  $A_{UT}^{\sin(\phi_h \pm \phi_S)}$  for charged hadrons, and their dependence on  $x_B$  and, for leading hadrons,  $z_h$ ,  $P_{h\perp}$ , were measured and found to be compatible with zero within statistical errors [82] [see Fig. 16 (right panel), p. 58 and Fig. 17 (right panel), p. 59]. The kinematical region covered was:  $Q^2 > 1$  (GeV/ $c$ )<sup>2</sup>,  $W > 5$  GeV,  $0.003 < x_B < 0.3$ ,  $0.1 < y < 0.9$ . Concerning the observed hadron, the cuts  $P_{h\perp} > 0.1$  GeV/ $c$ ,  $z_h > 0.2$  ( $z_h > 0.25$ ) have been imposed for all (leading) hadrons.

Recently, new high-precision measurements for the same observables and in the same kinematical region but with larger statistical significance have been published [83]. These results extend and essentially confirm those of Ref. [82], with statistical errors a factor of two smaller.

Interesting preliminary results have also been presented on  $A_{UT}^{\sin(\phi_h \pm \phi_S)}$  for charged pions and kaons, in the same kinematical configuration and using data collected in 2003-2004 [84, 85]. Again, all transverse spin effects investigated are found to be compatible with zero.

Very recently COMPASS has also presented preliminary results [86], in the same kinematical region, on the first measurement of the other six possible transverse azimuthal asymmetries (see, e.g., Ref. [87]),  $A_{UT}^{\sin(3\phi_h - \phi_S)}$ ,  $A_{LT}^{\cos(\phi_h - \phi_S)}$  (leading twist), and  $A_{UT}^{\sin \phi_S}$ ,  $A_{UT}^{\sin(2\phi_h - \phi_S)}$ ,  $A_{LT}^{\cos \phi_S}$ ,  $A_{LT}^{\cos(2\phi_h - \phi_S)}$  (subleading twist). All these asymmetries are compatible with zero within statistical errors.

### 2.2.3 JLAB-CLAS results

The JLAB-CLAS Collaboration has performed measurements of both longitudinal beam and target spin asymmetries for pion production in SIDIS off protons using an electron beam with energy 4.3 GeV and 5.7 GeV. More precisely, they have measured:

- 1) The  $\sin \phi_h$  moment of the subleading beam spin asymmetry,  $A_{LU}^{\sin \phi_h}$ , for the process  $ep \rightarrow e'\pi^+ + X$  above the baryon resonance region, in the range  $0.15 < x_B < 0.4$ ,  $0.5 < z_h < 0.8$ , using a polarized electron beam of 4.3 GeV [88] and of 5.7 GeV [89] (in this last case only preliminary results are available). The measured beam SSA is positive for a positive electron helicity, varying roughly in the range  $0.02 \div 0.08$ ; it increases with  $z_h$  and shows no significant dependence on the  $x_B$ -range;
- 2) The  $\sin \phi_h$ ,  $\sin 2\phi_h$  moments of the longitudinal target spin asymmetry,  $A_{UL}^{\sin \phi_h}$  and  $A_{UL}^{\sin 2\phi_h}$ , for both charged and neutral pions, in the range  $0.15 < x_B < 0.4$ ,  $0.5 < z_h < 0.8$ , using an electron beam of 5.7 GeV (preliminary results, see Refs. [89, 90]). Data for  $\pi^+$ 's show clear  $\sin \phi_h$  and  $\sin 2\phi_h$  modulations, leading to  $\langle \sin \phi_h \rangle = 0.058 \pm 0.011$  and  $\langle \sin 2\phi_h \rangle = -0.041 \pm 0.011$  (errors are statistical).

## 2.3 Azimuthal asymmetries in unpolarized processes

Several azimuthal asymmetries in unpolarized cross sections for SIDIS, Drell-Yan and  $e^+e^-$  processes have been measured. Among other explanations of their origin, intrinsic parton motion is one of the most accredited. Therefore, these asymmetries are intimately related to transverse single spin asymmetries and in particular to TMD parton distribution and fragmentation functions. For this reason, we find useful here to summarize some of the most relevant results.

### 2.3.1 SIDIS processes

The most general azimuthal dependence of the cross section for SIDIS off an unpolarized target can be written as (see, e.g., Ref. [91] and references therein):

$$\frac{d\sigma^{\ell N \rightarrow \ell' h X}}{d\phi_h} \propto A + B \cos \phi_h + C \cos 2\phi_h + D \sin \phi_h + E \sin 2\phi_h, \quad (3)$$

where the angle  $\phi_h$ , as mentioned above, is the azimuthal angle of the observed hadron momentum around the virtual photon direction, measured starting from the leptonic plane [see Fig. 14, p. 55].

In collinear pQCD,  $A$  is of order  $\mathcal{O}(\alpha_s^0)$ ; the first corrections to  $A$  and the  $B$ - $E$  contributions come from higher order terms, in particular  $B$ ,  $C$  are of order  $\mathcal{O}(\alpha_s)$ ,  $D$ ,  $E$  are of order  $\mathcal{O}(\alpha_s^2)$ . Furthermore, the T-odd contributions  $D$  and  $E$  are present only for parity violating weak interactions or for electromagnetic interactions with longitudinally polarized lepton beams. Nonperturbative transverse momentum effects and TMD functions may give leading-twist contributions to  $B$  and  $D$  terms which may be non-negligible even at very large  $Q^2$ .

The EMC Collaboration at CERN measured the azimuthal distribution [see Fig. 15, p. 55] and its  $\langle \cos \phi_h \rangle$ ,  $\langle \cos 2\phi_h \rangle$ ,  $\langle \sin \phi_h \rangle$  moments for charged hadron production in SIDIS with a muon beam of energy 280 GeV off a liquid hydrogen target [92]. Both the  $x_F$  and (for the moments)  $P_{h\perp}$  dependences

were measured. The main kinematical cuts considered were:  $Q^2 \geq 4 \text{ (GeV}/c)^2$ ,  $40 \leq W^2 \leq 450 \text{ GeV}^2$ ,  $\nu \geq 20 \text{ GeV}$ ,  $y \leq 0.8$ ,  $P_{h\perp} \geq 0.2 \text{ GeV}/c$ . The main results found were: A strong dependence of the  $\langle \cos \phi_h \rangle$  moment on  $x_F$ , which has a small and positive value for negative  $x_F$ , becomes negative at  $x_F \sim 0$  and falls below  $-0.1$  for  $x_F > 0.5$ . A small dependence of the  $\langle \cos \phi_h \rangle$ ,  $\langle \cos 2\phi_h \rangle$  moments on  $P_{h\perp}$ . The values of  $\langle \cos 2\phi_h \rangle$ ,  $\langle \sin \phi_h \rangle$  as functions of  $x_F$  were found to be close to zero. Previous results limited to the forward hemisphere were also available [93].

The Fermilab E665 Collaboration measured the azimuthal asymmetry of forward charged hadrons produced in SIDIS with a 490 GeV muon beam off proton and deuteron targets [94]. The main kinematical cuts imposed were:  $Q^2 > 3.0 \text{ (GeV}/c)^2$ ,  $100 < W^2 < 900 \text{ GeV}^2$ ,  $60 < \nu < 500 \text{ GeV}$ ,  $x_B > 0.003$ ,  $0.1 < y < 0.85$ ,  $P_h > 8 \text{ GeV}/c$ . They measured, among other observables, the  $\langle \cos \phi_h \rangle$  moment as a function of the minimum hadron transverse momentum up to  $2.5 \text{ GeV}/c$ , imposing  $W^2 > 300 \text{ GeV}^2$  and  $x_F > 0.2$ . Moment values are negative, starting from about  $-0.04$  at the lowest cutoff in  $P_{h\perp}$ , decreasing up to about  $-0.12$  for a  $P_{h\perp}$  cutoff of  $\sim 1.5 \text{ GeV}/c$  and then increasing again (but with larger errors) to  $\sim -0.03$  for the largest considered cutoff in  $P_{h\perp}$  of  $2.5 \text{ GeV}/c$ .

EMC and E665 results are consistent with theoretical models including parton transverse momenta arising both from intrinsic nonperturbative motions and NLO pQCD radiative corrections. Apparently, the nonperturbative contributions dominate in the kinematical regimes covered by these experiments.

The ZEUS Collaboration at HERA-DESY measured the azimuthal angle distribution for charged hadrons produced in neutral current deeply inelastic positron-proton scattering [95]. The dependence of the moments of the distribution,  $\langle \cos \phi_h \rangle$ ,  $\langle \cos 2\phi_h \rangle$  on (the minimum value of) the transverse momentum of the charged hadrons observed,  $P_{h\perp}^{\min}$ , was also studied. At low  $P_{h\perp}^{\min}$  a clear  $\langle \cos \phi_h \rangle$  contribution was observed, while as the value of  $P_{h\perp}^{\min}$  increased, a  $\langle \cos 2\phi_h \rangle$  term became evident;  $\langle \sin \phi_h \rangle$  was found to be consistent with zero independently of the  $P_{h\perp}^{\min}$  value chosen; ii) For hadrons produced at large transverse momenta the  $\langle \cos \phi_h \rangle$  moment was measured to be negative, in agreement with pQCD predictions; the  $\langle \cos 2\phi_h \rangle$  moment was measured for the first time and found to be non-zero and positive, with increasing magnitude as a function of  $P_{h\perp}^{\min}$ . These results were interpreted as giving clear evidence for a pQCD contribution to the azimuthal asymmetry, in contrast with the results of EMC and E665 Collaborations in different kinematical regimes.

The ZEUS Collaboration has also performed a study of the azimuthal asymmetry for inclusive jet production in neutral current deeply inelastic  $e^+p$  scattering. Again, NLO pQCD calculations seem to give a good description of the observed results [96].

More recently, the ZEUS Collaboration presented new results on the dependence of azimuthal moments on the pseudorapidity and the minimum transverse energy of the final-state hadrons [97]. Both neutral and charged hadrons were considered over an extended phase space as compared to Ref. [95]. The value of  $\langle \cos \phi_h \rangle$  was found to be negative for  $\eta < -2$ , becoming positive for larger  $\eta$ . NLO pQCD predictions reproduce reasonably well this behaviour but fail in describing the magnitude of the asymmetries. However, the predicted values of  $\langle \cos 2\phi_h \rangle$  agree with the data. A deviation of  $\langle \sin \phi_h \rangle$  from zero at the level of three standard deviations was observed, while  $\langle \sin 2\phi_h \rangle$  was consistent with zero.

### 2.3.2 Drell-Yan processes

Concerning the Drell-Yan (DY) process, it can be shown that after averaging over the initial hadron polarizations, summing over the final lepton spins, and applying invariance principles (permutation symmetry, gauge invariance, parity conservation and unitarity), the most general form of the lepton angular distribution, in the lepton-pair c.m. frame reads

$$\frac{1}{\sigma} \frac{d^2\sigma}{d\cos\theta d\phi} \propto 1 + \lambda \cos^2\theta + \mu \sin 2\theta \cos\phi + (\nu/2) \sin^2\theta \cos 2\phi, \quad (4)$$

where  $\theta$  and  $\phi$  are respectively the polar and azimuthal angle identifying the lepton-pair direction of motion [see also Fig. 10, p. 50]; the coefficients  $\lambda$ ,  $\mu$ ,  $\nu$  are in general functions of the other relevant

kinematical variables: the total c.m. energy  $\sqrt{s}$ , the lepton-pair invariant mass  $M$ , its transverse momentum  $q_T$ , and its fraction of longitudinal momentum  $x_F$ . The values of these coefficients depend on the choice of the reference frame, the so-called Collins-Soper (CS) frame being often adopted (other popular choices are the Gottfried-Jackson (GJ) frame and the  $u$ -channel frame). When the angular distributions in both  $\cos\theta$  and  $\phi$  are measured in a given frame, one can easily compute the coefficients in any other one. Notice however that this is not the case when only the  $\cos\theta$  distribution is measured.

In the naive parton model for the Drell-Yan process, the assumption of massless quarks implies that the virtual photon is transversely polarized, so that  $\lambda = 1$ ,  $\mu = \nu = 0$ , and one has  $d\sigma/d\cos\theta \sim 1 + \cos^2\theta$ . A general relation by Lam and Tung [98, 99, 100], analogous to the Callan-Gross relation in DIS, is expected to hold in any reference frame:  $\lambda = 1 - 2\nu$ . This relation is not modified by first-order QCD corrections [100], but can be influenced by parton intrinsic motions and other nonperturbative effects.

Concerning experimental results, we limit ourselves to mention some measurements that, as will be discussed in section 5, are relevant in the context of this review.

The NA3 [101] and NA10 [102, 103] Collaborations at CERN have measured the angular distributions of high-mass muon pairs produced by 140 GeV/c and 194 GeV/c  $\pi^-$  beams impinging on a tungsten target, and by a 286 GeV/c  $\pi^-$  beam on deuterium and tungsten targets. The dependence of the parameters  $\lambda$ ,  $\mu$ ,  $\nu$  on the c.m. energy  $\sqrt{s}$ , the invariant mass  $M$ , transverse momentum  $q_T$  and rapidity  $y$  of the lepton pair, and the fractional momentum of the parton in the pion,  $x_1$ , was measured. The kinematical region covered was indicatively (see Ref. [103] for more details):  $4.0 \leq M \leq 8.5$  GeV/c<sup>2</sup> and  $M \geq 11$  GeV/c<sup>2</sup>,  $0.32 \leq q_T \leq 2.60$  GeV/c,  $-0.14 \leq y \leq 0.71$ ,  $0.28 \leq x_1 \leq 0.80$ . No evidence for a c.m. energy dependence or a nuclear dependence of the angular distribution parameters was found. The value of  $\lambda$  was found close to 1, as predicted by the naive parton model, and substantially independent of any kinematical variable, apart from the high  $x_1$  region, where indications of a decrease of  $\lambda$  with  $x_1$ , as suggested by higher-twist effects [104, 105], were found. The value of  $\mu$  was found close to zero in the CS frame, as expected if both annihilating partons contribute equally to the transverse momentum of the lepton pair. The most important result of this analysis was the strong dependence of  $\nu$  on  $q_T$ , in clear disagreement with pQCD expectations. In particular, starting from  $\nu \sim 0$  at the lowest  $q_T$  values,  $\nu$  was found to grow up to  $0.15 \div 0.30$  (depending on  $\sqrt{s}$ ) at larger  $q_T$  values [see Fig. 11 (left panel), p. 51]. Since  $\lambda \sim 1$ , this result also implied a clear violation of the Lam-Tung relation.

The E615 Collaboration at Fermilab has measured the cross section, the transverse momentum distribution and the full angular distribution in  $\cos\theta$  and  $\phi$  as a function of  $M$ ,  $x_F$ , and  $q_T$ , for muon pairs produced by a 252 GeV  $\pi^-$  beam interacting with a tungsten target [106]. The dependence of the parameters  $\lambda$ ,  $\mu$ ,  $\nu$ , on the fractional momentum of the parton in the pion,  $x_1$ , was also measured. The kinematical region covered was:  $4.05 < M < 8.55$  GeV/c<sup>2</sup>,  $0 < q_T < 5.0$  GeV/c,  $0.2 < x_1 < 1.0$ . Again, a clear violation of the Lam-Tung relation, and a strong dependence of  $\nu$  on  $q_T$  were found. In this case also, starting from  $\nu \sim 0$  at the lowest  $q_T$  values,  $\nu$  was found to grow up to  $\sim 0.54(0.73)$  in the GJ(CS) frame at the largest  $q_T$  values.

Recently, the FNAL E866/NuSea Collaboration has presented results on the angular distributions of DY dimuons produced using an 800 GeV/c proton beam on a deuterium target [107], in the kinematical range  $4.5 < M < 15.0$  GeV/c<sup>2</sup>,  $q_T < 4$  GeV/c, and  $0 < x_F < 0.8$ . No significant  $\cos 2\phi$  dependence was found, in contrast with pion-induced DY data discussed above. These results put constraints on theoretical models that predict a large  $\cos 2\phi$  dependence originating from QCD vacuum effects and suggest that the sea-quark Boer-Mulders functions [108] are much smaller than those for valence quarks.

### 2.3.3 $e^+e^- \rightarrow \pi\pi + X$ processes

Recently the Belle Collaboration at the KEKB asymmetric-energy  $e^+e^-$  storage rings has published [109] very interesting results on the inclusive production of hadron pairs (namely charged pion pairs) in  $e^+e^-$  annihilation. Using two different reconstruction methods, they have found evidence of statistically



significant azimuthal asymmetries. The first method is based on the reconstruction of the thrust axis in the  $e^+e^-$  c.m. frame: combining two hadrons from different hemispheres in jet-like events, with azimuthal angles  $\phi_1$  and  $\phi_2$  defined w.r.t. the plane spanned by the lepton momenta and the thrust axis [see Fig. 12 (left), p. 52], a  $\cos(\phi_1 + \phi_2)$  modulation of the dihadron yield has been observed [see Fig. 13 (left panel), p. 53]. An alternative method does not require the knowledge of the thrust axis. In this case the dihadron yields are measured as a function of one angle,  $\phi_0$ , that is the angle between the plane spanned by the momentum vector of the first hadron and the lepton momenta and the plane defined by the two hadron momenta [see Fig. 12 (right), p. 52]. In this case a  $\cos(2\phi_0)$  modulation appears [see Fig. 13 (right panel), p. 53]. As it will be discussed in section 5.4, these results are related and give access to the product of two Collins functions.

The kinematical cuts imposed in both methods are the following:  $-0.6 < \cos(\theta_{\text{lab}}) < 0.9$ , where  $\theta_{\text{lab}}$  is the polar angle in the laboratory frame;  $z_{1,2} > 0.2$ , where  $z_i = 2E_{h_i}/Q$ , and  $Q$  is the c.m. energy;  $Q_T < 3.5 \text{ GeV}/c$ , where  $Q_T$  is the transverse momentum of the virtual photon in the rest frame of the hadron pair. Moreover, to cancel acceptance effects double ratios of normalized rates for unlike-sign ( $U$ ) over like-sign ( $L$ ) pion pairs ( $UL$  double ratios) have been considered. At large  $z_{1,2}$  values the measured asymmetries are significantly different from zero [see Fig. 13, p. 53]. In Ref. [110] preliminary results on the double ratios of unlike-sign,  $U$ , over all charged ( $C$ ) pion pairs have been presented. These  $UC$  double ratios can give useful additional information on the Collins function. Belle results have been confirmed by recent preliminary data with enlarged statistics and much smaller error bars [111].

### 3 Theoretical approaches to single spin asymmetries

We present here some of the approaches developed to explain the interesting features of the SSA data discussed so far. We will try to follow a historical perspective, starting with the former attempts to describe the SSA's observed in hadronic collisions and then entering into the latest developments.

The first approach we address is based on a pQCD factorization scheme with inclusion of spin and intrinsic transverse momentum dependent (TMD) effects: we will generally refer to it as the TMD approach. In particular we start with its application to inclusive hadron production in hadron-hadron collisions and its formulation as a phenomenological generalization of the parton model. This form of the TMD approach will be also referred to as the *Generalized Parton Model* (GPM) and will find a more detailed description within the helicity formalism in section 4. We then discuss more recent, and significant, QCD developments of the TMD approach with inclusion of initial and final state colour interactions which modify, to some extent, the partonic interpretation of the GPM approach. Some details on the impact parameter picture for SSA's, which gives a useful physical interpretation of the TMD approach, are also presented.

The second approach we consider extends the QCD collinear factorization theorems to higher-twist contributions: the so-called *twist-three approach*. We recall its basic ingredients, giving some details of its application to SSA's in  $pp \rightarrow \pi + X$  and its later extension to other processes.

The issues of validity, applicability and possible overlapping of these two approaches, for different kinematical regions and processes, as well as the status of factorization in pQCD, are also discussed. In particular, we will see how the TMD approach applies naturally to leading twist asymmetries, like SSA's in Drell-Yan processes and SIDIS, or azimuthal asymmetries in  $e^+e^- \rightarrow h_1 h_2 + X$ , at low transverse momentum, where also a second large scale (the virtuality of the exchanged boson) is present. With some caution, it can be also adopted in double inclusive production of hadrons (jets, or photon-jet) in hadronic collisions.

On the other hand, the collinear higher-twist approach applies in principle to subleading asymmetries, like SSA's in  $pp \rightarrow h + X$  and  $pp \rightarrow \gamma + X$ , where a single hard scale (the transverse momentum of the observed particle) appears. For these cases the GPM can be viewed as an effective and, as we



will see, phenomenologically successful, TMD description.

For completeness we will give some details of an alternative description of SSA's based on a semi-classical model: the so-called *orbiting valence quark model*.

Among other attempts to describe SSA's, even if on a more qualitative ground, we mention: *i*) a model discussed in Ref. [112], for  $pp \rightarrow \pi + X$ , and in Ref. [113], for SIDIS, where the quark chirality flip and the required T-odd phase (see below) are associated with instanton fluctuations in the QCD vacuum; *ii*) a soft rescattering mechanism [114] with a Pauli coupling that leads in SIDIS to a  $\sin(\phi_h + \phi_S)$  dependence (like that usually ascribed to the Collins effect in the TMD approach); *iii*) a coherence mechanism [115], where the entire hadron contributes to the scattering process, aimed to describe the sizable values of  $A_N$  observed in  $pp$  collisions at large  $x_F$ .

For technicalities and a comprehensive discussion of the topics addressed here we refer the reader to the original bibliography.

### 3.1 Parton model approaches including intrinsic transverse motion

It has been known for a long time, especially in the fixed target regime, that unpolarized cross sections for inclusive particle production in high-energy hadron-hadron collisions at moderate  $p_T$  (few GeV/c) cannot be properly described in the collinear factorized pQCD approach, neither at LO nor at NLO accuracy [116]. Only recently, improved NLO calculations including threshold resummation effects have been developed, see e.g. Ref. [117]. These results show how for inclusive cross sections integrated over all hadron rapidity range the agreement with data is much less problematic. On the other hand the rapidity-dependent case is still under study.

Even more dramatic is the failure of the description of the Drell-Yan low  $q_T$  spectrum, where  $q_T$  is the lepton-pair transverse momentum. Indeed, in this case no transverse momentum can be generated in the collinear LO approximation. All these facts have raised, starting from former work of Feynman and collaborators [118, 119], the interest in considering the role of intrinsic transverse momentum.

In the context of transverse SSA's the intrinsic transverse motion of partons has played an even more essential role. Indeed, as shown in Ref. [46], in collinear pQCD  $A_N$  appears only as the imaginary part of interference terms between spin-flip and no-spin-flip partonic scattering amplitudes. Since at LO these are real and helicity is conserved for massless partons, it was natural to expect  $A_N \simeq \alpha_s m/\sqrt{s}$ .

Contrary to these expectations several experimental observations, as seen in section 2, show sizable SSA's in the high-energy regime.

The cross section for a generic inclusive process  $AB \rightarrow C + X$ , in a phenomenological approach based on the generalization of the factorization theorem with the inclusion of intrinsic motions,  $\mathbf{k}_\perp$ , of partons inside a nucleon and of final hadrons relatively to the fragmenting parton, reads, schematically:

$$d\sigma \propto \sum_{a,b,c} \hat{f}_{a/A}(x_a, \mathbf{k}_{\perp a}) \otimes \hat{f}_{b/B}(x_b, \mathbf{k}_{\perp b}) \otimes d\hat{\sigma}^{ab \rightarrow cd}(x_a, x_b, \mathbf{k}_{\perp a}, \mathbf{k}_{\perp b}) \otimes \hat{D}_{C/c}(z, \mathbf{k}_{\perp C}), \quad (5)$$

where  $\otimes$  stands for appropriate convolutions both in the light-cone momentum fractions,  $x_{a,b}$ ,  $z$ , and in the  $\mathbf{k}_\perp$ 's. The  $\hat{f}$ 's and the  $\hat{D}$ 's are the TMD parton distribution (PDF) and fragmentation functions (FF), respectively;  $\mathbf{k}_{\perp a,b}$  is the transverse momentum of parton  $a, b$  w.r.t. the hadron  $A, B$  momentum and  $\mathbf{k}_{\perp C}$  the transverse momentum of hadron  $C$  w.r.t. the fragmenting parton direction of motion.

The above QCD factorization scheme – with unintegrated  $\mathbf{k}_\perp$  dependent distribution and fragmentation functions – has never been formally proven for the process under consideration, but only for the Drell-Yan process [120] and for two-particle inclusive production in  $e^+e^-$  annihilation [121] (somehow a time-reversed Drell-Yan process). Factorization at low transverse momentum for SIDIS has been recently addressed [122, 123] and proved at the same level as for the two above mentioned processes. Recent developments on the status of the more problematic  $k_\perp$ -factorization in  $AB \rightarrow CD + X$  will be discussed in section 3.1.1.

The study of spin asymmetries requires the extension of Eq. (5) to the polarized case. The inclusion of  $\mathbf{k}_\perp$  effects and TMD functions can in principle lead to sizable SSA's; however, if the TMD functions are symmetric in the azimuthal direction,  $A_N$  would be still negligible. It was then originally suggested by Sivers [18, 19] that there could exist a correlation between the azimuthal distribution of an unpolarized parton and the spin of its parent hadron. That is, we could have the following nonvanishing asymmetry:

$$\Delta \hat{f}_{a/A^\uparrow}(x, \mathbf{k}_\perp) \equiv \hat{f}_{a/A^\uparrow}(x, \mathbf{k}_\perp) - \hat{f}_{a/A^\downarrow}(x, \mathbf{k}_\perp) = \hat{f}_{a/A^\uparrow}(x, \mathbf{k}_\perp) - \hat{f}_{a/A^\uparrow}(x, -\mathbf{k}_\perp), \quad (6)$$

where the last relation comes from rotational invariance and  $\uparrow$  ( $\downarrow$ ) stands for the upwards (downwards) transverse spin direction of the hadron  $A$ . It is easy to see that  $\Delta \hat{f}_{a/A^\uparrow}$  must be, by parity conservation, proportional to  $(\mathbf{p}_A \times \mathbf{k}_\perp) \cdot \mathbf{S}_A$ , where  $\mathbf{p}_A, \mathbf{S}_A$  are the momentum and the spin of the hadron  $A$ , and  $\mathbf{k}_\perp$  the transverse momentum of the parton. This function is  $\mathbf{k}_\perp$ -odd and chiral-even, as will be clear in section 4. It is also naively time reversal odd (T-odd). Notice that the above asymmetry can be rephrased in terms of the number density of unpolarized partons inside a transversely polarized hadron ( $\hat{\mathbf{p}}_A, \hat{\mathbf{k}}_\perp$  being unit vectors and  $k_\perp = |\mathbf{k}_\perp|$ ):

$$\hat{f}_{a/A^\uparrow}(x, \mathbf{k}_\perp) = f_{a/A}(x, k_\perp) + \frac{1}{2} \Delta^N f_{a/A^\uparrow}(x, k_\perp) (\hat{\mathbf{p}}_A \times \hat{\mathbf{k}}_\perp) \cdot \mathbf{S}_A, \quad (7)$$

where  $\Delta^N f_{a/A^\uparrow}$  (related to  $f_{1T}^\perp$  [108], see Ref. [73]) is referred to as the *Sivers function*.

In this first formulation the numerator of  $A_N$ , see Eq. (1), assumed to be generated by the Sivers effect, was computed according to the following expression:

$$d\Delta\sigma^{\text{Sivers}} \propto \sum_{a,b,c} \Delta \hat{f}_{a/A^\uparrow}(x_a, \mathbf{k}_{\perp a}) \otimes f_{b/B}(x_b) \otimes d\hat{\sigma}^{ab \rightarrow cd}(x_a, x_b, \mathbf{k}_{\perp a}) \otimes D_{C/c}(z); \quad (8)$$

that is, by keeping TMD effects only where the collinear approximation would otherwise give zero (remember that the Sivers function vanishes for  $k_\perp = 0$  and is  $\mathbf{k}_\perp$ -odd).

In 1993 Collins proposed a proof of the vanishing of the Sivers function [20]. By imposing, in the light-cone gauge (this point would have become crucial), parity and time reversal invariance, he showed that strong interactions forbid such an asymmetry. However, on the basis of possible initial state interactions between the two colliding hadrons, in Ref. [124] it was argued that this asymmetry might be allowed. By a reasonable parameterization of this function a good description of E704 data was then obtained [124, 125].

In Refs. [20, 21] another possible asymmetric azimuthal angular dependence was proposed: a left-right asymmetry in the fragmentation of a transversely polarized quark into a spinless (or, more generally, unpolarized) hadron. This implies a new TMD and spin dependent twist-two function ( $\mathbf{p}_q$  and  $\mathbf{s}_q$  being the momentum and the spin of the quark and  $\mathbf{p}_C \simeq z\mathbf{p}_q + \mathbf{k}_\perp$  the hadron momentum),

$$\hat{D}_{C/q^\uparrow}(z, \mathbf{k}_\perp) = D_{C/q}(z, k_\perp) + \frac{1}{2} \Delta^N D_{C/q^\uparrow}(z, k_\perp) (\hat{\mathbf{p}}_q \times \hat{\mathbf{k}}_\perp) \cdot \mathbf{s}_q, \quad (9)$$

where  $\Delta^N D_{C/q^\uparrow}$  (or  $H_1^\perp$  in Refs. [126, 108], see also Ref. [73]) is the *Collins function*. Again we have

$$\Delta \hat{D}_{C/q^\uparrow}(z, \mathbf{k}_\perp) \equiv \hat{D}_{C/q^\uparrow}(z, \mathbf{k}_\perp) - \hat{D}_{C/q^\downarrow}(z, \mathbf{k}_\perp) = \hat{D}_{C/q^\uparrow}(z, \mathbf{k}_\perp) - \hat{D}_{C/q^\uparrow}(z, -\mathbf{k}_\perp), \quad (10)$$

where  $\uparrow$  ( $\downarrow$ ) stands for the upwards (downwards) transverse spin direction of the fragmenting quark. In this case, due to the rescattering of the hadron with the remnants of the jet (or, in more formal words, since the final hadron, contrary to the incoming one, cannot be represented as a plane wave state), time-reversal invariance does not imply any constraint, allowing the existence of such an asymmetry.

This new effect in the fragmentation mechanism was then proposed as a transverse quark polarimeter with the aim of extracting information on the transverse polarization of a quark, i.e., as a tool to measure the transversity distribution. This function, denoted by  $h_{1q}(x)$  (or  $\Delta_{Tq}, \delta q$ ), and defined as

$$h_{1q}(x) = f_{q^\uparrow/p^\uparrow}(x) - f_{q^\downarrow/p^\uparrow}(x), \quad (11)$$

is the difference between the probabilities to find a quark polarized along the transverse proton polarization and against it. This chiral-odd function, in contrast with the unpolarized and the helicity distribution functions (both chiral-even), is much more difficult to measure. Indeed, it cannot be accessed in DIS, since it implies a helicity flip at the parton level whereas QED and QCD for massless quarks conserve helicity. It has therefore to be accompanied by another chiral-odd quantity. As originally proposed by Ralston and Soper in Ref. [127], the most promising source of information on  $h_{1q}$ , is the double transverse spin asymmetry,  $A_{TT}$ , in Drell-Yan processes, where it appears quadratically, but unfortunately no data are still available.

Collins idea was to consider a new process where another chiral-odd function could appear: this is the SIDIS process with a transversely polarized proton target,  $ep^\uparrow \rightarrow e'h + X$ , where the azimuthal dependence of the final hadron distribution, w.r.t. the lepton scattering plane, would probe at the same time the transversity distribution function, the transverse spin dependence of the hard scattering and, eventually, the spin dependence in the fragmentation. This process, as we will discuss in section 5, has become, indeed, the first source of phenomenological information on the transversity distribution.

A calculation of the Collins function, based on a sigma model for pions with an effective Lagrangian incorporating chiral symmetry breaking, showed that  $\Delta\hat{D}_{C/q^\uparrow}(z, \mathbf{k}_\perp)$  could be different from zero [20].

This idea was then extended to the study of  $A_N$  in  $p^\uparrow p \rightarrow \pi + X$  collisions. In the factorized approach discussed above, the numerator of the SSA generated by the Collins effect would read

$$d\Delta\sigma^{\text{Collins}} \propto \sum_{a,b,c} h_{1a}(x_a) \otimes f_{b/p}(x_b) \otimes d\Delta\hat{\sigma}^{ab \rightarrow cd}(x_a, x_b, \mathbf{k}_\perp) \otimes \Delta\hat{D}_{\pi/c^\uparrow}(z, \mathbf{k}_\perp), \quad (12)$$

where  $d\Delta\hat{\sigma}^{ab \rightarrow cd}$  is the partonic double transverse spin asymmetry related to the partonic spin transfer,  $D_{NN} = d\Delta\hat{\sigma}/d\hat{\sigma}$ . Notice once again that only the leading  $\mathbf{k}_\perp$ -dependence is kept.

A first phenomenological attempt to explain the SSA in terms of such effect was presented in Ref. [128]. The azimuthal asymmetry in the fragmentation process was generated via the Lund string mechanism [129]. According to this model, in the breaking of the string spanned between the scattered quark and the target, the quark and the antiquark of every pair created acquire a transverse momentum (w.r.t. the direction of the string) and a polarization which are strongly correlated. Namely, the antiquark polarization goes like  $\mathbf{P}_{\bar{q}} \simeq -\hat{z} \times \mathbf{k}_\perp$  where  $\hat{z}$  is the unit vector along the string direction.

In order to form a pion, the polarized scattered quark (coming from the hard scattering) has to combine with the antiquark (belonging to the string pair) into a spin singlet. This implies a correlation between the  $q$  and  $\bar{q}$  polarizations, resulting in an asymmetric azimuthal distribution of the pion w.r.t. the quark polarization. In this model the Collins effect is introduced only for leading, or “first-rank”, pions (those containing the original quark spanning the string): the azimuthal distribution of higher-rank (subleading) pions is assumed to be symmetric. It is worth to mention that even starting from Eq. (12), that is a pQCD inspired formula, the authors of Ref. [128] adopted a partonic spin-transfer  $D_{NN}$  equal to one (as it is for very small scattering angles) and a simple power-like  $p_T$ -dependent partonic cross-section based on the observed inclusive pion spectra. By assuming that the transverse polarization of the  $u$  and  $d$  quarks in the proton are  $+1$  and  $-1$  at  $x = 1$ , respectively, they obtained qualitative agreement with the E704 data, although underestimating their size.

Among the peculiar features of this model we recall that for spin-1 meson (e.g. the  $\rho$ ) production the spin- $\mathbf{k}_\perp$  correlation gives a very different Collins effect; as a consequence,  $A_N(\rho) \simeq -(1/3)A_N(\pi)$  [130]. No SSA is expected for  $K^-$  production (which has no valence quark in common with the polarized proton) since the subleading fragmentation mechanism is assumed to be symmetric.

A more detailed phenomenological study of the Collins effect in  $pp$  collisions, based on the factorized scheme of Eq. (12), was performed in Ref. [131], where the authors adopted the helicity formalism with inclusion of TMD effects. We postpone the details of this approach to section 4. Here we only recall that by a reasonable parameterization of the Collins function and the transversity distribution a good description of the E704 data was obtained. As we will discuss in section 5 a complete treatment of the

kinematics, taking into account the full  $\mathbf{k}_\perp$  dependences in the factorized formula of Eq. (12), plays a big role and leads to a strong revision of this conclusion. More generally we will see how the correct  $\mathbf{k}_\perp$  kinematics is crucial in the TMD approach to inclusive particle production.

Almost in the same years, a first systematic classification of the twist-two and twist-three transverse momentum and spin dependent parton distribution and fragmentation functions was presented in Refs. [126, 108]. For the twist-three case these functions have no partonic interpretation since they are related to quark-quark-gluon matrix elements. Further improvements beyond leading twist in the above classification were reached in Ref. [132]. This work has been recently reassessed and completed in Ref. [87] where some new developments (see also Refs. [133, 134]) have been taken into account; in particular, a systematic presentation of the relevant observables for all combinations of lepton and hadron polarizations at small transverse momentum and twist-three accuracy has been given. For space reasons, and given its relevance, in the following we will restrict to the leading-twist TMD sector. We refer the reader to the above mentioned papers for a more detailed discussion.

The starting point in this classification is the correlator of quark fields ( $\psi$ ) for a polarized nucleon (with spin  $S$ ) entering the DIS processes in the diagrammatic expansion of the hard scattering amplitude,

$$\Phi_{ij}(P, S, k) = \int \frac{d^4y}{(2\pi)^4} e^{ik \cdot y} \langle P, S | \bar{\psi}_j(0) \psi_i(y) | P, S \rangle, \quad (13)$$

and the analogous correlator for the fragmentation sector

$$\Delta_{ij}(P_h, S_h, k) = \sum_X \int \frac{d^4y}{(2\pi)^4} e^{ik \cdot y} \langle 0 | \psi_i(y) | P_h, S_h, X \rangle \langle P_h, S_h, X | \bar{\psi}_j(0) | 0 \rangle. \quad (14)$$

By integrating over  $k^- = (k^0 - k^3)/\sqrt{2}$ , where  $k^\mu = xP^\mu + k_\perp^\mu$  and  $k_\perp^\mu = (0, \mathbf{k}_\perp, 0)$ , and keeping the leading twist terms, one gets, for the distribution sector,

$$\begin{aligned} \Phi(x, \mathbf{k}_\perp, S) = & \frac{1}{2} \left[ f_1 \not{h}_+ + f_{1T}^\perp \frac{\epsilon_{\mu\nu\rho\sigma} \gamma^\mu n_+^\nu k_\perp^\rho S_T^\sigma}{M} + \left( S_L g_{1L} + \frac{\mathbf{k}_\perp \cdot \mathbf{S}_T}{M} g_{1T} \right) \gamma^5 \not{h}_+ \right. \\ & \left. + h_{1T} i\sigma_{\mu\nu} \gamma^5 n_+^\mu S_T^\nu + \left( S_L h_{1L}^\perp + \frac{\mathbf{k}_\perp \cdot \mathbf{S}_T}{M} h_{1T}^\perp \right) \frac{i\sigma_{\mu\nu} \gamma^5 n_+^\mu k_\perp^\nu}{M} + h_1^\perp \frac{\sigma_{\mu\nu} k_\perp^\mu n_+^\nu}{M} \right], \quad (15) \end{aligned}$$

where  $n_\pm$  are auxiliary light-like vectors and  $M$  is the nucleon mass. All functions above depend on  $x$  and  $|\mathbf{k}_\perp|$ . Few words on the above notation are helpful:  $f$ ,  $g$  and  $h$  stand for unpolarized, longitudinally polarized, and transversely polarized quarks, respectively: the subscript “1” stands for leading twist; the apex  $\perp$  indicates the explicit presence of transverse momenta with a noncontracted index [126]; the subscripts  $L$ ,  $T$  stand for the longitudinal and transverse polarization of the hadron. Therefore, for instance,  $f_1$  is the TMD unpolarized PDF,  $f_{1T}^\perp$  is the Sivers function and  $h_{1T}$ ,  $h_{1T}^\perp$  are related to the TMD transversity distribution. For relations among different notations see also Refs. [73, 12, 135].

By appropriate Dirac projections,  $\Phi^{[\Gamma]} = \text{Tr}(\Gamma\Phi)$ , one can single out the various sectors of distribution functions. In particular,  $\Gamma = (n_-)_\alpha \gamma^\alpha / 2$  projects out the  $f_1$  sector, and  $\Gamma = \frac{1}{2} i\sigma_{\mu\nu} (n_-)^\mu \frac{(S_T)^\nu}{2} \gamma^5$  gives the  $h_1$  sector. Among the others we only mention, in particular, the function  $h_1^\perp$ , also known as the Boer-Mulders function, which has been proposed in Ref. [136] as a possible tool to explain the azimuthal asymmetry observed in unpolarized Drell-Yan processes.

The partonic meaning of the eight functions appearing in Eq. (15) and their relations with those defined in a complementary formalism, the helicity approach, will be discussed in more detail in section 4.

The same structure can be obtained for the fragmentation sector, starting from the corresponding correlator, Eq. (14). In this case one gets, among the others, the Collins function,  $\Delta^N D_{C/q^\dagger}$ , and a chiral-even TMD fragmentation function of an unpolarized quark into a transversely polarized hadron (denoted consistently as  $\Delta^N D_{C^\dagger/q}$ ). This function, also known as the *polarizing* FF, could play a role in describing the observed transverse polarization of  $\Lambda$  hyperons produced in unpolarized  $pp$  collisions [137].

For the sake of clarity we give here the relation between two standard notations for the most relevant TMD functions appearing in the sequel (the Sivers and Boer-Mulders distributions; the Collins and polarizing fragmentation functions):

$$\begin{aligned}\Delta^N f_{q/p^\uparrow}(x, |\mathbf{k}_\perp|) &= -\frac{2|\mathbf{k}_\perp|}{M} f_{1T}^{\perp q}(x, |\mathbf{k}_\perp|) & \Delta^N f_{q^\uparrow/p}(x, |\mathbf{k}_\perp|) &= -\frac{|\mathbf{k}_\perp|}{M} h_1^{\perp q}(x, |\mathbf{k}_\perp|) \\ \Delta^N D_{h/q^\uparrow}(z, |\mathbf{k}_{\perp h}|) &= \frac{2|\mathbf{k}_{\perp h}|}{zM_h} H_1^{\perp q}(z, |\mathbf{k}_{\perp h}|) & \Delta^N D_{h^\uparrow/q}(z, |\mathbf{k}_{\perp h}|) &= \frac{|\mathbf{k}_{\perp h}|}{zM_h} D_{1T}^{\perp q}(z, |\mathbf{k}_{\perp h}|).\end{aligned}\quad (16)$$

It is also customary to consider  $k_\perp$ -moments of the TMD distributions. The most relevant ones in the PDF sector are defined as (similar relations hold also for the FF case, see e.g. Eq. (76))

$$f_{1T}^{\perp(1)}(x) \equiv \int d^2\mathbf{k}_\perp \frac{\mathbf{k}_\perp^2}{2M^2} f_{1T}^\perp(x, |\mathbf{k}_\perp|) \quad f_{1T}^{\perp(1/2)}(x) \equiv \int d^2\mathbf{k}_\perp \frac{|\mathbf{k}_\perp|}{2M} f_{1T}^\perp(x, |\mathbf{k}_\perp|). \quad (17)$$

### 3.1.1 QCD developments

An important and clear improvement of the TMD approach, in particular concerning the distribution sector, came with the discovery of a mechanism to generate a transverse spin asymmetry at leading twist [138]. Here, by considering the deeply inelastic lepton-proton scattering process, the authors showed that final-state interactions due to gluon exchange between the outgoing quark and the target spectator system lead to single spin asymmetries at leading twist in pQCD; *i.e.*, the rescattering corrections are not power-law suppressed. The existence of such SSA's requires a phase difference between two amplitudes coupling the proton target with  $J_p^z = \pm\frac{1}{2}$  (where  $J_p$  is the total proton angular momentum) to the same final state. These same amplitudes are necessary to produce a nonzero proton anomalous magnetic moment. The calculation of Ref. [138] was performed in a field-theoretic model in which QCD, with massive quarks, is supplemented by a coloured scalar diquark field and an elementary proton field. Soon afterwards this mechanism was reanalyzed by Collins [139] who proved that it is compatible with factorization and due to a spin asymmetry in the  $\mathbf{k}_\perp$  distribution of quarks in a transversely polarized hadron: the ‘‘Sivers asymmetry’’. The earlier statement by Collins, that the Sivers asymmetry has to vanish because of time-reversal invariance, gets invalidated by the path-ordered exponential of the gluon field in the operator definition of TMD parton densities. What the time-reversal argument shows is instead that the Sivers distribution is reversed in sign in Drell-Yan processes w.r.t. the SIDIS case. This result, which would imply a violation of naive universality of parton densities, offers a clear test of our understanding of the TMD approach in pQCD.

The origin of this sign change can be understood by looking at the gauge link entering the correlator. Therefore it is crucial to start with the properly defined gauge-invariant parton density for a hadron with momentum  $P$  and transverse spin  $S$  ( $\uparrow, \downarrow$ ), that has the following operator definition

$$\hat{f}_{q/A^\uparrow}(x, \mathbf{k}_\perp) = \int \frac{d\xi^- d^2\xi_\perp}{(2\pi)^3} e^{-ixp^+\xi^- + i\mathbf{k}_\perp \cdot \xi_\perp} \langle P, S | \bar{\psi}(0, \xi^-, \xi_\perp) W_{\xi_\infty}^\dagger \frac{\gamma^+}{2} W_{0\infty} \psi(0) | P, S \rangle. \quad (18)$$

Here, light-front coordinates are used:  $\xi^\pm = (\xi^0 \pm \xi^z)/\sqrt{2}$  and  $\xi_\perp^\mu = (0, \xi_\perp, 0)$ . The symbol  $W_{\xi_\infty}$  indicates a Wilson-line operator, also called gauge-link, going out from the point  $\xi$  to future infinity. These links are path-ordered exponentials, defined as [140, 141]

$$W_{\xi_\infty} = \mathcal{P} \exp\left(-ig_s \int_{\xi^-}^{\infty} dz^- \hat{A}^+(z^-, \xi_\perp)\right) \cdot \mathcal{P} \exp\left(-ig_s \int_{\xi_\perp}^{\infty} dz_\perp \cdot \hat{A}_\perp(z^- = \infty, z_\perp)\right), \quad (19)$$

where  $\hat{A}^\mu = \sum_a t^a A_a^\mu$ , with  $t^a = \lambda^a/2$  being the Gell-Mann colour matrices.

In particular, in the light-cone gauge ( $\hat{A}^+ = 0$ ) the first piece in Eq. (19) reduces to one and we are left with the pure transverse gauge link, depending on the nonvanishing vector potential at infinity. As



extensively discussed in Ref. [141], this link in the transverse direction is crucial to maintain the gauge invariance of TMD parton distributions under residual gauge transformations; at the same time, it is responsible for the final(initial) state interactions in SIDIS(DY) [138, 139]. In nonsingular gauges, like covariant gauges, where the vector potential at infinity vanishes, in Eq. (19) only the gauge link along the light-like direction,  $z^\mu \simeq (0, \mathbf{0}, z^-)$ , survives. In this case, as discussed in Ref. [121] and reassessed in Ref. [142] severe light-cone divergences arise from contributions of virtual gluons with vanishing light-cone plus momentum. A standard way to cut them off is the use of a Wilson line slightly out of the light-like direction ( $z^+ \sim 0$ ) [143]. Notice that this complication does not affect model calculations of TMD distributions at lowest order.

The original proof on the vanishing of the Sivers function [20], obtained applying space- and time-reversal to the quark fields in the operator definition of the parton densities, was then incomplete, because it ignored the presence of Wilson lines. Under time-reversal the future-pointing Wilson lines are replaced by past-pointing Wilson lines so that the correct version of the proof gives [139]

$$\hat{f}_{q/A^\uparrow}(x, \mathbf{k}_\perp)|_{\text{future-pointing } W} = \hat{f}_{q/A^\downarrow}(x, \mathbf{k}_\perp)|_{\text{past-pointing } W}. \quad (20)$$

Note the change in direction of the transverse spin-vector ( $\uparrow$  goes into  $\downarrow$ ). Since the past-pointing Wilson lines are appropriate for factorization in the Drell-Yan process [139, 144], the correct result is not that the Sivers asymmetry, Eq. (6), vanishes, but that it has opposite signs in DIS and in Drell-Yan:

$$\Delta \hat{f}_{q/A^\uparrow}(x, \mathbf{k}_\perp)|_{\text{DIS}} = -\Delta \hat{f}_{q/A^\uparrow}(x, \mathbf{k}_\perp)|_{\text{DY}}. \quad (21)$$

The TMD spin-independent parton distribution keeps its universality.

A complementary study for the fragmentation sector has been developed in Refs. [145, 146], where the authors compare SIDIS processes and  $e^+e^-$  annihilation into two hadrons. The relevant result is that spin and  $\mathbf{k}_\perp$  dependent fragmentation functions are universal, also in sign. This finding has played a crucial role in the first extraction of the transversity distribution from a global analysis of the azimuthal asymmetries observed in  $e^+e^- \rightarrow \pi\pi + X$  and SIDIS (see sections 5.4, 5.5.2).

The role of the gauge links in TMD distributions has then been further and systematically investigated in a series of papers [140, 141, 122, 123, 147, 148], which focus mainly on the gauge invariant definition of TMD distributions and the proper factorization in QCD at leading twist for SIDIS and Drell-Yan processes at low transverse momentum. We only mention here that according to the  $k_\perp$  factorization for SIDIS, in the convolution of  $k_\perp$  dependent PDF's and FF's with the hard scattering parts another term appears: a soft factor coming from soft gluon radiations and defined by a matrix element of Wilson lines in QCD vacuum [122, 146]. One of its effects is that the transverse momentum of the observed hadron in SIDIS could be generated not only by the intrinsic motion of the quarks in the nucleon and in the quark fragmentation process but also via soft gluon radiation. Notice that, at the present stage, all phenomenological studies have neglected this extra unknown factor.

In Ref. [147] the energy evolution of the spin and TMD distributions is also discussed. The authors, following Ref. [121], show how the Collins-Soper equation in the impact parameter space can be applied also to these distributions. This equation, intimately related to the regularization of the light-cone singularities of TMD distributions in covariant gauges, allows to resum the large logarithms arising in perturbative calculations for SIDIS (or DY) process at low transverse momentum.

Another interesting issue related to the TMD azimuthal asymmetries is the potential suppression due to Sudakov factors coming from soft gluon radiation. This problem has been analyzed in Ref. [149] for a class of processes, like the Drell-Yan process or two-hadron production in  $e^+e^-$  annihilation, where two energy scales (for DY: the transverse momentum of the lepton pair,  $q_T$ , and its invariant mass,  $Q$ ) are present. In order to extend the TMD factorization picture beyond the region of very small  $q_T$  (where tree-level formulas are sufficient) to the region where the transverse momentum becomes moderate (still  $q_T \ll Q$ ) one has to include the Sudakov factors by proper resummation. This implies a broadening of the  $q_T$  distribution and a suppression effect, that becomes more important with rising energy [149].

The scale dependence, at LO, of the first moments of the TMD distribution and fragmentation functions has been studied in Ref. [150], by using Lorentz invariance and the QCD equations of motion in the large  $N_c$  limit. A phenomenological study on the  $Q^2$ -evolution (via resummation of soft and collinear parton emissions at LO) of unpolarized TMD distributions in SIDIS has been presented in Refs. [151, 152].

Before completing this short overview of the TMD approach we want to mention the recent study of the gauge links in more complicated processes, like  $pp \rightarrow h_1 h_2 + X$ , where the elementary scattering involves many subprocesses and hadrons are present both in the initial and final state.

Indeed, in the simplest hadronic scattering processes, such as SIDIS, DY and  $e^+e^-$ -annihilation, only a limited number of different gauge-link structures appear. These are the future and past-pointing Wilson lines mentioned above. When going beyond these processes one may encounter more complex gauge-link structures. In Refs. [153, 154] the paths that can appear in general scattering processes have been analyzed (some technical aspects are presented in Ref. [155]). It was then shown that the presence of gauge links can lead to modified hard parts, referred to as *gluonic pole cross sections*, for SSA's in  $p^\uparrow p \rightarrow \pi\pi + X$  [154, 156]. By taking suitable  $k_\perp$ -moments of the SSA's (with proper weights) the net effect coming from these highly non-trivial structures is to modify the usual sum of Feynman diagrams representing the standard partonic cross sections into gauge invariant weighted sums, with  $SU(3)$  colour factors as weights (analogous to the  $\pm 1$  factors discussed above for SIDIS and DY).

Very recently the double inclusive hadron (or jet) production in hadron-hadron collisions with a small  $q_T$  imbalance, has received a special attention, in particular concerning the validity of the  $k_\perp$  factorization. In Ref. [157] by adopting a simplified Abelian model, Collins and Qiu argue that factorization is violated, even in the extended version of the TMD approach including gluonic pole cross sections. On the other hand, another approach [158, 159], based on a careful analysis of one-gluon radiation contributions, led apparently to the opposite result. Some light on this apparent discrepancy has been shed in Refs. [160, 161] and further clarified in Ref. [162], showing a mutual consistency among the different approaches.

Summarizing, the main findings are: *i*) by expanding the gauge link in the correlators entering the colour gauge invariant approach [154, 156] at first order in the coupling constant one recovers the results of Refs. [158, 159]; *ii*) by extending, and properly adapting, the calculations of Refs. [158, 159] to two-gluon exchange, a non factorizable term in the TMD unpolarized cross section appears, in agreement with the results found in Ref. [157, 160]. This extra piece can be taken into account by redefining the gauge link entering the TMD parton distribution [161]. A similar complication (i.e. a non factorizable hard part, or equivalently, a redefinition of the gauge link entering the TMD distribution) for the SSA (Sivers effect) is expected at the next order of perturbation theory. In Ref. [162], by assuming factorization at the diagrammatic level, the authors obtain a manifest gauge invariant expression for the TMD cross sections in terms of gluonic pole cross sections and TMD distributions with process-dependent Wilson lines. In this sense the TMD distributions are in general non universal. In this approach, beside confirming the results of Refs. [158, 159], gluonic pole cross sections in TMD unpolarized cross sections as well as ordinary partonic cross sections in unweighted SSA's arise together with universality-breaking parts, in agreement with Refs. [160, 161]. However, these pieces are shown to vanish for the integrated and weighted observables considered in Refs. [154, 156, 163, 164]. The identification of these process dependent pieces could be an important step towards a unified picture of TMD factorization for hadronic processes. Further work is still needed.

### 3.1.2 The impact parameter picture

This physical picture, mostly applied to the Sivers effect, has been discussed in a series of papers by Burkardt and collaborators [31, 32, 33, 165]. It is based on two main ingredients: the distortion in the transverse plane of the distribution of partons inside a polarized target and the attractive(repulsive)

final(initial) state interactions in SIDIS(DY). The first aspect is strongly related to the information one can extract from the generalized parton distributions (GPD).

GPD's are generalizations of ordinary parton distributions to non-forward matrix elements of a lightlike correlation function. They can be accessed for instance in deeply virtual Compton scattering,  $\gamma^*p \rightarrow \gamma p'$ , where a finite momentum is transferred to the proton. GPD's depend on two longitudinal momentum fractions ( $x$  and  $x + \xi$ , where  $\xi$  is the so-called skewness parameter) and on the invariant momentum transfer to the proton,  $t = \Delta^2$ . In the simpler case where  $\xi = 0$  the Fourier transform of the GPD w.r.t.  $t$  gives the parton distribution in position space,  $q(x, \mathbf{b})$ , where  $\mathbf{b}$  is the impact parameter giving the transverse distance of the struck quark from the center of mass of the proton.

When the proton is transversely polarized (for instance along the  $+Y$  axis) two GPD's describe the distribution of unpolarized quarks, namely  $H(x, 0, t)$  (related to the unpolarized PDF) and  $E(x, 0, t)$ , whose Fourier transform gives the distortion of the distribution.

By relating the integral of  $E_q(x, 0, 0)$  to the  $q$ -flavour contribution ( $\kappa_q$ ) to the proton anomalous magnetic moment one can get an estimate of such distortions. On this basis one can expect an opposite sign of the distortion for  $u$  and  $d$  quarks, with  $u$  quarks mostly displaced along  $-X$ . Notice that this left-right asymmetry in  $b$ -space is T-even, in contrast with the left-right asymmetry in momentum space.

Let us come to the second ingredient in this picture, by considering SSA's for the production of  $\pi^+, \pi^0$  in SIDIS. Due to charge factors and the fact that  $u \rightarrow \pi^+, \pi^0$  fragmentation is favoured, most of  $\pi^+, \pi^0$  mesons come from an initial  $u$  quark in the polarized proton. We now recall that any left-right asymmetry in the transverse momentum space at the quark level requires final state interactions (FSI). Intuitively one then expects that the FSI's are on average attractive, since it costs energy to build up the string of gauge fields that connects the struck quark with the spectators. More precisely, if the photon, moving along the  $-Z$  axis, collides with a nucleon polarized along the  $+Y$  axis, from the previous results we expect that a  $u$  quark tends to be displaced in the  $-X$  direction in impact parameter space. If the FSI's are attractive, this quark experiences a force along the  $+X$  direction. This translates into the preferred direction of  $\pi^+, \pi^0$  mesons along  $+X$ , in agreement with model calculations of the Sivers function as well its phenomenological extractions. In the Drell-Yan process the initial state interactions, expected to be repulsive, imply an opposite sign for the Sivers function.

### 3.1.3 Models and constraints for TMD distributions

The Sivers function, being a naively T-odd entity, requires the interference between two complex amplitudes with different phases. Spectator models at tree level cannot provide these nontrivial phases. However they can arise as soon as a gluon is exchanged between the struck quark and the target spectator [138]. In other words the presence of the gauge link, which insures the colour gauge invariance of parton distributions, at the same time could provide the nontrivial, relevant, phases.

Starting from the work of Brodsky, Hwang and Schmidt (BHS) [138], different models for the Sivers function as well as for the Boer-Mulders function have been developed. In Ref. [166] the authors extended the BHS calculation, based on a scalar spectator diquark model of the nucleon with a point-like form factor, to DY processes. They also computed the Boer-Mulders function for  $u$  quarks, finding  $h_1^{\perp u} = f_{1T}^{\perp u}$ . The same relation was found in Refs. [167, 168], still with a scalar spectator but adopting a Gaussian form factor. In both cases a negative  $f_{1T}^{\perp}$  for  $u$  quarks came out. The MIT bag model was adopted by Yuan in Ref. [169], where he still found a negative Sivers function for  $u$  quarks and  $f_{1T}^{\perp d} = -(1/4) f_{1T}^{\perp u}$  (model [A] in Fig. 1, left panel). Moreover he obtained  $h_1^{\perp u} = (3/2) f_{1T}^{\perp u}$  and  $h_1^{\perp d} = -3 f_{1T}^{\perp d} = (3/4) f_{1T}^{\perp u}$ . In Ref. [170] the Sivers function has been calculated in a spectator model with scalar and axial-vector diquarks (model [B] in Fig. 1, left panel), with yet a different choice for the form factor w.r.t. Ref. [168]. The  $d$  quark Sivers function turns out to have the opposite sign compared to the  $u$  quark one and to be much smaller in size; again  $h_1^{\perp} \simeq f_{1T}^{\perp}$ .

Analogous results have been obtained in Ref. [171] both with scalar and vector diquarks in a light-

cone  $SU(6)$  quark-diquark model. The instanton liquid model for QCD vacuum with MIT bag model wave functions for quarks was adopted in Ref. [172] (model [C] in Fig. 1, left panel). In this model, the two independent perturbative and instanton terms sum up to give the total contribution to the Sivvers function. For  $d$  quarks the two terms almost cancel each other, leading to a small, negative Sivvers function. On the contrary, in the case of the  $u$ -quark Sivvers function, the instanton contribution and the perturbative one add together in fair agreement with the other models.

From these models the emerging common result is the sign of the Sivvers function for  $u$  quarks. It is worth to stress that while this is in agreement with the phenomenological extractions, a clear discrepancy is found concerning the overall size. In this respect, the study in Ref. [173], based on the QCD counting rules, could help in putting useful constraints on the Sivvers function, which should be one power of  $(1-x)$  suppressed relative to the unpolarized PDF. Concerning the Boer-Mulders function new results

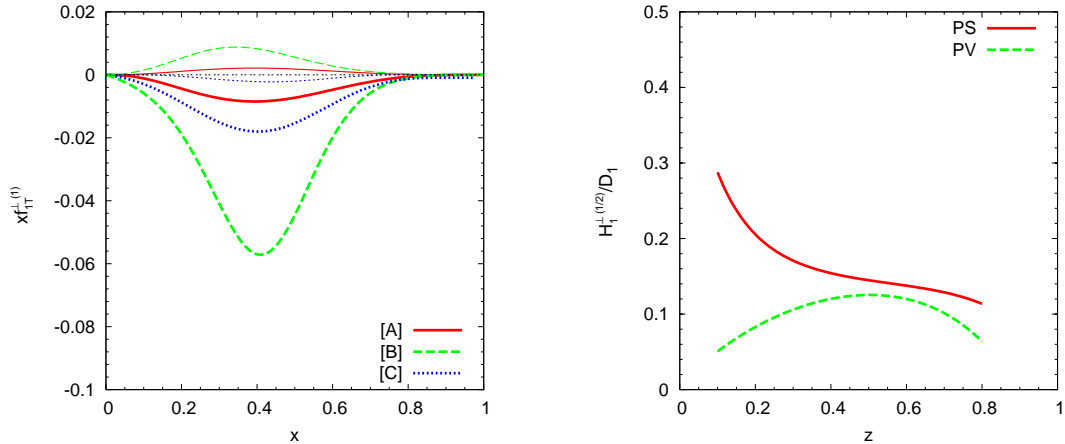


Figure 1: Left panel: Comparison of models calculations of  $x f_{1T}^{\perp(1)}$  for up (thick lines) and down (thin lines) quark Sivvers function according to Refs. [169] [A], [170] [B], and [172] [C]. Right panel: Model calculations of  $H_1^{\perp(1/2)}/D_1$  for the favoured Collins function normalized to the unpolarized FF [174]. Results for pseudoscalar (solid line) and pseudovector (dashed line) pion-quark coupling with gluon loops are shown.

have appeared [175, 176]. With the exception of a previous calculation [170], all models, including the new findings in the diquark spectator model [175] predict a negative Boer-Mulders function for both  $u$  and  $d$  quarks. The same conclusion has been reached in Ref. [176] through the calculation of the chirally odd GPD  $\bar{E}_T$  (which has opposite sign w.r.t.  $h_1^{\perp}$  [33]) in different models both for nucleon and pion targets.

Let us now consider the Collins function. Four model calculations for the fragmentation of a transversely quark into a pion have been presented so far in the literature [177, 178, 179, 180] (besides the former attempts by Collins [20] and Artru [128], discussed above). All of them produce the necessary imaginary parts by adopting a simple model for the fragmentation process at tree level and inserting one-loop corrections. Two possibilities for the tree-level amplitudes and two possible kinds of one-loop corrections have been investigated, for a total of four different models: pseudoscalar pion-quark coupling with pion loops [177] and with gluon loops [179, 174]; pseudovector pion-quark coupling with pion loops [178] and with gluon loops [180]. For gluon loop cases see Fig. 1 (right panel). We refer the reader to Ref. [174] for further details.

In the above-mentioned approaches disfavoured fragmentation functions (e.g.  $d \rightarrow \pi^+$ ) vanish, something apparently not supported by data, see section 5. In principle, these functions could be calculated in these models by considering diagrams with the emission of two pions, one of which goes unobserved.

The different results obtained for the Collins function do not allow to draw any conclusion even about its sign. The fact that more than one diagram with a different structure contributes to the Collins function makes it also difficult, if not impossible, to interpret the resulting effect, as we do for the Sivers function, in terms of simple attractive/repulsive interactions.

Some useful constraints on TMD distribution and fragmentation functions in terms of bounds and sum rules are available. In Ref. [181] by considering the combined Dirac  $\otimes$  target spin space and requiring the positivity of the spin-matrix eigenvalues, they found, beside the well-known Soffer bound [182] ( $2|h_1| \leq (f_1 + g_{1L})$ ), new bounds on the eight TMD distributions entering the correlator in Eq. (15).

The first sum rule for a T-odd TMD function was discussed in Ref. [183]: the authors considered the Collins function and, by imposing conservation of the intrinsic transverse momentum in parton fragmentation, obtained

$$\sum_h \int dz z H_1^{\perp(1)q}(z) = \sum_h \int dz \int d^2\mathbf{k}_\perp \frac{|\mathbf{k}_\perp|}{M_h} \Delta^N D_{h/q^\uparrow}(z, |\mathbf{k}_\perp|) = 0, \quad (22)$$

where  $H_1^{\perp(1)q}(z)$  is defined analogously as in Eq. (17) and the sum is over all hadrons.

More recently a somewhat corresponding sum rule for the Sivers function has been derived by Burkardt [184]. This rule states that the net transverse momentum due to the Sivers mechanism must vanish; more formally

$$\langle \mathbf{k}_\perp \rangle = \sum_{a=q,\bar{q},g} \langle \mathbf{k}_\perp \rangle_a = \int dx \int d^2\mathbf{k}_\perp \mathbf{k}_\perp \sum_{a=q,\bar{q},g} \Delta \hat{f}_{a/p^\uparrow}(x, \mathbf{k}_\perp) = 0. \quad (23)$$

Even if intuitively expected, the nontrivial fact is its validity in presence of final state interactions, which might spoil the simple partonic interpretation. The Burkardt sum rule (BSR) has been also checked explicitly in the diquark model calculations of the Sivers function [185]. Its role in SSA phenomenology will be discussed in Section 5.

### 3.2 Twist-three effects in collinear pQCD

The origin of this approach could be traced back to the early paper by Kane et al. [46], where it was shown how in a collinear QCD parton model any single spin asymmetry should be proportional to the quark mass. Although this result cannot explain the large values of  $A_N$  observed, it was read as a signal of a higher twist effect. Another step towards this interpretation was developed by Efremov and Teryaev [186, 187, 188] who pointed out that a nonvanishing SSA can be obtained in pQCD beyond the leading power expansion. However, the first consistent calculation in collinear pQCD of a sizable SSA in the forward region (large  $x_F$ ) was given by Qiu and Sterman in their paper on hadronic direct photon production [189, 190] and their subsequent application to pion production [191]. The asymmetries are evaluated in the framework of pQCD generalized factorization theorems with the introduction of new twist-three quark-gluon correlator functions convoluted with ordinary twist-two parton distribution functions and a short-distance hard scattering part. The new functions, being expectation values between the hadronic states of three field operators, do not have a simple partonic interpretation. More precisely, for the numerator of  $A_N$  in the process  $A^\uparrow B \rightarrow C + X$  ( $C$  unpolarized) they obtain, neglecting higher power corrections (we keep here the original notation of Ref. [191]),

$$\begin{aligned} d\Delta\sigma_{A^\uparrow B \rightarrow C+X} &= \sum_{abc} \phi_{a/A^\uparrow}^{(3)}(x_1, x_2) \otimes \phi_{b/B}(x') \otimes H_{a+b \rightarrow c} \otimes D_{c \rightarrow C}(z) \\ &+ \sum_{abc} \delta q_{a/A}^{(2)}(x) \otimes \phi_{b/B}^{(3)}(x'_1, x'_2) \otimes H''_{a+b \rightarrow c} \otimes D_{c \rightarrow C}(z) \\ &+ \sum_{abc} \delta q_{a/A}^{(2)}(x) \otimes \phi_{b/B}(x') \otimes H'_{a+b \rightarrow c} \otimes D_{c \rightarrow C}^{(3)}(z_1, z_2), \end{aligned} \quad (24)$$



where  $a, b, c$  represent parton flavours ( $q, \bar{q}, g$ ), and  $\phi_{b/B}(x')$  and  $D_{c \rightarrow C}(z)$  are ordinary twist-two parton distribution and fragmentation functions, respectively;  $\delta q_{a/A}^{(2)}(x)$  is the twist-two transversity distribution function. The new pieces, namely twist-three functions (see apexes), depend on two light-cone variables and can give three different contributions, from the initial polarized hadron, the initial unpolarized hadron, the final unpolarized hadron. As in ordinary pQCD factorization, only the hard scattering functions  $H$  are calculable and their forms depend on the definition of the twist-three distributions.

In order to present this formalism we consider in some detail the first term (first line) in Eq. (24).

Keeping in mind that the asymmetries are larger in the forward region, one can restrict to the valence flavour approximation for  $a$  in  $\sum_{abc}$ , and then consider only a valence twist-three distribution. Another important simplification comes from the fact that the  $H_{a+b \rightarrow c}$  part involves two contributions: one proportional to  $\delta(x_1 - x_2)$  and another one proportional to  $\delta(x_i)$ . The first case sets the gluon momentum in the correlator to zero; in the second case, one of the quarks carries a vanishing momentum. These are referred to as *soft gluon* and *soft fermion* poles respectively. Moreover, while soft gluon poles enter with derivatives of the twist-three distribution, soft fermion ones do not. If, as for ordinary twist-two functions, the derivatives of twist-three functions are enhanced near the edges of phase space, then soft gluon poles could give the leading contribution to the large asymmetries for  $x_F \rightarrow 1$ .

To get the master formula in this approach one has to start with the factorized expression in a diagrammatic representation of the process

$$d\Delta\sigma \approx \sum_a \int \frac{d^4 k_1}{(2\pi)^4} \frac{d^4 k_2}{(2\pi)^4} T_a(k_1, k_2) S_a(k_1, k_2), \quad (25)$$

where  $k_{1,2}$  are valence quark momenta,  $T_a$  is proportional to the non perturbative matrix element of the quark-quark-gluon operator between polarized initial hadron states (a twist-three matrix element) and  $S_a$  refers to the rest of the process. Expanding  $S_a$  in the collinear approximation enables to reduce the four-dimensional integrals to convolutions in the momentum fractions of partons with  $k_i \simeq x_i P$ . Notice that in this approach a nonzero spin dependence is found only from pole terms in the hard scattering. Without them the symmetries of the strong interactions would forbid any SSA. Keeping the first nonvanishing term in  $d\Delta\sigma$ , that is the leading pole structure of  $S_a$ , one gets

$$d\Delta\sigma \approx \sum_a \int dx_1 dx_2 i\epsilon^{\rho s_T n \bar{n}} \frac{\partial S_a}{\partial k_2^\rho}(x_1, x_2) T_{a,F}(x_1, x_2), \quad (26)$$

where  $n, \bar{n}$  are light-like unit vectors and

$$T_{a,F}(x_1, x_2) = \int \frac{dy_1^- dy_2^-}{4\pi} e^{ix_1 P^+ y_1^- + i(x_2 - x_1) P^+ y_2^-} \langle P, \mathbf{s}_T | \bar{\psi}_a(0) \gamma^+ [\epsilon^{s_T \sigma n \bar{n}} F_\sigma^+(y_2^-)] \psi_a(y_1^-) | P, \mathbf{s}_T \rangle, \quad (27)$$

with  $F_\sigma^+$  the gluon field strength. Since  $T_{a,F}$  is real only the poles of  $S_a$  can contribute.

The last step is to factorize the remaining function  $S_a$  into a perturbatively calculable partonic term,  $H_{a+b \rightarrow c}$ , a corresponding target parton distribution,  $\phi_{b/B}$ , and a fragmentation function,  $D_{c \rightarrow C}$ :

$$S_a(k_1, k_2) \approx \sum_{bc} \int \frac{dx'}{x'} \phi_{b/B}(x') \int dz H_{a+b \rightarrow c}(k_1, k_2, x', p_c) D_{c \rightarrow C}(z), \quad (28)$$

where  $\sum_{bc}$  runs over all parton flavours.

Finally, the full factorized expression for  $d\Delta\sigma$  reads

$$d\Delta\sigma = \frac{1}{2s} \sum_{abc} \int dz D_{c \rightarrow C}(z) \int \frac{dx'}{x'} \phi_{b/B}(x') \int dx_1 dx_2 T_{a,F}(x_1, x_2) \left[ i\epsilon^{\rho s_T n \bar{n}} \frac{\partial}{\partial k_2^\rho} H_{a+b \rightarrow c}(x_1, x_2, x', z) \right]_{k_2^0=0}, \quad (29)$$

where the integration over either  $x_1$  or  $x_2$  can be done by using the poles in  $H_{a+b \rightarrow c}$ .

Notice that this results in a factorization formula with only a single momentum fraction for each hadron, similar to that for the spin-averaged cross section with  $\phi_{a/A}(x)$  replaced by  $T_{a,F}(x, x)$ .

A way to understand why  $T_{a,F}$  is expected to be the dominant contribution is the following. From the sources of the  $k_i$  ( $i = 1, 2$ ) dependence in  $H_{a+b \rightarrow c}(k_1, k_2, x', p_c)$  (on-shellness of the unobserved final parton  $d$ , on- and off-shellness of the propagators and the explicit dependence in the numerator) we get two kinds of terms: one proportional to  $(\partial/\partial x)T_{a,F}(x, x)$  and one proportional to  $T_{a,F}(x, x)$ .

One has to remember that this approach was intended to address the description of the asymmetries in the forward region, where  $x_F$  is large. Here the dominant contribution comes from large net momentum fraction  $x$  for the polarized beam hadron, coupled with relatively small momentum fraction  $x'$  from the partons of the unpolarized target hadron. Since all distributions vanish for large  $x$  as  $(1-x)^\beta$ , with  $\beta > 0$ ,  $(\partial/\partial x)T_{a,F}(x, x) \gg T_{a,F}(x, x)$  when  $x \rightarrow 1$ . Therefore, in the forward region, terms proportional to derivatives of the distributions  $T_{a,F}$  dominate. Moreover it is only the matrix element  $T_{a,F}$  that inherits derivative terms, as a result of the collinear expansion involving soft gluon poles. Soft fermion poles have no such derivatives at LO and also do not correspond to the valence quark approximation. In this spirit only the derivative term was kept and the corresponding hard part was calculated.

A recent development of this approach has been discussed in Ref. [192]. Still neglecting the soft fermion poles, the complete soft-gluon pole structure, including the non derivative term, has been computed. The main result of this work is that one can incorporate the two terms in a simple way since they have a common hard scattering part. This comes from a remarkable property of the hard scattering functions recently proven by Koike and Tanaka [193]. On the other hand the phenomenological role of this extra piece in the forward region is found to be negligible, as assumed in former papers.

Without giving further details of the calculation (see [191, 192]), we only mention that by properly exploiting the pole structure of  $H_{a+b \rightarrow c}(k_1, k_2)$  (initial and final-state poles), one gets for the numerator of the SSA, restoring all factors,

$$E_C \frac{d^3 \Delta \sigma}{d^3 \mathbf{p}_C} = \frac{\alpha_s^2}{s} \sum_{a,b,c} \int_{z_{\min}}^1 \frac{dz}{z^2} D_{c \rightarrow C}(z) \int_{x'_{\min}}^1 \frac{dx'}{x'} \frac{1}{x' s + t/z} \phi_{b/B}(x') \quad (30)$$

$$\times \sqrt{4\pi\alpha_s} \left( \frac{e^{PCSTn\bar{n}}}{z\hat{u}} \right) \frac{1}{x} \left[ T_{a,F}(x, x) - x \left( \frac{d}{dx} T_{a,F}(x, x) \right) \right] H_{a+b \rightarrow c}(\hat{s}, \hat{t}, \hat{u}) ,$$

where  $s, t, u$  ( $\hat{s}, \hat{t}, \hat{u}$ ) are the standard hadronic (partonic) Mandelstam variables, and  $x, x'_{\min}, z_{\min}$  are fixed by the usual elastic scattering condition.

The  $H_{a+b \rightarrow c}$  are the final hard-scattering functions and read

$$H_{a+b \rightarrow c} = H_{a+b \rightarrow c}^I(\hat{s}, \hat{t}, \hat{u}) + H_{a+b \rightarrow c}^F(\hat{s}, \hat{t}, \hat{u}) \left( 1 + \frac{\hat{u}}{\hat{t}} \right) , \quad (31)$$

where  $H_{a+b \rightarrow c}^I$  ( $H_{a+b \rightarrow c}^F$ ) denotes the contributions due to initial (final) -state interactions. An important feature is that they are given in terms of the same Feynman diagrams needed to calculate the usual unpolarized partonic cross sections for the  $ab \rightarrow cd$  process but with different colour factors due to the extra initial (final) state interactions, see Appendix of Ref. [192]. Two aspects of the final result in Eq. (30) deserve a word: the denominator  $\hat{u}$  gives explicitly the power suppression of the SSA and the extra factor  $\sqrt{\alpha_s}$  w.r.t. the unpolarized cross section comes from the additional interaction with a gluon field.

It is also worth to mention that both in the original and the more recent works the contributions involving the three-gluon twist-three correlation function, which would enter the  $gg$  partonic process and could probably be relevant in the mid-rapidity region, have been ignored.

In order to perform a phenomenological study one has to rely on some parameterizations of the  $T_{a,F}$  twist-three functions. Since the operator defining it contains the same quark field operators as the

ordinary twist-two parton distribution functions, the most natural ansatz is:

$$T_{a,F}(x, x) = N_a(x)\phi_a(x). \quad (32)$$

In Refs. [189, 190, 191] a simple functional form with  $N_a(x) = \kappa_a\lambda$  was adopted, where  $\lambda$  has the dimension of a mass and  $\kappa_{u,d} = \pm 1$  (for a proton). In the recent developments of this formalism [192], with more data having become available, a more general form has been adopted, i.e.  $N_a(x) = N_a x^{\alpha_a} (1-x)^{\beta_a}$ . In both cases the main features of the data for  $A_N$  in pion production in  $pp$  as well as in  $\bar{p}p$  collisions can be described rather well. Notice, however, that all these papers use leading order, leading twist expressions for the unpolarized cross section in the denominator of  $A_N$ .

This approach, applied to SSA's in prompt photon production, by adopting the same twist-three functions as extracted from the analysis of pion data (positive for  $up$  and negative for *down* quarks) gives a sizable negative asymmetry. This result, as we will discuss in section 5, could be of extreme relevance in discriminating between the GPM approach, based on TMD distribution and fragmentation functions, and the twist-three formalism.

A complementary study has been also devoted to the role of the other two sources of SSA's in  $pp \rightarrow \pi + X$  in the twist-three approximation, namely the chiral-odd contributions in Eq. (24) (second and third lines). The twist-three distribution,  $\phi_{b/B}^{(3)}(x'_1, x'_2)$  and its relative hard scattering parts have been discussed in Refs. [194, 195]. This contribution, expected to be relevant in the negative  $x_F$  region, comes out to be negligible over all ranges in  $x_F$  due to the smallness of the hard scattering partonic asymmetry. In Ref. [196] a detailed analysis of the chiral-odd twist-three fragmentation function was performed, showing how, with some difficulties, a description of E704 data can be obtained.

Remaining in the context of inclusive particle production in hadron-hadron collisions, this approach has been also applied to the study of the transverse  $\Lambda$  polarization in unpolarized  $pp$  collisions. In this case two twist-three effects could contribute: the twist-three chiral-odd distribution  $\phi_{a/p}^{(3)}(x_1, x_2)$ , coupled with a twist-two unpolarized PDF and a twist-two chiral-odd fragmentation function (analogous to the twist-two transversity PDF); a twist-three chiral-even FF, that, following the same notation adopted in Eq. (24), would read  $D_{c \rightarrow \Lambda^\uparrow}^{(3)}(z_1, z_2)$ , coupled with two twist-two unpolarized PDF's. The first contribution has been studied in Ref. [197], where by adopting a simple ansatz on  $\phi_{a/p}^{(3)}(x_1, x_2)$ , namely a proportionality relation with the chiral-odd transversity distribution, the main features of the data are reproduced, although some discrepancies still remain.

The twist-three formalism has been also applied to SIDIS azimuthal asymmetries [198, 199] at large  $p_T \simeq Q$  (with  $Q$  the virtuality of the exchanged photon). In these papers the authors show that among the two possible mechanisms, the first coming from the twist-three chiral-even distribution and the second from the twist-three chiral-odd fragmentation (coupled with the transversity PDF), the last one is negligible. In particular they calculated the soft-gluon pole contributions for both cases. They also improved their calculation for the first and most relevant case, identifying all pole contributions (soft-fermion and hard-gluon poles included) and providing a systematic collinear expansion for this approach in SIDIS.

Before concluding this section we mention some attempts to connect the TMD approach to the twist-three formalism. A first study has been presented in Ref. [200], showing that the inclusion of transverse gauge links, which lead to  $T$ -odd effects, is connected to the Qiu-Sterman mechanism. More precisely, it was shown that the first  $k_\perp$  moment of the Sivers function is equal to the twist-three chiral-even distribution,  $T_{a,F}$ . This connection has been also addressed in Ref. [201].

Recently a unified picture in terms of the twist-three approach and the TMD formalism [202, 203, 204, 205] both in SIDIS and Drell-Yan processes has been presented. The main result is that although the two mechanisms have their own domain of validity, they describe the same physics in the kinematic region where they overlap. More precisely, focusing on SIDIS for the sake of clarity, when the transverse momentum of the observed hadron,  $p_T$ , and the photon virtuality,  $Q$ , are much larger than  $\Lambda_{\text{QCD}}$ , the

spin-dependent cross section can be calculated in terms of a twist-three quark-gluon correlation. On the other hand, when  $p_T \simeq \Lambda_{\text{QCD}} \ll Q$ , single spin asymmetries can be generated from a spin-dependent TMD quark distribution. There is, however, a common kinematic region,  $\Lambda_{\text{QCD}} \ll p_T \ll Q$ , where both mechanisms should work. In this region  $p_T$  is large, so that the asymmetry is a twist-three effect, but at the same time  $p_T \ll Q$ , so that the TMD factorization formalism also applies. The same arguments work for the Drell-Yan process by simply replacing the  $p_T$  of the observed hadron with the transverse momentum of the lepton pair. The resulting connection unifies the physical pictures for the underlying dynamics of transverse SSA's and imposes important constraints on phenomenological studies.

We finally stress that both in the TMD and in the twist-three approach, on-shell massless partons are considered in the soft as well as in the hard parts. The role of off-shellness, still largely unknown, has been recently emphasized and investigated in Refs. [206, 207, 208] (see also references therein).

### 3.3 A semiclassical model

Among the nonperturbative models proposed to describe the SSA's observed in inclusive hadron production in hadron-hadron collisions we mention a picture based on a semiclassical geometrical approach: the *orbiting valence quark model* [9, 209, 210, 211, 212, 213, 214]. The main ideas behind this approach can be summarized as follows: *i*) The constituents of a polarized hadron are assumed to perform an orbital motion about the polarization axis. Their relativistic ground state wave functions allow to calculate the polarization of valence quarks in a polarized proton. The results show that there is a flavour dependent asymmetry in the valence-quark polarization. The sea quarks come out unpolarized. *ii*) In the fragmentation region the main contribution to hadron production comes from quark-antiquark annihilation via a direct-formation mechanism. *iii*) Since hadrons are extended objects, a surface effect is expected in such production processes.

Let us consider a proton-proton collision along the  $Z$  axis in the rest frame of the polarized proton. In the transversely upward ( $+X$ ) polarized hadron,  $u$  quarks, being on average polarized along the hadron polarization, have an orbital motion such that they go preferably left ( $-Y$ ) at the front surface and right ( $+Y$ ) at the back surface of the hadron. When the polarized target interacts with the unpolarized projectile this preferred direction is preserved at the front surface (when the projectile and the target start overlapping) while it is partially spoiled at the back surface (when they start separating again) because of the colour interactions acting during the transition of the projectile through the target. The net result is that in the fusion mechanism of a  $u$  quark from the polarized proton and a suitable antiquark from the unpolarized proton, the formed meson goes preferably left, i.e. along  $-Y$ . More generally this means that, when a polarized proton collides, only colour singlet  $q\bar{q}$  pairs formed at the front surface can get an extra momentum due to the orbiting motion of valence quarks. This determines the observed asymmetry in the distribution of the produced mesons.

In this model one then expects that for  $p^\uparrow p \rightarrow \pi + X$  in the fragmentation region of the polarized proton, where mainly valence quarks contribute,  $\pi^+$  and  $\pi^0$  mesons go left, whereas  $\pi^-$ 's go right. For the case of a polarized antiproton  $\pi^+$ 's and  $\pi^-$ 's reverse their direction, whereas  $\pi^0$ 's keep going left. The left-right asymmetry is more significant at large  $x_F$ . According to this mechanism, also Drell-Yan lepton pairs should exhibit a left-right asymmetry.

One of the main features of this model is that in order to have a nonzero SSA the produced hadron must have at least a common valence quark with the polarized hadron. In particular, for kaon production in  $p^\uparrow p$  collisions one expects that for  $K^+(u\bar{s})$   $A_N$  is similar (in size and sign) to  $A_N(\pi^+)$ , whereas for  $K^-(\bar{u}s)$  it should vanish.

This model has been also applied to the description of the transverse polarization of hyperons  $[P_T(Y)]$  produced in unpolarized hadron-hadron collisions [215, 216].

For a detailed and comprehensive description of this approach and its phenomenological applications see Ref. [9] and references therein.

## 4 Spin asymmetries in the generalized parton model

In this section we will present and discuss in detail the generalized, spin and  $\mathbf{k}_\perp$  dependent, parton model approach to polarization effects in high-energy hadronic collisions. As discussed in section 3, there are several approaches available in the literature. In what follows we will adopt the one developed in a series of papers, starting from the middle of 90s. This approach is an extension of early attempts to deal with parton intrinsic motion and unintegrated, transverse momentum dependent (TMD) parton distribution (PDF) and fragmentation functions (FF). It consistently includes spin and polarization effects, requiring the introduction of a new class of leading twist TMD distributions. Like any theoretical approach, the formalism we will use has both advantages and drawbacks. The main advantages are the following: a) It is a QCD-improved, generalized parton model approach, with direct inclusion, in the spirit of the parton model itself, of spin and transverse momentum ( $\mathbf{k}_\perp$ ) effects; b) It retains the simple partonic interpretation of all soft, leading-twist TMD distributions; c) Using the helicity formalism, it very clearly shows the connection among the polarization states of the particles involved and the role of spin effects in the soft and hard processes; d) It fully includes kinematical  $\mathbf{k}_\perp$  effects, without approximations. It has of course also some drawbacks: a) For some of the processes considered, factorization has not been proven explicitly yet. It is rather taken as a reasonable assumption for this generalized scheme; b) It only accounts for leading-twist soft distributions (in this sense its application to subleading-twist SSA's can be considered as an effective approach); c) It does not properly account for initial and final state interactions, which have been shown to be crucial for the nonvanishing of naively time-odd PDF's and FF's. Despite these problems, its phenomenological success is presently remarkable. In our opinion it is also the most convenient approach for a simple illustration of the pQCD-based formalisms and of their main phenomenological applications. In section 5 we will discuss and compare the results and predictions of this approach with available experimental results and with those of other theoretical approaches. In particular, we will emphasize measurements which could help in disentangling among different formalisms and are at reach of present experiments.

### 4.1 Polarized cross sections and helicity formalism

Let us consider, to be definite, the doubly polarized hadronic process  $A(S_A) + B(S_B) \rightarrow C + X$  at high energy and moderately large transverse momentum,  $p_T$ . Here  $p_T$  is the transverse momentum of the observed hadron with respect to the direction of the colliding beams.  $A, B, C$  are generic hadrons, respectively with spin state  $S_A, S_B, S_C$  ( $S_h = 0, 1/2, 1$ ). Using the helicity formalism the invariant differential cross section for the production of an unpolarized particle in the polarized processes under consideration can be expressed through the following *master formula*:

$$\frac{E_C d\sigma^{(A,S_A)+(B,S_B)\rightarrow C+X}}{d^3\mathbf{p}_C} = \sum_{a,b,c,d,\{\lambda\}} \int \frac{dx_a dx_b dz}{16\pi^2 x_a x_b z^2 s} d^2\mathbf{k}_{\perp a} d^2\mathbf{k}_{\perp b} d^3\mathbf{k}_{\perp C} \delta(\mathbf{k}_{\perp C} \cdot \hat{\mathbf{p}}_c) J(\mathbf{k}_{\perp C}) \quad (33)$$

$$\times \rho_{\lambda_a, \lambda'_a}^{a/A, S_A} \hat{f}_{a/A, S_A}(x_a, \mathbf{k}_{\perp a}) \rho_{\lambda_b, \lambda'_b}^{b/B, S_B} \hat{f}_{b/B, S_B}(x_b, \mathbf{k}_{\perp b}) \hat{M}_{\lambda_c, \lambda_d; \lambda_a, \lambda_b} \hat{M}_{\lambda'_c, \lambda'_d; \lambda'_a, \lambda'_b}^* \delta(\hat{s} + \hat{t} + \hat{u}) \hat{D}_{\lambda_c, \lambda'_c}^{\lambda_C, \lambda'_C}(z, \mathbf{k}_{\perp C}).$$

Notice that with generic  $\lambda_C, \lambda'_C$  helicities (i.e. replacing  $\sum_{\lambda_C} D_{\lambda_c, \lambda'_c}^{\lambda_C, \lambda'_C}$  with  $D_{\lambda_c, \lambda'_c}^{\lambda_C, \lambda'_C}$ ) on the r.h.s. of the above equation, we get the (unnormalized) helicity density matrix for the final particle  $C$  that allows to evaluate its polarization state. This is particularly relevant for the case of transverse hyperon polarization in unpolarized hadronic collisions. However, since here we want to focus on the basic ideas of the approach, for simplicity we will consider the production of unpolarized particles in the collisions of spin 1/2 hadrons. A detailed treatment of spin 1/2 particle production using the helicity formalism in a generalized parton model is under completion [217]. We will shortly discuss the formalism for the spin 1/2 case in section 4.3.2, and the phenomenology for transverse  $\Lambda$  polarization in section 5.1.3.



Eq. (33) gives the cross section for the polarized hadronic process under consideration as a factorized convolution of all possible hard elementary QCD processes,  $ab \rightarrow cd$ , with soft, spin and  $\mathbf{k}_\perp$  dependent PDF's and FF's. Let us briefly comment on the notation and physical content of this equation. Further details can be found in the original papers [135, 218, 219] and in references therein.

- (i)  $A$  and  $B$  are initial, spin 1/2 hadrons in pure spin states denoted by  $S_A$  and  $S_B$  and corresponding polarization (pseudo)vectors  $\mathbf{P}^A$  and  $\mathbf{P}^B$ , respectively;
- (ii) Unless differently stated, we always consider the c.m. frame of the initial colliding hadrons, the  $AB$  c.m. frame or hadronic c.m. frame; in this frame, hadron  $A$ ,  $B$ , move respectively along the  $\pm Z_{\text{cm}}$ -axis direction and the final hadron  $C$  is produced in the  $(XZ)_{\text{cm}}$  plane, with  $(p_C)_{X_{\text{cm}}} > 0$ ;
- (iii) The notation  $\{\lambda\}$  indicates a sum over all helicity indices;  $x_a$ ,  $x_b$  and  $z$  are the usual light-cone momentum fractions of partons  $a, b$  inside the initial hadrons  $A, B$  and of hadron  $C$  produced in the fragmentation of parton  $c$ ;  $\mathbf{k}_{\perp a}$  ( $\mathbf{k}_{\perp b}$ ) are the (two-dimensional) transverse momenta of parton  $a$  ( $b$ ) with respect to hadron  $A$  ( $B$ );  $\mathbf{k}_{\perp C}$  is the generic three-momentum of hadron  $C$  in the hadronic c.m. frame; notice that the delta function  $\delta(\mathbf{k}_{\perp C} \cdot \hat{\mathbf{p}}_c)$  constrains  $\mathbf{k}_{\perp C}$  to be effectively two-dimensional and always orthogonal to parton  $c$  three-momentum,  $\mathbf{p}_c$ ;
- (iv) The factor  $(16\pi^2 x_a x_b s)^{-1}$ , where  $s = (p_A + p_B)^2$  is the total energy of the colliding beams, collects phase space factors related to the elementary cross sections and the corresponding flux factor for the noncollinear (when viewed in the hadronic c.m. frame) parton scattering process;
- (v) The phase-space factor  $J(\mathbf{k}_{\perp C})/z^2$  is the invariant TMD Jacobian factor for massless particles connecting the parton momentum  $\mathbf{p}_c$  with the hadron momentum  $\mathbf{p}_C$ , (see e.g. Appendix A of Ref. [218]);
- (vi)  $\rho_{\lambda_a, \lambda_a}^{a/A, S_A}$  is the helicity density matrix of parton  $a$  inside hadron  $A$  with spin state  $S_A$ , and analogously for  $\rho_{\lambda_b, \lambda_b}^{b/B, S_B}$ ; notice that the helicity density matrix always describes the polarization state of the particle in its helicity rest frame; for a massless particle no rest frame exists and the helicity frame is defined as the standard frame, reached from the hadronic c.m. frame, in which the particle four-momentum is  $p^\mu = (p, 0, 0, p)$  [13];
- (vii)  $f_{a/A, S_A}(x_a, \mathbf{k}_{\perp a})$  is the spin and TMD distribution function of the unpolarized parton  $a$  inside the polarized hadron  $A$ , and similarly for parton  $b$  inside hadron  $B$ ; these leading-twist TMD distributions generalize the usual partonic distributions in the collinear configuration; notice that in this paper, for the sake of clarity, we adopt the following convention: for *all*  $\mathbf{k}_\perp$  dependent distribution and fragmentation functions and soft amplitudes we will use a “hat” to indicate full, vectorial dependence on  $\mathbf{k}_\perp$ , while we will not use it for dependence on  $k_\perp = |\mathbf{k}_\perp|$ , with factorized azimuthal dependence; notice also that this notation is partially at variance with those adopted in the papers where the original formulation of the GPM was developed, which by the way slightly differ from paper to paper;
- (viii) The  $\hat{M}_{\lambda_c, \lambda_d; \lambda_a, \lambda_b}$ 's are the helicity amplitudes for the elementary process  $ab \rightarrow cd$ , opportunely normalized according to the kinematical phase-space factors explicitly shown in Eq. (33);
- (ix)  $\hat{D}_{\lambda_c, \lambda_c}^{\lambda_C, \lambda_C}(z, \mathbf{k}_{\perp C})$  is the product of nonperturbative *fragmentation amplitudes* for the polarized fragmentation process  $c \rightarrow C + X$ .

We will now consider in more detail the quantities which describe how the polarization of the initial hadrons is transferred, through the soft and hard elementary processes, to the final partons and to the produced hadron (if its polarization state is observed).

## 4.2 Spin and TMD parton distribution functions at leading twist

The quantity  $\rho_{\lambda_a, \lambda_a}^{a/A, S_A} \hat{f}_{a/A, S_A}(x_a, \mathbf{k}_{\perp a})$  in Eq. (33) encodes complete information on the polarization state of parton  $a$  with spin  $s_a$ , as determined by the polarization state of the parent hadron  $A$  (which is fixed by the experimental conditions considered) and by the soft, nonperturbative processes related to the hadron structure (analogously for parton  $b$  inside hadron  $B$ ). Indeed, introducing soft, nonperturbative

helicity amplitudes for the inclusive process  $A \rightarrow a + X$ ,  $\hat{\mathcal{F}}_{\lambda_a, \lambda_{X_A}; \lambda_A}(x_a, \mathbf{k}_{\perp a})$ , we can write:

$$\rho_{\lambda_a, \lambda'_a}^{a/A, S_A} \hat{f}_{a/A, S_A}(x_a, \mathbf{k}_{\perp a}) = \sum_{\lambda_A, \lambda'_A} \rho_{\lambda_A, \lambda'_A}^{A, S_A} \not\int_{X_A, \lambda_{X_A}} \hat{\mathcal{F}}_{\lambda_a, \lambda_{X_A}; \lambda_A} \hat{\mathcal{F}}_{\lambda'_a, \lambda_{X_A}; \lambda'_A}^* \equiv \sum_{\lambda_A, \lambda'_A} \rho_{\lambda_A, \lambda'_A}^{A, S_A} \hat{F}_{\lambda_A, \lambda'_A}^{\lambda_a, \lambda'_a}, \quad (34)$$

where  $\not\int_{X_A, \lambda_{X_A}}$  stands for a spin sum and phase space integration over the undetected system of hadron  $A$  remnants,  $\rho_{\lambda_A, \lambda'_A}^{A, S_A}$  is in turn the helicity density matrix of hadron  $A$ ,

$$\rho_{\lambda_A, \lambda'_A}^{A, S_A} = \frac{1}{2} \begin{pmatrix} 1 + P_Z^A & P_X^A - iP_Y^A \\ P_X^A + iP_Y^A & 1 - P_Z^A \end{pmatrix}_{A, S_A} = \frac{1}{2} \begin{pmatrix} 1 + P_L^A & P_T^A e^{-i\phi_{S_A}} \\ P_T^A e^{i\phi_{S_A}} & 1 - P_L^A \end{pmatrix}_{A, S_A}, \quad (35)$$

$\mathbf{P}^A = (P_T^A \cos \phi_{S_A}, P_T^A \sin \phi_{S_A}, P_L^A)$  is its polarization vector and  $\phi_{S_A}$  the corresponding azimuthal angle, defined in the helicity reference frame of hadron  $A$ . We have also defined

$$\hat{F}_{\lambda_A, \lambda'_A}^{\lambda_a, \lambda'_a}(x_a, \mathbf{k}_{\perp a}) \equiv \not\int_{X_A, \lambda_{X_A}} \hat{\mathcal{F}}_{\lambda_a, \lambda_{X_A}; \lambda_A}(x_a, \mathbf{k}_{\perp a}) \hat{\mathcal{F}}_{\lambda'_a, \lambda_{X_A}; \lambda'_A}^*(x_a, \mathbf{k}_{\perp a}). \quad (36)$$

The product of nonperturbative helicity amplitudes  $\hat{F}_{\lambda_A, \lambda'_A}^{\lambda_a, \lambda'_a}$  has a simple physical interpretation and is directly related to the leading twist part of the well known hand-bag diagrams for the hadronic correlator in deeply inelastic scattering processes. The distribution amplitudes  $\hat{\mathcal{F}}_{\lambda_a, \lambda_{X_A}; \lambda_A}$  depend on the parton light-cone momentum fraction  $x_a$  and on its intrinsic transverse momentum  $\mathbf{k}_{\perp a}$ , with modulus  $k_{\perp a}$  and azimuthal angle  $\phi_a$  (all defined in the parent hadron helicity frame), in the following way:

$$\hat{\mathcal{F}}_{\lambda_a, \lambda_{X_A}; \lambda_A}(x_a, \mathbf{k}_{\perp a}) = \mathcal{F}_{\lambda_a, \lambda_{X_A}; \lambda_A}(x_a, k_{\perp a}) \exp[i\lambda_A \phi_a]. \quad (37)$$

Rotational and parity invariance imply that only eight functions as defined in Eq. (36) are independent. Notice that since some parity relations are different according to the parton type involved (quark or gluon), the two cases must be treated separately. For quarks, keeping in mind that upper (lower) helicity indices refer to the parton (hadron) respectively, one can easily associate the eight functions

$$F_{++}^{++}, \quad F_{++}^{--}, \quad F_{+-}^{+-}, \quad F_{+-}^{-+}, \quad F_{+-}^{++}, \quad F_{+-}^{--}, \quad F_{+-}^{+-}, \quad F_{+-}^{-+}, \quad (38)$$

to the eight independent, leading twist, polarized TMD quark distribution functions:

- 1) The combinations  $F_{++}^{++} \pm F_{++}^{--}$  are respectively related to the unpolarized and longitudinally polarized PDF's,  $f_{a/A}$  and  $\Delta_L f_{a/A}$  (denoted as  $f_1$  and  $g_{1L}$  in Ref. [108]);
- 2) The combinations  $F_{+-}^{+-} \pm F_{+-}^{-+}$  are in turn related to the two possible TMD contributions to the transversity PDF,  $\Delta_T \hat{f}_{a/A}$  (corresponding to  $h_{1T}$  and  $h_{1T}^\perp$  in Ref. [108]);
- 3) The combinations  $F_{+-}^{++} \pm F_{+-}^{--}$  are respectively related to the probability of finding an unpolarized (longitudinally polarized) quark inside a transversely polarized hadron, that is to the well-known Siverts function [18, 19]  $\Delta^N f_{a/A^\uparrow}$  (or  $f_{1T}^\perp$  [73]), and to the function  $\Delta \hat{f}_{a, s_z/A, S_T}$ , (related to  $g_{1T}$  of Ref. [108]);
- 4) Finally, the combinations  $F_{+-}^{+-} \pm F_{+-}^{-+}$  are related to the probability of finding a transversely polarized quark respectively inside an unpolarized hadron (that is, to the Boer-Mulders function [108],  $\Delta^N f_{a^\uparrow/A}$  or  $h_1^\perp$ ) or inside a longitudinally polarized hadron (that is, to the PDF  $\Delta \hat{f}_{a, s_T/A, S_L}$  or  $h_{1L}^\perp$  [108]).

One can also see that: the functions  $F_{++}^{\pm\pm}$ , are obviously purely real; the  $F_{+-}^{\pm\mp}$  are purely real (purely imaginary) for quarks (gluons); the last four functions in Eq. (38) are complex but not independent, and their sums and differences can be also expressed as the real and imaginary parts of  $F_{+-}^{++}$  and  $F_{+-}^{-+}$ .

Some additional comments are in order here to clarify the physical content of these functions and summarize their main features: among the eight functions, the only ones that survive in the collinear configuration (that is, under  $\mathbf{k}_{\perp}$  integration) are the three usual leading twist PDF's,  $f_{a/A}$ ,  $\Delta_L f_{a/A}$ ,

$\Delta_T f_{a/A}$ . Those which are off-diagonal in the parton helicity indices, like  $\Delta_T f_{a/A}$ , are chiral odd; therefore, they cannot be directly measured in DIS processes with on-shell, massless partons. In any physical observable, they must combine with some other helicity-odd term (e.g., in SIDIS, with a chiral-odd FF, like the Collins function, or with higher twist terms due to parton masses and off-shellness); those functions proportional to the imaginary part of the  $F$ 's are in turn naively T-odd, and require initial/final state interactions in order to be nonvanishing [138, 139] (see also section 3).

The most general expression for the helicity density matrix of quark  $a$  inside a hadron,  $A$ , with polarization state  $S_A$  is

$$\rho_{\lambda_a, \lambda'_a}^{a/A, S_A} = \begin{pmatrix} \rho_{++}^a & \rho_{+-}^a \\ \rho_{-+}^a & \rho_{--}^a \end{pmatrix}_{A, S_A} = \frac{1}{2} \begin{pmatrix} 1 + P_z^a & P_x^a - iP_y^a \\ P_x^a + iP_y^a & 1 - P_z^a \end{pmatrix}_{A, S_A} = \frac{1}{2} \begin{pmatrix} 1 + P_L^a & P_T^a e^{-i\phi_{s_a}} \\ P_T^a e^{i\phi_{s_a}} & 1 - P_L^a \end{pmatrix}_{A, S_A}, \quad (39)$$

where  $\mathbf{P}^a = (P_x^a, P_y^a, P_z^a) = (P_T^a \cos \phi_{s_a}, P_T^a \sin \phi_{s_a}, P_L^a)$  is the quark polarization vector and  $\phi_{s_a}$  its azimuthal angle, in the quark helicity frame (to which the  $x, y, z$  axes refer). In specific calculations, when performing the sum over the helicity indices  $\lambda_a, \lambda'_a$ , and  $\lambda_b, \lambda'_b$  in Eq. (33), one obtains terms of the form ( $j = x, y, z$ )

$$P_j^a \hat{f}_{a/A, S_A} = \hat{f}_{s_j/S_A}^a - \hat{f}_{-s_j/S_A}^a \equiv \Delta \hat{f}_{s_j/S_A}^a, \quad (40)$$

where, as often in the sequel, we do not show the functional dependence of the  $\hat{f}$ 's on  $x$  and  $\mathbf{k}_\perp$ . These terms refer to polarized quarks inside hadron  $A$ . Additionally, we can have also terms corresponding to unpolarized quarks inside polarized hadrons (the Sivers asymmetry)

$$\Delta \hat{f}_{a/S_A} = \hat{f}_{a/S_A} - \hat{f}_{a/-S_A}. \quad (41)$$

Parity and rotational invariance allows this function to be nonzero for transversely polarized hadrons only.

By employing Eq. (34), the relations among the functions in Eq. (38) and those defined in Eqs. (40), (41) can be more precisely cast in the following form:

$$\begin{aligned} f_{a/A} &= f_{a/A, S_L} = (F_{++}^{++} + F_{++}^{--}) \\ \hat{f}_{a/A, S_T} &= f_{a/A} + \frac{1}{2} \Delta \hat{f}_{a/S_T} = (F_{++}^{++} + F_{++}^{--}) + 2 \text{Im} F_{+-}^{++} \sin(\phi_{S_A} - \phi_a) \\ P_x^a f_{a/A, S_L} &= \Delta f_{s_x/S_L} = 2 \text{Re} F_{++}^{+-} \\ P_x^a \hat{f}_{a/A, S_T} &= \Delta \hat{f}_{s_x/S_T} = (F_{+-}^{+-} + F_{+-}^{-+}) \cos(\phi_{S_A} - \phi_a) \\ P_y^a f_{a/A, S_L} &= P_y^a f_{a/A} = \Delta f_{s_y/S_L} = \Delta f_{s_y/A} = -2 \text{Im} F_{++}^{+-} \\ P_y^a \hat{f}_{a/A, S_T} &= \Delta \hat{f}_{s_y/S_T} = \Delta f_{s_y/A} + \Delta^- \hat{f}_{s_y/S_T} = -2 \text{Im} F_{+-}^{+-} + (F_{+-}^{+-} - F_{+-}^{-+}) \sin(\phi_{S_A} - \phi_a) \\ P_z^a f_{a/A, S_L} &= \Delta f_{s_z/S_L} = (F_{++}^{++} - F_{++}^{--}) \\ P_z^a \hat{f}_{a/A, S_T} &= \Delta \hat{f}_{s_z/S_T} = 2 \text{Re} F_{+-}^{++} \cos(\phi_{S_A} - \phi_a), \end{aligned} \quad (42)$$

where  $\phi_{S_A}$  and  $\phi_a$  are the azimuthal angles of the hadron polarization vector and of the quark transverse momentum  $\mathbf{k}_{\perp a}$  respectively, in the hadronic c.m. frame. Notice that  $P_x^a f_{a/A} = \Delta f_{s_x/A} = 0$ , and that the function  $\Delta \hat{f}_{s_y/S_T}$  can be decomposed into two terms, one independent of the hadron transverse polarization,  $\Delta f_{s_y/A}$ , and a term that changes sign when the hadron polarization is reversed,  $\Delta^- \hat{f}_{s_y/S_T} = (1/2)[\Delta \hat{f}_{s_y/S_T} - \Delta \hat{f}_{s_y/-S_T}]$ . Analogous relations hold for quark  $b$  inside hadron  $B$ .

As already said, apart from the well-known PDF's surviving in the collinear configuration, two of the remaining functions are of particular phenomenological relevance for the study of azimuthal and single spin asymmetries: the Sivers function, which may be responsible for several transverse single spin asymmetries; the Boer-Mulders function  $\Delta f_{s_y/A}$  that, besides contributing with additional terms to the transverse SSA's, may be responsible for azimuthal asymmetries in unpolarized processes, e.g. in

Drell-Yan. Appendix C of Ref. [135] gives a detailed comparison of the above notation with the one of the Amsterdam group [108], often adopted in the literature (see also Eq. (16)).

For an on-shell massless particle with spin 1 the helicity density matrix is formally very similar to that of a spin 1/2 particle, considered above for the quark case. Therefore, most of the discussion and treatment presented there can be directly translated to the gluon case. There are two main differences: a) gluons cannot carry any transverse spin; there is however a formal analogy between *transversely* polarized quarks and *linearly* polarized gluons; b) the complete specification of the gluon polarization state requires the introduction of a polarization tensor  $T_{ij}$ . Below, we briefly summarize the results for the gluon sector, emphasizing where they differ in some respect from the quark case.

The helicity density matrix for an on-shell gluon inside hadron  $A$  in a spin state  $S_A$  can be cast as

$$\rho_{\lambda_g, \lambda'_g}^{g/A, S_A} = \frac{1}{2} \begin{pmatrix} 1 + P_z^g & \mathcal{T}_1^g - i\mathcal{T}_2^g \\ \mathcal{T}_1^g + i\mathcal{T}_2^g & 1 - P_z^g \end{pmatrix}_{A, S_A} = \frac{1}{2} \begin{pmatrix} 1 + P_{circ}^g & -P_{lin}^g e^{-2i\phi} \\ -P_{lin}^g e^{2i\phi} & 1 - P_{circ}^g \end{pmatrix}_{A, S_A}. \quad (43)$$

$P_{circ}^g$  corresponds to  $P_z^g$ , the gluon longitudinal polarization. The off-diagonal elements of Eq. (43) are related to the linear polarization of the gluons in the transverse ( $xy$ ) plane at an angle  $\phi$  and  $\phi + \pi/2$  w.r.t. the  $x$  axis. The  $x$ ,  $y$  and  $z$  axes refer to the standard gluon helicity frame, as reached from the hadronic c.m. frame, in which its momentum is  $p^\mu = (p, 0, 0, p)$ .  $P_{lin}^g$  can be expressed in terms of the parameters  $\mathcal{T}_1^g$  and  $\mathcal{T}_2^g$ , which are closely related to the Stokes parameters used in classical optics; they play a role formally analogous to that of the  $x$  and  $y$ -components of the quark polarization vector in the quark sector. The use of the parameters  $\mathcal{T}_1^g$  and  $\mathcal{T}_2^g$  makes the gluon distribution functions formally similar to those for the quarks and considerably simplifies the formulae for the spin asymmetries.

The nonperturbative helicity amplitudes  $\hat{\mathcal{F}}_{\lambda_a, \lambda_{X_A}; \lambda_A}(x_a, \mathbf{k}_{\perp a})$  and their products  $\hat{F}_{\lambda_A, \lambda'_A}^{\lambda_a, \lambda'_a}$  now refer to the process  $A \rightarrow g + X$  and their parity properties are then slightly different. The rest of the calculation goes along the same way, i.e. adopting the eight functions in Eq. (38), with the difference that the functions  $F_{+-}^{+-}$  and  $F_{+-}^{-+}$  are now purely imaginary quantities.

Without giving the detailed expressions of the gluon TMD distributions (see Ref. [135]) we only mention that the Sivers function exists also for gluons and in this approach maintains the same physical interpretation as for the quark case. There is also an analogue of the quark Boer-Mulders function, referred to in the sequel as the Boer-Mulders-like gluon function,  $\mathcal{T}_1^g f_{g/A} = \Delta f_{\mathcal{T}_1/A}^g$ . However, the physical interpretation of this function is more involved: it represents the difference between the probabilities of finding, inside an unpolarized hadron, a gluon with linear polarization in the plane containing the gluon and hadron three-momenta and in the direction orthogonal to this plane. Similarly, there exists an analogue of the quark transversity distribution, involving again linearly polarized gluons. A more detailed comparison with the corresponding notation of the Amsterdam group [220] can be found in Appendix C of Ref. [135] (see also Ref. [35]).

### 4.3 Spin and TMD fragmentation functions at leading twist

Leading twist fragmentation functions can be described within the same formalism presented for PDF's in the previous section. Let us define the nonperturbative helicity *fragmentation amplitudes*,  $\hat{\mathcal{D}}_{\lambda_C, \lambda_X; \lambda_c}$ , for the process  $c \rightarrow C + X$  in which parton  $c$ , coming from the elementary hard scattering process  $ab \rightarrow cd$ , hadronizes into a jet containing the detected final hadron  $C$ , with light-cone momentum fraction  $z$  and transverse momentum  $\mathbf{k}_{\perp C}$ . We then define the product of fragmentation amplitudes

$$\hat{\mathcal{D}}_{\lambda_c, \lambda'_c}^{\lambda_C, \lambda'_C}(z, \mathbf{k}_{\perp C}) = \int_{X, \lambda_X} \hat{\mathcal{D}}_{\lambda_C, \lambda_X; \lambda_c}(z, \mathbf{k}_{\perp C}) \hat{\mathcal{D}}_{\lambda'_C, \lambda_X; \lambda'_c}^*(z, \mathbf{k}_{\perp C}). \quad (44)$$

Denoting by  $\phi_C^H$  the azimuthal angle of hadron  $C$  momentum in the parton  $c$  helicity frame, one has

$$\hat{\mathcal{D}}_{\lambda_C, \lambda_X; \lambda_c}(z, \mathbf{k}_{\perp C}) = \mathcal{D}_{\lambda_C, \lambda_X; \lambda_c}(z, k_{\perp C}) e^{i\lambda_c \phi_C^H}. \quad (45)$$

In the sequel, apart from a short discussion of transverse  $\Lambda$  polarization in sections 4.3.2, 5.1.3, we will always refer to unpolarized final hadrons. In this case, the generalized FF  $\hat{D}_{\lambda_c, \lambda'_c}^{\lambda_C, \lambda'_C}(z, \mathbf{k}_{\perp C})$  simplifies to

$$\hat{D}_{\lambda_c, \lambda'_c}^{C/c}(z, \mathbf{k}_{\perp C}) \equiv \sum_{\lambda_C} \hat{D}_{\lambda_c, \lambda'_c}^{\lambda_C, \lambda'_C}(z, \mathbf{k}_{\perp C}) = D_{\lambda_c, \lambda'_c}^{C/c}(z, k_{\perp C}) e^{i(\lambda_c - \lambda'_c) \phi_C^H}, \quad (46)$$

and its azimuthal independent term fulfills the simplified parity relations

$$D_{-\lambda_c, -\lambda'_c}^{C/c}(z, k_{\perp C}) = (-1)^{2s_c} (-1)^{\lambda_c + \lambda'_c} D_{\lambda_c, \lambda'_c}^{C/c}(z, k_{\perp C}), \quad (47)$$

which again imply some differences between the quark ( $s_c = 1/2$ ) and the gluon ( $s_c = 1$ ) case.

### 4.3.1 Quark and gluon fragmentation into an unpolarized hadron

From parity and rotational constraints we can easily see that for quark fragmentation into an unpolarized hadron there are only two independent fragmentation functions at leading twist:

$$\hat{D}_{\pm\pm}^{C/q}(z, \mathbf{k}_{\perp C}) = D_{\pm\pm}^{C/q}(z, k_{\perp C}) \equiv D_{C/q}(z, k_{\perp C}) \quad (48)$$

$$\hat{D}_{\pm\mp}^{C/q}(z, \mathbf{k}_{\perp C}) = D_{\pm\mp}^{C/q}(z, k_{\perp C}) e^{\pm i\phi_C^H} = -D_{\mp\pm}^{C/q}(z, k_{\perp C}) e^{\pm i\phi_C^H}, \quad (49)$$

with

$$[D_{+-}^{C/q}(z, k_{\perp C})]^* = -D_{+-}^{C/q}(z, k_{\perp C}). \quad (50)$$

$D_{C/q}(z, k_{\perp C})$  is the unpolarized TMD fragmentation function. When integrated over the intrinsic transverse momentum it gives the usual unpolarized FF in the collinear configuration,  $D_{C/q}(z)$ ,

$$D_{C/q}(z) = \frac{1}{2} \sum_{\lambda_q} \int d^2\mathbf{k}_{\perp C} D_{\lambda_q, \lambda_q}^{C/q}(z, k_{\perp C}) = \frac{1}{2} \sum_{\lambda_q, \lambda_C} \int d^2\mathbf{k}_{\perp C} D_{\lambda_q, \lambda_q}^{\lambda_C, \lambda_C}(z, k_{\perp C}). \quad (51)$$

$D_{+-}^{C/q}(z, k_{\perp C})$  is a purely imaginary quantity, related to the Collins FF,  $\Delta^N D_{C/q^\uparrow}(z, k_{\perp C})$ ,

$$-2i D_{+-}^{C/q}(z, k_{\perp C}) = 2 \text{Im} D_{+-}^{C/q}(z, k_{\perp C}) = \Delta^N D_{C/q^\uparrow}(z, k_{\perp C}), \quad (52)$$

which gives the difference between the number densities of unpolarized hadrons  $C$  produced in the fragmentation of a quark polarized transversely to the hadronization plane (containing the quark,  $\mathbf{p}_q$ , and hadron,  $\mathbf{p}_C$ , three-momenta) in the  $\mathbf{p}_q \times \mathbf{p}_C$  direction and in the opposite one.

We can summarize these results in a form similar to Eq. (42):

$$D_{C/q} = D_{C/q, s_L} = D_{++}^{C/q} \quad \Delta \hat{D}_{C/q, s_T} = -2 \text{Im} D_{+-}^{C/q} \sin(\phi_{s_q} - \phi_C^H), \quad (53)$$

where  $\phi_{s_q}$  and, as already explained,  $\phi_C^H$  are the azimuthal angles of the fragmenting quark polarization vector and of  $\mathbf{k}_{\perp C}$  in the quark helicity frame, as reached from the hadronic c.m. frame.

The gluon generalized fragmentation functions  $D_{\pm\pm}^{C/g}(z, k_{\perp C})$  with equal helicity indices obey the same relations as for the quark case, see Eq. (48) with  $q \rightarrow g$ , whereas, due to the different parton spins and parity properties, the gluon analogues of Eqs. (49), (50) for unequal helicity indices read

$$\begin{aligned} \hat{D}_{\pm\mp}^{C/g}(z, \mathbf{k}_{\perp C}) &= D_{\pm\mp}^{C/g}(z, k_{\perp C}) e^{\pm 2i\phi_C^H} = D_{\mp\pm}^{C/g}(z, k_{\perp C}) e^{\pm 2i\phi_C^H} \\ [D_{+-}^{C/g}(z, k_{\perp C})]^* &= D_{+-}^{C/g}(z, k_{\perp C}). \end{aligned} \quad (54)$$

Therefore,  $D_{+-}^{C/g}(z, k_{\perp C})$  is now a purely real quantity. Similarly to what happens for the gluon parton distributions,  $D_{+-}^{C/g}(z, k_{\perp C})$  is related to the fragmentation process of a *linearly polarized* gluon into an unpolarized hadron. In analogy to Eq. (52) we define for gluons a Collins-like FF:

$$2 D_{+-}^{C/g}(z, k_{\perp C}) = 2 \text{Re} D_{+-}^{C/g}(z, k_{\perp C}) \equiv \Delta^N \hat{D}_{C/\mathcal{T}_1^g}(z, k_{\perp C}). \quad (55)$$

In the gluon helicity frame, in which the fragmentation process takes place in the  $(xz)$  plane, this quantity gives the difference between the number densities of unpolarized hadrons  $C$  resulting from the fragmentation of gluons linearly polarized along the  $x$ -direction and along the  $y$ -direction.



### 4.3.2 Quark fragmentation into a spin 1/2 hadron

In this section we shortly describe the helicity formalism for the polarized TMD fragmentation functions for the production of spin 1/2 particles. We will limit to the case of quark partons. Clearly, in this case there is a strong analogy with the polarized TMD distribution functions for parton quarks inside a spin 1/2 hadron, discussed in section 4.2. The extension to the case of gluon fragmentation can be easily performed along the same lines, using the results presented in the previous sections.

The polarization state of a spin 1/2 hadron  $C$ , produced in the fragmentation of an on-shell massless quark is described by its helicity density matrix

$$\rho_{\lambda_C, \lambda'_C}^C \hat{D}_{C/q, s_q}(z, \mathbf{k}_{\perp C}) = \sum_{\lambda_q, \lambda'_q} \hat{D}_{\lambda_q, \lambda'_q}^{\lambda_C, \lambda'_C}(z, \mathbf{k}_{\perp C}) \rho_{\lambda_q, \lambda'_q}^{q, s_q}, \quad (56)$$

and depends on the polarization state of the fragmenting quark, through its own helicity density matrix  $\rho_{\lambda_q, \lambda'_q}^{q, s_q}$ , and on the nonperturbative dynamics of the polarized hadronization process, through the generalized fragmentation functions introduced in the previous sections. The polarization state, and the helicity density matrix, of the fragmenting quark depend in turn on its production process.

Analogously to the PDF sector, by using rotational and parity invariance we can easily see that at leading twist there are eight independent polarized TMD fragmentation functions, which can be connected to the generalized functions

$$D_{++}^{++}, \quad D_{++}^{--}, \quad D_{+-}^{+-}, \quad D_{+-}^{-+}, \quad D_{+-}^{++}, \quad D_{+-}^{--}, \quad D_{+-}^{+-}, \quad D_{--}^{+-}, \quad (57)$$

through relations very similar to those of Eqs. (42) for the PDF case.

Even if we will discuss spin 1/2 particle production only marginally, let us stress the following points: 1) There are only three TMD fragmentation functions that do not vanish under  $\mathbf{k}_{\perp C}$  integration, that is the three usual FF's of the collinear approach: the unpolarized, longitudinally polarized and transversely polarized FF's (like in the PDF case, the last one has two TMD contributions; only the dominant one survives under  $\mathbf{k}_{\perp C}$  integration); 2) There is a term corresponding to the Collins effect, describing the fragmentation of a transversely polarized quark into an unpolarized spin 1/2 hadron, as already discussed in section 4.3.1; 3) There is a very interesting new distribution,  $\Delta D_{S_V/q} = \Delta^N D_{C\uparrow/q}$ , related to the fragmentation of an unpolarized quark into a transversely polarized (in its helicity frame) spin 1/2 hadron. This TMD function, first introduced in Ref. [126], needs not to vanish, and is in a sense the analogue of the Sivers PDF in the fragmentation sector. As it will be discussed in section 5, it can play a relevant role for the description of transverse  $\Lambda$  polarization in unpolarized hadronic collisions within a pQCD approach. Its phenomenological relevance was pointed out for the first time in Ref. [137], where it was also named, given its role, as *polarizing* fragmentation function.

## 4.4 Helicity amplitudes for the elementary process $ab \rightarrow cd$

Another essential ingredient of the master formula, Eq.(33), are the helicity amplitudes for the hard elementary process  $ab \rightarrow cd$ . These enter in the combination  $\hat{M}_{\lambda_c, \lambda_d; \lambda_a, \lambda_b} \hat{M}_{\lambda'_c, \lambda'_d; \lambda'_a, \lambda'_b}^*$ , which is diagonal only in the helicity indices of the unobserved parton  $d$  (fragmenting into a jet). For particles  $a, b, c$ , both diagonal and non diagonal helicity terms play a role, in different combinations corresponding to all the allowed contributions to a given polarized process. These contributions will be discussed in more detail in section 4.5, where the structure of Eq. (33) will be explicitly given for some of the terms appearing in the case of doubly polarized processes. Helicity amplitudes are normalized so that the unpolarized cross section, *for a collinear collision*, is given by

$$\frac{d\hat{\sigma}^{ab \rightarrow cd}}{d\hat{t}} = \frac{1}{16\pi\hat{s}^2} \frac{1}{4} \sum_{\lambda_a, \lambda_b, \lambda_c, \lambda_d} |\hat{M}_{\lambda_c, \lambda_d; \lambda_a, \lambda_b}|^2. \quad (58)$$

It is important to keep in mind that all hadronic polarization observables are measured in the hadronic c.m. frame. On the other hand, in the helicity formalism the polarization state of each particle involved in the process (including partons) is given via its helicity density matrix, defined in the appropriate helicity frame, as reached by the chosen overall hadronic frame. Therefore, one must carefully connect all helicity frames with the hadronic c.m. frame. A similar connection must be found between the helicity amplitudes  $\hat{M}^0$ , given in the *canonical partonic c.m. frame* (that is, a frame in which partons  $a$  and  $b$  collide head-on moving along the  $\pm z$ -axis direction respectively, creating particles  $c, d$ , laying in the  $xz$  plane), and their expressions in the hadronic c.m. frame,  $\hat{M}$ , which enter the master formula for cross sections. While this connection is irrelevant for any process involving only unpolarized elementary scatterings, it plays an essential role for the *polarized* case, which in principle introduces azimuthal factors that are not Lorentz invariants. As we will see in more detail in section 5, these factors, in addition to those coming from the polarized PDF's and FF's discussed previously, are crucial for a proper understanding of each term contributing to spin and azimuthal asymmetries.

Let us now start from the hadronic c.m. frame for the process  $AB \rightarrow C+X$ . Neglecting for simplicity all masses, the hadronic four-momenta are given by

$$p_A^\mu = \frac{\sqrt{s}}{2}(1, 0, 0, 1), \quad p_B^\mu = \frac{\sqrt{s}}{2}(1, 0, 0, -1), \quad p_C^\mu = (E_C, p_T, 0, p_L), \quad (59)$$

with  $E_C = \sqrt{p_T^2 + p_L^2}$ , and  $s = (p_A + p_B)^2$ . As for partons, we introduce the usual light-cone momentum fractions  $x_a = p_a^+ / p_A^+$ ,  $x_b = p_b^+ / p_B^+$ ,  $z = p_C^+ / p_c^+$  and transverse momenta  $\mathbf{k}_{\perp a}$ ,  $\mathbf{k}_{\perp b}$  and  $\mathbf{k}_{\perp C}$ .

Due to the simplified kinematics, in the  $\mathbf{k}_\perp$ -integrated, collinear configuration the hadronic reaction plane (the  $(XZ)_{\text{cm}}$  plane of our overall c.m. frame) and the partonic scattering plane coincide. The hadronic and partonic c.m. frames are connected by a simple Lorentz boost along the direction of the colliding beams. Clearly, this situation does not apply to a generalized parton model including all kinematical TMD effects. The elementary scattering,  $a(\mathbf{p}_a) + b(\mathbf{p}_b) \rightarrow c(\mathbf{p}_c) + d(\mathbf{p}_d)$ , is not planar anymore in the generic  $\mathbf{k}_\perp$  configuration and takes place out of the  $(XZ)_{\text{cm}}$  plane.

There are two different ways to find the elementary helicity amplitudes in the hadronic frame:

- 1) One can directly compute the amplitudes  $\hat{M}$  in this frame, with the given kinematical configuration, using well known effective calculational techniques. As a result, the amplitudes will be given in terms of azimuthal phase factors directly measured in the hadronic frame, having therefore a simple interpretation. However, they will have complicated, not very illuminating, expressions. Moreover, their general properties, e.g. under parity transformations, will be not so evident.
- 2) One can alternatively use the amplitudes  $\hat{M}^0$  in the canonical partonic frame, that are well known and have very simple expressions at leading order, together with their parity properties, which are also well known. As a second step, one can relate the amplitudes  $\hat{M}^0$  to the amplitudes  $\hat{M}$  by considering the Lorentz transformation connecting the partonic and hadronic frames and its action on the helicity states of the particles involved. This method, which will be used in the sequel, leads to simple expressions for the amplitudes  $\hat{M}$ , related by simple azimuthal phase factors to the amplitudes  $\hat{M}^0$ . However, the azimuthal phases will be given as very involved combinations of all angular variables coming from the kinematics and the Lorentz transformation.

Following this procedure, the elementary scattering amplitudes computed in the hadronic c.m. system are related to those computed in the partonic c.m. system (in the  $XZ$  plane) by:

$$\hat{M}_{\lambda_c, \lambda_d; \lambda_a, \lambda_b} = \hat{M}_{\lambda_c, \lambda_d; \lambda_a, \lambda_b}^0 e^{-i(\lambda_a \xi_a + \lambda_b \xi_b - \lambda_c \xi_c - \lambda_d \xi_d)} e^{-i[(\lambda_a - \lambda_b) \tilde{\xi}_a - (\lambda_c - \lambda_d) \tilde{\xi}_c]} e^{i(\lambda_a - \lambda_b) \phi_c''}, \quad (60)$$

where  $\xi_i$ ,  $\tilde{\xi}_i$  and  $\phi_c''$  are phases acquired as a result of the boost and rotations [13, 135].

The parity properties of the canonical c.m. amplitudes  $\hat{M}^0$  are the usual ones [13]:

$$\hat{M}_{-\lambda_c, -\lambda_d; -\lambda_a, -\lambda_b}^0 = \eta_a \eta_b \eta_c \eta_d (-1)^{s_a + s_b - s_c - s_d} (-1)^{(\lambda_a - \lambda_b) - (\lambda_c - \lambda_d)} \hat{M}_{\lambda_c, \lambda_d; \lambda_a, \lambda_b}^0, \quad (61)$$

where  $\eta_i$  is the intrinsic parity factor for particle  $i$ . From Lorentz and rotational invariance properties [13] one can also obtain useful expressions relating, up to an overall phase factor, irrelevant here, the canonical amplitudes for processes which only differ by the exchange of the two initial partons,  $a \leftrightarrow b$ , or of the two final partons,  $c \leftrightarrow d$ :

$$\hat{M}_{\lambda_c, \lambda_d; \lambda_b, \lambda_a}^{0, ba \rightarrow cd}(\theta) = \hat{M}_{\lambda_c, \lambda_d; \lambda_a, \lambda_b}^{0, ab \rightarrow cd}(\pi - \theta) e^{-i\pi(\lambda_c - \lambda_d)} \quad \hat{M}_{\lambda_d, \lambda_c; \lambda_a, \lambda_b}^{0, ab \rightarrow dc}(\theta) = \hat{M}_{\lambda_c, \lambda_d; \lambda_a, \lambda_b}^{0, ab \rightarrow cd}(\pi - \theta) e^{-i\pi(\lambda_a - \lambda_b)}, \quad (62)$$

where the scattering angle  $\theta$  is defined in the canonical partonic c.m. frame.

## 4.5 Kernels for doubly polarized processes

The computation of the invariant differential cross section corresponding to any polarized hadronic process  $A(S_A) + B(S_B) \rightarrow C + X$ , see Eq. (33), requires the evaluation and integration, for each elementary process  $ab \rightarrow cd$ , of the general kernel

$$\Sigma(S_A, S_B)^{ab \rightarrow cd} = \sum_{\{\lambda\}} \rho_{\lambda_a, \lambda'_a}^{a/A, S_A} \hat{f}_{a/A, S_A}(x_a, \mathbf{k}_{\perp a}) \rho_{\lambda_b, \lambda'_b}^{b/B, S_B} \hat{f}_{b/B, S_B}(x_b, \mathbf{k}_{\perp b}) \hat{M}_{\lambda_c, \lambda_d; \lambda_a, \lambda_b} \hat{M}_{\lambda'_c, \lambda'_d; \lambda'_a, \lambda'_b}^* \hat{D}_{\lambda_c, \lambda'_c}^{\lambda_C, \lambda'_C}(z, \mathbf{k}_{\perp C}). \quad (63)$$

All the ingredients of the kernels have been separately discussed in detail in the previous sections. We have stressed the fact that, including  $\mathbf{k}_{\perp}$  effects, the non-collinearity of soft processes, together with the non-planarity of the elementary scattering processes, generate non trivial azimuthal phase factors that must be properly taken into account in the calculations. As it will be shown in section 5, these phase factors have direct consequences on the behaviour of spin and azimuthal asymmetries in term of the kinematical variables and can be experimentally tested.

Before giving explicit kernels, Eq. (63), for some representative partonic channels contributing to the doubly polarized process  $A(S_A) + B(S_B) \rightarrow C + X$ , we note that for on-shell, massless partons there are only three nonvanishing, independent helicity amplitudes for the process  $ab \rightarrow cd$ :

$$\begin{aligned} \hat{M}_{++; ++} &= \hat{M}_{++; ++}^0 e^{i\varphi_1} = \hat{M}_1^0 e^{i\varphi_1} \\ \hat{M}_{-+; -+} &= \hat{M}_{-+; -+}^0 e^{i\varphi_2} = \hat{M}_2^0 e^{i\varphi_2} \\ \hat{M}_{-+; +-} &= \hat{M}_{-+; +-}^0 e^{i\varphi_3} = \hat{M}_3^0 e^{i\varphi_3}, \end{aligned} \quad (64)$$

where the phases  $\varphi_i$ ,  $i = 1, 2, 3$ , can be obtained from Eq. (60) by inserting the proper values for the helicities  $\lambda_j$ ,  $j = a, b, c, d$  and are such that they change sign by helicity inversion. The (+) and (-) subscripts correspond respectively to  $(\pm 1/2)$  helicities for quarks and to  $(\pm 1)$  helicities for gluons. For shortness, in the kernels we will not show explicitly the PDF and FF dependences on the parton light-cone fractions and transverse momenta. Kernels for processes related to those presented by the exchange  $a \leftrightarrow b$ , and/or  $c \leftrightarrow d$  can be easily obtained by using Eq. (62) and exchanging properly some labels. The elementary amplitudes  $\hat{M}_i^0$ ,  $i = 1, 2, 3$ , and their products, can be found, e.g., in Ref. [135].

(1)  $q_a q_b \rightarrow q_c q_d$  processes

$$\begin{aligned} &2 \Sigma(S_A, S_B)^{q_a q_b \rightarrow q_c q_d} = \\ &\left\{ \hat{f}_{a/S_A} \hat{f}_{b/S_B} \left( |\hat{M}_1^0|^2 + |\hat{M}_2^0|^2 + |\hat{M}_3^0|^2 \right) + \Delta \hat{f}_{s_z/S_A} \Delta \hat{f}_{s_z/S_B} \left( |\hat{M}_1^0|^2 - |\hat{M}_2^0|^2 - |\hat{M}_3^0|^2 \right) \right. \\ &\quad + 2 \left[ \left( \Delta \hat{f}_{s_x/S_A} \Delta \hat{f}_{s_x/S_B} + \Delta \hat{f}_{s_y/S_A} \Delta \hat{f}_{s_y/S_B} \right) \cos(\varphi_3 - \varphi_2) \right. \\ &\quad \left. \left. - \left( \Delta \hat{f}_{s_x/S_A} \Delta \hat{f}_{s_y/S_B} - \Delta \hat{f}_{s_y/S_A} \Delta \hat{f}_{s_x/S_B} \right) \sin(\varphi_3 - \varphi_2) \right] \hat{M}_2^0 \hat{M}_3^0 \right\} D_{C/c} \end{aligned} \quad (65)$$

$$\begin{aligned}
& - \left\{ \left[ \Delta \hat{f}_{s_x/S_A}^a \hat{f}_{b/S_B} \sin(\varphi_1 - \varphi_2 + \phi_C^H) - \Delta \hat{f}_{s_y/S_A}^a \hat{f}_{b/S_B} \cos(\varphi_1 - \varphi_2 + \phi_C^H) \right] \hat{M}_1^0 \hat{M}_2^0 \right. \\
& \quad \left. + \left[ \hat{f}_{a/S_A} \Delta \hat{f}_{s_x/S_B}^b \sin(\varphi_1 - \varphi_3 + \phi_C^H) - \hat{f}_{a/S_A} \Delta \hat{f}_{s_y/S_B}^b \cos(\varphi_1 - \varphi_3 + \phi_C^H) \right] \hat{M}_1^0 \hat{M}_3^0 \right\} \Delta^N D_{C/c^\dagger}.
\end{aligned}$$

This case includes all channels involving quarks and antiquarks like e.g.  $\bar{q}_a \bar{q}_b \rightarrow \bar{q}_c \bar{q}_d$ ,  $q_a \bar{q}_b \rightarrow q_c \bar{q}_d$ .

(2)  $qg \rightarrow qg$  processes

$$\begin{aligned}
& 2 \Sigma(S_A, S_B)^{qg \rightarrow qg} = \\
& \left[ \hat{f}_{q/S_A} \hat{f}_{g/S_B} (|\hat{M}_1^0|^2 + |\hat{M}_2^0|^2) + \Delta \hat{f}_{s_z/S_A}^q \Delta \hat{f}_{s_z/S_B}^g (|\hat{M}_1^0|^2 - |\hat{M}_2^0|^2) \right] D_{C/q} \\
& - \left[ \Delta \hat{f}_{s_x/S_A}^q \hat{f}_{g/S_B} \sin(\varphi_1 - \varphi_2 + \phi_C^H) - \Delta \hat{f}_{s_y/S_A}^q \hat{f}_{g/S_B} \cos(\varphi_1 - \varphi_2 + \phi_C^H) \right] \hat{M}_1^0 \hat{M}_2^0 \Delta^N D_{C/c^\dagger}.
\end{aligned} \tag{66}$$

Notice that in this case the amplitude  $\hat{M}_3^0$  is zero because of helicity conservation.

(3)  $gg \rightarrow gg$  processes

$$\begin{aligned}
& 2 \Sigma(S_A, S_B)^{gg \rightarrow gg} = \\
& \left\{ \hat{f}_{g/S_A} \hat{f}_{g/S_B} (|\hat{M}_1^0|^2 + |\hat{M}_2^0|^2 + |\hat{M}_3^0|^2) + \Delta \hat{f}_{s_z/S_A}^g \Delta \hat{f}_{s_z/S_B}^g (|\hat{M}_1^0|^2 - |\hat{M}_2^0|^2 - |\hat{M}_3^0|^2) \right. \\
& \quad + 2 \left[ (\Delta \hat{f}_{\mathcal{T}_1/S_A}^g \Delta \hat{f}_{\mathcal{T}_1/S_B}^g + \Delta \hat{f}_{\mathcal{T}_2/S_A}^g \Delta \hat{f}_{\mathcal{T}_2/S_B}^g) \cos(\varphi_3 - \varphi_2) \right. \\
& \quad \left. \left. - (\Delta \hat{f}_{\mathcal{T}_1/S_A}^g \Delta \hat{f}_{\mathcal{T}_2/S_B}^g - \Delta \hat{f}_{\mathcal{T}_2/S_A}^g \Delta \hat{f}_{\mathcal{T}_1/S_B}^g) \sin(\varphi_3 - \varphi_2) \right] \hat{M}_2^0 \hat{M}_3^0 \right\} D_{C/g} \\
& + \left\{ \left[ \Delta \hat{f}_{\mathcal{T}_1/S_A}^g \hat{f}_{g/S_B} \cos(\varphi_1 - \varphi_2 + 2\phi_C^H) + \Delta \hat{f}_{\mathcal{T}_2/S_A}^g \hat{f}_{g/S_B} \sin(\varphi_1 - \varphi_2 + 2\phi_C^H) \right] \hat{M}_1^0 \hat{M}_2^0 \right. \\
& \quad \left. + \left[ \hat{f}_{g/S_A} \Delta \hat{f}_{\mathcal{T}_1/S_B}^g \cos(\varphi_1 - \varphi_3 + 2\phi_C^H) + \hat{f}_{g/S_A} \Delta \hat{f}_{\mathcal{T}_2/S_B}^g \sin(\varphi_1 - \varphi_3 + 2\phi_C^H) \right] \hat{M}_1^0 \hat{M}_3^0 \right\} \Delta^N D_{C/\mathcal{T}_1^g}.
\end{aligned} \tag{67}$$

A few comments are in order here:

- 1) The explicit expressions of the polarized TMD quark distributions, for specific  $S_A$  and  $S_B$  combinations, can be read from Eq. (42) (for gluons see Ref. [135]). Notice that in general these functions still depend on the azimuthal phases (given in the hadronic frame) of the hadron polarization vector and of the parton transverse momentum. These angles will therefore appear in the final azimuthal phase factors of a specific polarized cross section;
- 2) Since for the fragmentation process into an unpolarized hadron there are only two independent TMD functions, the unpolarized FF and the Collins function, and only the last one depends on the azimuthal phase  $\phi_C^H$ , this dependence has been explicitly factored out in the azimuthal phase factors;
- 3) When considering processes obtained from those listed above by the exchange  $a \leftrightarrow b$ , and/or  $c \leftrightarrow d$ , it is important to recall that this concerns also the phases  $\varphi_i$ ,  $i = 1, 2, 3$  already factored out from the amplitudes  $\hat{M}_i^0$ , see Eq. (60).
- 4) The unintegrated kernels still depend on the parton transverse momenta  $\mathbf{k}_{\perp a}$ ,  $\mathbf{k}_{\perp b}$ ,  $\mathbf{k}_{\perp C}$ . As a result, we have seen that the partonic process is not planar and does not lay on the hadronic production plane. Therefore, the kernels still contain terms that, under  $\mathbf{k}_{\perp}$  integration, must vanish for some specific asymmetry (as it has been checked both analytically and numerically). As an example, there are terms corresponding to longitudinal SSA's, that are forbidden, for the overall hadronic process, by parity and rotational invariance. This is somehow analogous to the case of single spin azimuthal asymmetries measured (in the virtual photon-target proton reference frame) in SIDIS off longitudinally polarized (in the laboratory reference frame) protons. Since the two ref. frames are not coplanar, the longitudinal proton polarization vector has a transverse component, of order  $M/Q$ , in the  $\gamma^* - p$  c.m. frame.

To conclude, given its phenomenological interest we show, as an example, the kernel for the  $q_a q_b \rightarrow q_c q_d$  channel for the transverse polarization of spin 1/2 particles in unpolarized  $AB$  collisions.

$$\begin{aligned}
P_{Y_{\text{cm}}} \Sigma(0, 0)^{q_a q_b \rightarrow q_c q_d} = & \quad (68) \\
& \frac{1}{2} \left\{ f_{a/A} f_{b/B} \left[ |\hat{M}_1^0|^2 + |\hat{M}_2^0|^2 + |\hat{M}_3^0|^2 \right] + 2 \Delta \hat{f}_{s_y/A}^a \Delta \hat{f}_{s_y/B}^b \cos(\varphi_3 - \varphi_2) \hat{M}_2^0 \hat{M}_3^0 \right\} \Delta D_{S_Y/c}^{C/c} \cos \tilde{\phi} \\
& + \hat{f}_{a/A} \Delta \hat{f}_{s_y/B}^b \hat{M}_1^0 \hat{M}_3^0 \left\{ \Delta^- \hat{D}_{S_Y/s_T}^{C/c} \cos(\varphi_1 - \varphi_3 + \phi_C^H) \cos \tilde{\phi} - \Delta D_{S_X/s_T}^{C/c} \sin(\varphi_1 - \varphi_3 + \phi_C^H) \sin \tilde{\phi} \right\} \\
& + \Delta \hat{f}_{s_y/A}^a \hat{f}_{b/B} \hat{M}_1^0 \hat{M}_2^0 \left\{ \Delta^- D_{S_Y/s_T}^{C/c} \cos(\varphi_1 - \varphi_2 + \phi_C^H) \cos \tilde{\phi} - \Delta D_{S_X/s_T}^{C/c} \sin(\varphi_1 - \varphi_2 + \phi_C^H) \sin \tilde{\phi} \right\},
\end{aligned}$$

where the polarized fragmentation functions for the process  $c \rightarrow C + X$  are the analogues of the quark distributions discussed in section 4.2.  $P_{Y_{\text{cm}}}$  is the transverse polarization of the spin 1/2 final particle w.r.t. the production plane, which is the  $(XZ)_{\text{cm}}$  plane of the hadronic c.m. frame. The angle  $\tilde{\phi}$  projects the transverse polarization of the particle, as given in its helicity frame, on the transverse direction in the hadronic frame just defined above. Notice that  $\cos \tilde{\phi} = Y_{\text{cm}} \cdot (\hat{\boldsymbol{p}}_c \times \hat{\boldsymbol{k}}_{\perp C})$ .

## 5 Phenomenology of single spin asymmetries

In this section we will consider in more detail, and from a phenomenological point of view, the theoretical computations aiming to a description of unpolarized and single-polarized cross section data for various high-energy processes of interest. We will consider in particular the generalized parton model approach in the helicity formalism (GPM), presented in section 4, making when possible a comparison with analogous results obtained within the other theoretical approaches discussed in section 3.

Following an historical perspective, we will first consider single and, to a lesser extent, double inclusive particle production in  $pp$  collisions. We will give an overview on how spin and  $\boldsymbol{k}_{\perp}$  effects play a role in explaining some former and well-known observations, as well as the most recent data collected at RHIC on SSA's. Consideration of several final particles, like pions, kaons, heavy mesons, hyperons, and photons, in different kinematical configurations, will guide us in showing the most interesting aspects of SSA's and their description in the GPM approach. Let us recall however that for the above processes factorization in the TMD approach is still under investigation and, for the single inclusive case, SSA's appear at subleading-twist level.

We will then move to a class of processes for which the  $\boldsymbol{k}_{\perp}$  factorization has been proved and SSA's show up already at leading twist. First we will discuss the Drell-Yan process, where both the unpolarized and single-polarized cases present interesting features to be analyzed in the context of the TMD approach. Finally,  $e^+e^-$  and SIDIS processes will be also addressed, with emphasis on some recent data collected by the Belle, HERMES and COMPASS Collaborations. We will then give a discussion of the latest extractions of the Sivers function, the transversity distribution and the Collins function.

We will show how rich this phenomenology can be, focusing also on the information one can gather from a combined careful study of all these cases.

In the theoretical estimates at LO accuracy the MRST01 set [221] is adopted for the collinear unpolarized PDF,  $f_{a/p}(x)$ . Where it appears together with the helicity PDF,  $\Delta_L f_{a/p}$ , the GRV98 [222] and the GRSV2000 [223] sets or, in some cases, the MRST01 and the LSS01 [224] sets are consistently used. For the FF ( $D_{h/c}(z)$ ), the KKP [225] and the Kretzer (K) [226] sets are adopted.

### 5.1 Unpolarized cross sections and SSA's in $pp \rightarrow C + X$

The inclusive production of large  $p_T$  particles in high-energy hadronic collisions has been for a long time a crucial testing ground for perturbative QCD. We will focus here on the role of intrinsic transverse momentum effects, utilizing the helicity formalism for the computation of (un)polarized cross sections.



### 5.1.1 Pion, kaon and heavy meson production

Pion production is by far the most representative case: a relatively large sample of data is already available, and more are going to come in the near future; moreover, pion SSA's may be considered as the original motivation behind the GPM approach.

A crucial and distinguishing ingredient of this approach is the proper inclusion of full  $\mathbf{k}_\perp$  kinematics and its interplay with the azimuthal phase factors appearing in the expressions of the polarized cross sections. We fix for the  $pp \rightarrow \pi + X$  inclusive process the following configuration: we adopt the  $pp$  c.m. frame (the hadronic frame), with the  $Z$  axis along the direction of the colliding protons, and the pion produced in the  $XZ$  plane with positive  $(p_\pi)_X$ . For the proton moving along  $+Z$ , the transverse polarization is defined along the  $Y$  axis with  $\uparrow (\downarrow) \equiv \pm Y$  [ $\phi_{S_A} = \pm\pi/2$  in Eq. (42)].

Let us start with the unpolarized case. The corresponding differential cross section for inclusive pion production is given in terms of the kernels in Eq. (63),  $\Sigma(0,0) = 1/2[\Sigma(\uparrow,0) + \Sigma(\downarrow,0)]$ , one for each active partonic channel,  $ab \rightarrow cd$ . As discussed in Ref. [135], the main new result of the GPM approach is the appearance of additional terms besides the usual contribution from the unpolarized  $\mathbf{k}_\perp$  dependent PDF's and FF's, coupled with the unpolarized partonic cross sections. This term, once integrated over all  $\mathbf{k}_\perp$ 's, would be the only one in the factorization scheme in collinear configuration. It is also the only contribution considered in previous approaches using the parton model with TMD effects but neglecting the new spin and  $\mathbf{k}_\perp$  dependent, leading-twist, PDF's and FF's [227, 228, 229, 230]. In fact, focusing here on the  $qq \rightarrow qq$  channel, the additional contributions come from: a) The convolution of two (chiral-odd) Boer-Mulders functions with the double transverse spin asymmetry for the  $qq$  interaction; 2) The convolution of one Boer-Mulders function and the Collins function (again, two chiral-odd quantities) coupled with the partonic spin-transfer factor. Analogously, all the other partonic channels contain some extra pieces as compared to the naive TMD extension of the collinear factorized approach.

The study of so many additional contributions, given in terms of new unknown distributions, might look as hopeless from the phenomenological point of view. It is however the very structure behind this scheme, and its exact kinematical formulation, to offer a way out.

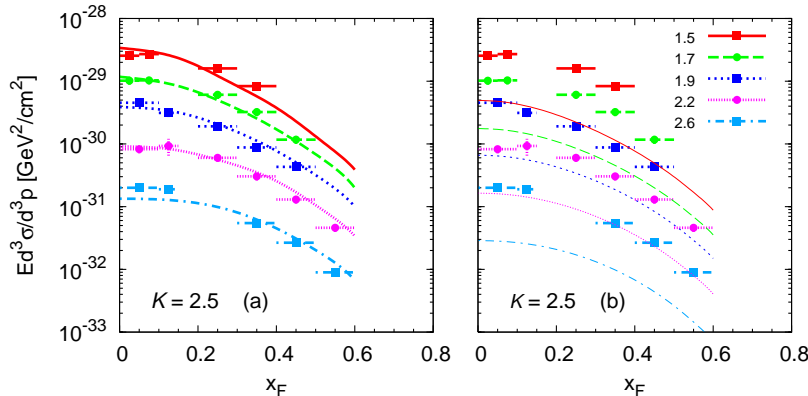


Figure 2: Invariant differential cross section for  $pp \rightarrow \pi^0 + X$  at  $\sqrt{s} = 19.4$  GeV and for different  $p_T$  values (in GeV/c) vs.  $x_F$  [231]. The corresponding results in the GPM approach with  $\mathbf{k}_\perp$  effects (a) and in the collinear partonic configuration (b) are also shown. All curves are rescaled by a fixed  $K$ -factor,  $K = 2.5$ . Unpolarized PDF and FF sets: MRST01-KKP.

Once the integrations over the nonobservable intrinsic motions have been performed, the many azimuthal phases appearing in the elementary interactions, due to the noncollinear configuration, lead to large cancellations of most of the contributions involving the new unknown TMD functions. However, the inclusion of  $\mathbf{k}_\perp$  effects in the standard unpolarized contribution in collinear configuration could be

relevant for a good description of the unpolarized cross section data measured in inclusive particle production in different kinematical configurations. These cross sections are otherwise often underestimated by a factor of up to one order of magnitude [218]. As discussed in Ref. [117] threshold resummation effects might reduce to some extent this discrepancy.

As an example, in Fig. 2 we show the invariant differential cross section for inclusive  $\pi^0$  production in  $pp$  collisions, at  $\sqrt{s} = 19.4$  GeV and for different  $p_T$  values, as a function of  $x_F$ . In the left panel we plot the estimated cross sections, obtained with inclusion of  $\mathbf{k}_\perp$  effects, while the corresponding results in the usual collinear partonic configuration are plotted in the right panel (all curves are rescaled by a fixed  $K$ -factor,  $K = 2.5$ ). With the aim of giving a consistent treatment of both SSA's and unpolarized cross sections at the same level of accuracy (namely leading order pQCD calculations with leading twist soft functions) a large collection of data on Drell-Yan, direct photon production and pion production in  $pp$ ,  $pA$  collisions has been considered. NLO corrections to the unpolarized cross sections, usually parameterized as  $K$ -factors, having values around 2-3, are assumed to cancel, at least partly, in the SSA. Some of the relevant parameters of this approach, namely the Gaussian widths of  $\mathbf{k}_\perp$ -dependent PDF's and FF's, could then be reasonably fixed. For details see Ref. [218].

For higher-energy kinematical configurations, like e.g. that of the RHIC-BNL experiments, the dominance of the standard unpolarized term,  $f_{a/p} \otimes f_{b/p} \otimes D_{\pi/c}$  (but with inclusion of  $\mathbf{k}_\perp$  effects), w.r.t. all other additional contributions, comes out again in a neat way. In this case, however, the enhancing factor coming from the  $\mathbf{k}_\perp$  effects is much less important.

In this context, in Ref. [116] it has been claimed that experimental data on pion SSA's observed at fixed target experiments (moderate c.m. energies) cannot be explained by pQCD, since the collinear approach (LO and NLO) fails to reproduce the corresponding unpolarized cross sections. On the contrary, at high energy a good description can be obtained at NLO accuracy. As shown in Fig. 2 the inclusion of  $k_\perp$  effects reduces the gap between theoretical estimates in pQCD and data on unpolarized cross sections even for fixed target experiments. Therefore, a consistent treatment in the GPM approach of both unpolarized cross sections and SSA's for pion production can be given.

Let us now consider the numerator of  $A_N$ , focusing on two partonic channels:

(1)  $q_a q_b \rightarrow q_c q_d$  processes

$$\begin{aligned}
[\Sigma(\uparrow, 0) - \Sigma(\downarrow, 0)]^{q_a q_b \rightarrow q_c q_d} &= \frac{1}{2} \Delta \hat{f}_{a/p\uparrow}(x_a, \mathbf{k}_{\perp a}) f_{b/p}(x_b, k_{\perp b}) \left[ |\hat{M}_1^0|^2 + |\hat{M}_2^0|^2 + |\hat{M}_3^0|^2 \right] D_{\pi/c}(z, k_{\perp\pi}) \\
&+ \left[ \Delta^- \hat{f}_{s_y/\uparrow}^a(x_a, \mathbf{k}_{\perp a}) \cos(\varphi_1 - \varphi_2 + \phi_\pi^H) - \Delta \hat{f}_{s_x/\uparrow}^a(x_a, \mathbf{k}_{\perp a}) \sin(\varphi_1 - \varphi_2 + \phi_\pi^H) \right] \\
&\quad \times f_{b/p}(x_b, k_{\perp b}) \hat{M}_1^0 \hat{M}_2^0 \Delta^N D_{\pi/c\uparrow}(z, k_{\perp\pi}) \\
&+ 2 \left[ \Delta^- \hat{f}_{s_y/\uparrow}^a(x_a, \mathbf{k}_{\perp a}) \cos(\varphi_3 - \varphi_2) - \Delta \hat{f}_{s_x/\uparrow}^a(x_a, \mathbf{k}_{\perp a}) \sin(\varphi_3 - \varphi_2) \right] \\
&\quad \times \Delta f_{s_y/p}^b(x_b, k_{\perp b}) \hat{M}_2^0 \hat{M}_3^0 D_{\pi/c}(z, k_{\perp\pi}) \\
&+ \frac{1}{2} \Delta \hat{f}_{a/p\uparrow}(x_a, \mathbf{k}_{\perp a}) \Delta f_{s_y/p}^b(x_b, k_{\perp b}) \cos(\varphi_1 - \varphi_3 + \phi_\pi^H) \hat{M}_1^0 \hat{M}_3^0 \Delta^N D_{\pi/c\uparrow}(z, k_{\perp\pi});
\end{aligned} \tag{69}$$

(2)  $qg \rightarrow qg$  processes

$$\begin{aligned}
[\Sigma(\uparrow, 0) - \Sigma(\downarrow, 0)]^{qg \rightarrow qg} &= \frac{1}{2} \Delta \hat{f}_{q/p\uparrow}(x_q, \mathbf{k}_{\perp q}) f_{g/p}(x_g, k_{\perp g}) \left[ |\hat{M}_1^0|^2 + |\hat{M}_2^0|^2 \right] D_{\pi/q}(z, k_{\perp\pi}) \\
&+ \left[ \Delta^- \hat{f}_{s_y/\uparrow}^q(x_q, \mathbf{k}_{\perp q}) \cos(\varphi_1 - \varphi_2 + \phi_\pi^H) - \Delta \hat{f}_{s_x/\uparrow}^q(x_q, \mathbf{k}_{\perp q}) \sin(\varphi_1 - \varphi_2 + \phi_\pi^H) \right] \\
&\quad \times f_{g/p}(x_g, k_{\perp g}) \hat{M}_1^0 \hat{M}_2^0 \Delta^N D_{\pi/q\uparrow}(z, k_{\perp\pi}).
\end{aligned} \tag{70}$$

Let us recall that the above equations have been obtained by properly exploiting the phases coming from the scattering helicity amplitudes and the fragmentation process, while the phases entering the spin and TMD initial distributions, if present, are still implicitly included in their vectorial  $\mathbf{k}_\perp$  dependence.

Again we briefly comment on the  $qq \rightarrow qq$  case. In the first term of Eq. (69) we find the contribution due to the Sivers effect; in the second term we have the Collins effect coupled with the two pieces of the TMD transversity distribution. Notice that these contributions, already familiar from previous work adopting a simplified  $\mathbf{k}_\perp$  kinematics, enter now with a complete phase structure without any simplification. Two extra terms appear: the third one contains the Boer-Mulders effect coupled again with the TMD transversity distribution; finally, the fourth term comes from a combination of the Sivers, Collins and Boer-Mulders effects. Notice that in the  $gg \rightarrow qq$  case only the Sivers effect and, separately, the transversity + Collins effect, could be active. For the  $gg \rightarrow gg$  process one gets an analogous structure as in the  $qq \rightarrow qq$  case, with a corresponding number of effects (involving linear gluon polarizations instead of transverse quark polarizations).

The complex structure in terms of azimuthal phases plays an even more crucial role in the numerator of the SSA. To show that one can saturate all unknown polarized TMD distribution functions, using the corresponding positivity bounds. In some cases this is certainly an overestimate: e.g., for the transversity distribution it violates the Soffer bound [182].

In Fig. 3 (left panel) we plot all different maximized contributions to  $A_N$  for the  $p^\uparrow p \rightarrow \pi^+ + X$  process in the E704 experimental configuration, for which very large values of  $A_N$  have been measured [47, 48, 49]. Notice that, whenever different terms could combine with different signs (e.g., Sivers or Collins functions for different quark flavours), their contributions have been summed always with *the same sign*, in order to avoid any kind of cancelations not resulting from azimuthal factors and phase-space integrations. One sees that potentially the Sivers mechanism is largely dominant, some role could be played by the Collins mechanism, while all other contributions are negligible [135].

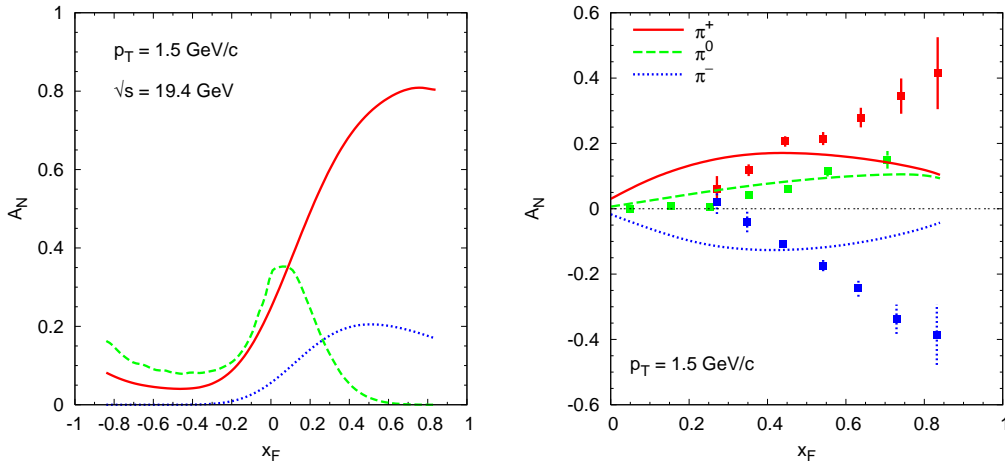


Figure 3: Left panel: Maximized contributions to  $A_N$ , plotted as a function of  $x_F$ , for  $p^\uparrow p \rightarrow \pi^+ + X$  processes and E704 kinematics. Solid line: quark Sivers mechanism alone; dashed line: gluon Sivers mechanism alone; dotted line: transversity  $\otimes$  Collins effect. All other contributions are negligible. Unpolarized PDF and FF sets: MRST01-K. Right panel: Values of  $A_N$  vs.  $x_F$  (E704 kinematics), due to the Collins mechanism alone, obtained by saturating all proper bounds on the unknown soft functions. Data are from Refs. [47, 48, 49]. (Un)polarized PDF and FF sets: (MRST01)LSS01-K.

However, a clear-cut statement on the relevance of the Collins effect in  $A_N(p^\uparrow p \rightarrow \pi + X)$  would require the combined study of the SSA for both charged pions.

In Ref. [219] a detailed study on this issue was performed, by imposing the proper bounds for the TMD transversity distributions [181] with the LSS01 set for the helicity PDF's. This analysis showed how the phases involved, when the  $\mathbf{k}_\perp$  kinematics is treated carefully, are crucial, leading to a strong suppression of the asymmetry generated by the Collins mechanism, see Fig. 3 (right panel).

The role of the azimuthal phases can be checked more explicitly by performing the simple exercise of setting all of them to zero (somewhat an analogue of the former simplified studies with planar kinematics): in such a case, as expected, one obtains considerably larger results. However, the competing contributions from  $qq \rightarrow qq$  and  $qg \rightarrow qg$  processes (due to the opposite sign in the partonic spin transfer factor), still prevent to get  $A_N$  values as large as those observed at large  $x_F$ . This result is in contrast with former believes, that the remarkably large SSA measured *e.g.* by the E704 experiment could be generated by the Collins mechanism alone [131]. In fact, in these former studies, only the leading  $\mathbf{k}_\perp$  effects were taken into account in a simplified planar configuration for the hard scattering.

It is worth to mention here that the Collins effect is not completely out of reach in hadronic collisions: indeed it has been recently shown that by measuring the azimuthal distribution of a pion inside a jet inclusively produced in  $p^\uparrow p$  collisions, one can select this mechanism (see Refs. [232] and [233]).

From Fig. 3 (left panel) one also sees that the contribution of the gluon Sivers mechanism for E704 kinematics at negative  $x_F$  could be important. Indeed, very similar results can be obtained for the  $p^\uparrow \bar{p} \rightarrow \pi + X$  process in the kinematical configuration of the proposed PAX experiment at GSI [234], where at large negative  $x_F$  one could gain some information on the poorly known gluon Sivers function.

The STAR experiment at RHIC-BNL has also measured non zero values of  $A_N$  in  $p^\uparrow p \rightarrow \pi^0 + X$  processes at forward rapidity [59, 235]. Again, in the STAR kinematical regime the Sivers mechanism gives the largest contribution to  $A_N$ . There might remain some contribution from the Collins mechanism, while all other contributions are negligible. In this case, however, in contrast with the lower energy case, at negative  $x_F$  all contributions are vanishingly small.

Let us now try to explain some of the above results, namely, the different behaviour of the Sivers mechanism in different kinematical configurations. The azimuthal phase factor  $\cos \phi_a$  entering the Sivers function, see section 4, plays a crucial role and deserves some additional comments. The only other term depending on  $\phi_a$  in the contribution of the Sivers effect to the numerator of  $A_N$  is the partonic cross section, in particular via the corresponding Mandelstam variable  $\hat{t}$ . At large positive  $x_F$  and moderately large  $p_T$  the (average) values of  $\hat{t}$  are relatively small. Therefore, the (dominant)  $\hat{t}$ -channel contributions, proportional to  $1/\hat{t}^2$ , depend sizably on  $\phi_a$ , so that  $A_N$  is not necessarily suppressed. This explains the potentially large effect at large  $x_F$ . Instead, for negative values of  $x_F$ , all partonic Mandelstam variables are much less dependent on  $\phi_a$ , so that one is roughly left with the  $d^2\mathbf{k}_{\perp a} \cos \phi_a$  integration alone, which cancels the potentially large Sivers contribution. As a consequence, the possibility of gaining information on the gluon Sivers distribution from the recent STAR and BRAHMS data at negative values of  $x_F$  is frustrated. Notice that, due to the much lower values of  $\sqrt{s}$  involved, this suppression caused by the  $\cos \phi_a$  dependence is much less effective for the kinematical regimes of E704 and of the proposed PAX [234] experiment.

On the basis of the above results it is clear that in the GPM approach the Sivers effect is the only mechanism which could by itself describe the large  $A_N$  values observed by the E704, STAR and BRAHMS collaborations in the forward region.

In Ref. [218], in order to perform numerical estimates and carry out a comparison with available experimental data a simple factorized form for the Sivers function was introduced:

$$\Delta^N f_{q/p^\uparrow}(x, k_\perp) = 2\mathcal{N}_q^S(x) f_{q/p}(x) \mathcal{H}(k_\perp) \frac{\beta^2}{\pi} e^{-\beta^2 k_\perp^2}, \quad (71)$$

where  $\beta^2 = 1/\langle k_\perp^2 \rangle$  is a flavour-independent width parameter defining the Gaussian  $k_\perp$  shape of the unpolarized PDF (as extracted from the unpolarized cross section analysis:  $\langle k_\perp^2 \rangle = 0.64$  (GeV/c)<sup>2</sup> [218]). Notice that the natural positivity bounds are automatically fulfilled by imposing  $\mathcal{N}_q^S$  and  $\mathcal{H}$  to be separately smaller than unity in magnitude in the full  $x$  and  $k_\perp$  range respectively (see section 5.5.2).

To start with, only valence  $u$  and  $d$  quark Sivers functions (QSF) have been considered, neglecting (for what concerns the Sivers effect only) possible contributions from antiquarks and gluons. The fact that sizable values of  $A_N$  set up at large positive  $x_F$  somehow supports this choice.

In order to describe the E704 data invoking the Siverts effect alone, one needs a positive (negative)  $u$  ( $d$ ) quark Siverts function,  $\Delta^N f_{q/p^\uparrow}(x, k_\perp)$  [recall the opposite sign between  $\Delta^N f_{q/p^\uparrow}$  and  $f_{1T}^{\perp q}$ , see Eq. (16)]. Therefore, in the subsequent fragmentation process the unfavoured flavour contributions (e.g.  $d \rightarrow \pi^+$ ) enter with opposite sign (all other factors in the kernel being positive) w.r.t. the favoured ones (e.g.  $u \rightarrow \pi^+$ ) in the charged pion SSA's. This implies that the extraction of the quark Siverts functions is sensitive to the relative weight of the leading and non-leading terms in a specific set of FF's.

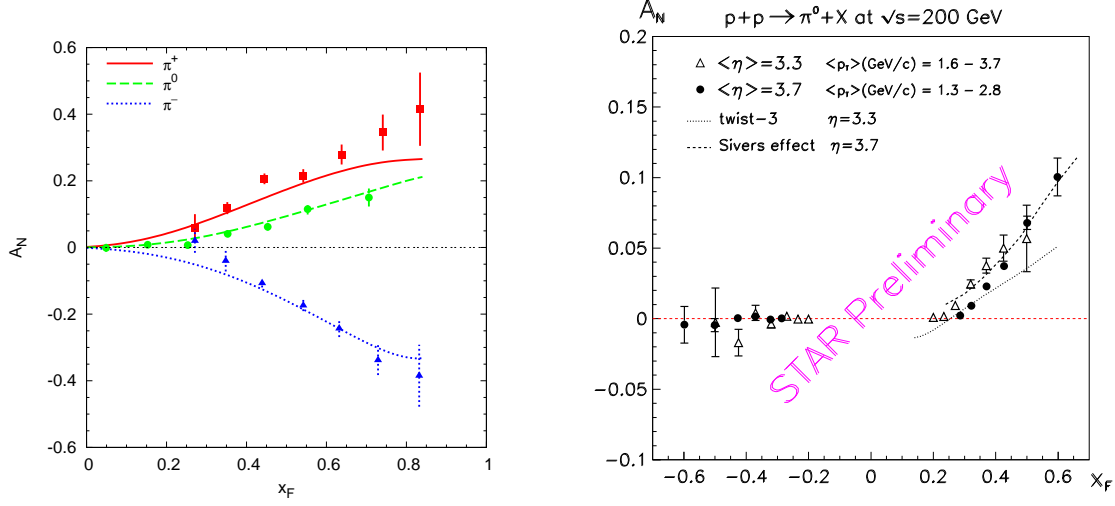


Figure 4: Left:  $A_N(p^\uparrow p \rightarrow \pi + X)$  vs.  $x_F$ , at  $\sqrt{s} = 19.4$  GeV and fixed  $p_T = 1.5$  GeV/c (Siverts effect); unpolarized PDF and FF sets: MRST01-KKP; data are from [47, 48, 49]. Right:  $A_N(p^\uparrow p \rightarrow \pi^0 + X)$  at  $\sqrt{s} = 200$  GeV; data are from [63]. A comparison with the Siverts effect in the GPM approach (dashed line) [218] and twist-three calculations (dotted line) [192] is also shown.

Under these assumptions, a good description of E704 data was obtained, see Fig. 4 (left panel). Although somehow expected, the most striking feature of the Siverts functions so obtained was the marked valence-like behaviour (that is,  $\Delta^N f_{q/p^\uparrow}(x, k_\perp)$  is strongly suppressed at small  $x$ ). This analysis, which consistently treats the full  $\mathbf{k}_\perp$  kinematics in the calculation of both the numerator and the denominator of  $A_N$ , also confirms all the main features of the Siverts contribution and of the Siverts function parameterizations found in previous papers based on a simplified planar kinematics [124, 125].

The so extracted Siverts function has been adopted to give predictions at much larger energies as those reached at RHIC [218]. The results have been found in good agreement with the subsequent published data [59] both in the positive and in the negative  $x_F$  region. Latest STAR results, with enhanced statistics, have confirmed the peculiar  $x_F$  behaviour of  $A_N$ . In Fig. 4 (right panel) we show the theoretical estimates obtained by adopting the Siverts functions as extracted from E704 data (dashed line) and compare them with preliminary data from STAR collaboration [63]. As predicted theoretically, sizable pion SSA's, with features similar to those found in the E704 kinematical regime, are confirmed experimentally even at such large c.m. energies. In Fig. 4 (right panel) we also show theoretical results in the twist-three approach (dotted line). In order to compare the two phenomenological studies some words are mandatory: in Ref. [192], adopting the twist-three approach a *global* fit on all available E704, STAR and BRAHMS data has been performed, leading to a good description of SSA results (see also Fig. 5); LO cross sections in collinear configuration have been adopted to compute the denominator of  $A_N$ ; in order to describe both low and high energy SSA data, calculations for E704 kinematics have been rescaled by a factor of 2.



Further data for charged pion SSA's have been collected by the BRAHMS collaboration [72], covering a different kinematical region (most of the data is at lower  $p_T$ ) and at two energy values. In this case, adopting the parameterization of the quark Sivers functions extracted by fitting E704 data, theoretical results underestimate the high-energy data (dotted lines in Fig. 5). This indicates that an extension of the GPM fit procedure including all data is required to better fix the Sivers function. Indeed the global fit based on the twist-three approach gives a better description (Fig. 5, solid lines).

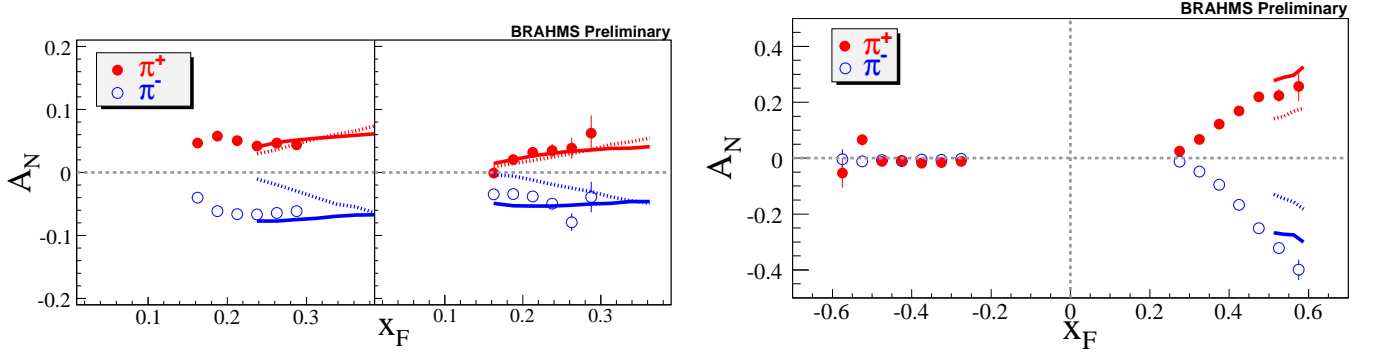


Figure 5: Left panel:  $A_N(p^\uparrow p \rightarrow \pi^\pm + X)$  at  $\sqrt{s} = 200$  GeV for two scattering angles,  $2.3^\circ$  (left) and  $4^\circ$  (right). Right panel:  $A_N$  at  $\sqrt{s} = 62$  GeV. Dotted line: GPM, Sivers effect; solid line: twist-three approach. Curves are calculated at  $p_T > 1$  GeV/c. Data are from [72].

In Fig. 6 we show preliminary STAR data on  $A_N(p^\uparrow p \rightarrow \pi^0 + X)$ , as a function of  $p_T$  [63] in different  $x_F$  bins and compare them with theoretical predictions based on the Sivers effect alone. With the possible exception of the lowest  $p_T$  points, at small  $x_F$ ,  $A_N$  is reasonably reproduced, taking into account that the GPM approach (based on pQCD), should be better suited for  $p_T$  bigger than 1-2 GeV/c. Let us also remind that the theoretical curves are (genuine) predictions obtained from a simple parameterization of the quark Sivers functions, aimed to describe the main features of the large  $x_F$  E704 data (at much lower energy). A similar  $p_T$ -behaviour is also expected in the twist-three approach.

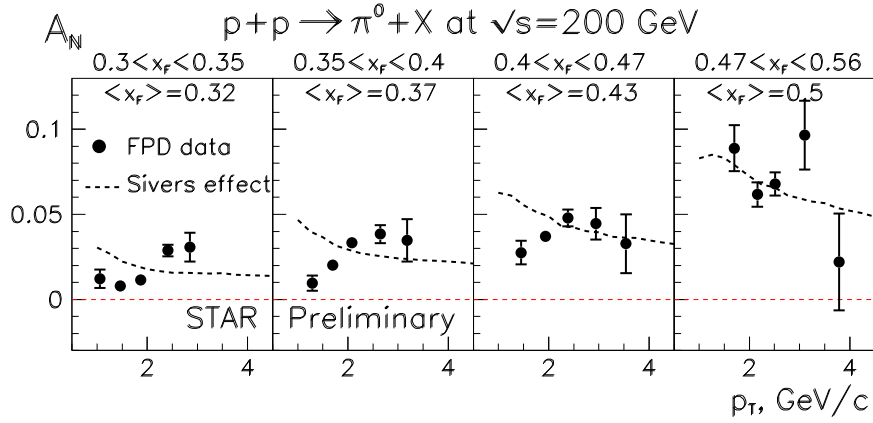


Figure 6:  $A_N(p^\uparrow p \rightarrow \pi^0 + X)$  at  $\sqrt{s} = 200$  GeV as a function of  $p_T$  and for different  $x_F$  bins. Data are from [63]. Predictions for the Sivers effect in the GPM approach are also shown.

We mention here that a preliminary study adopting the parameterizations of the Sivers function extracted from the azimuthal asymmetries observed in SIDIS (see section 5.5.2) leads to a much better agreement with BRAHMS data, still preserving a fair description of STAR data [233].

Let us focus now on the mid-rapidity region. As already mentioned above, in this region only the Siverson effect could generate a sizable SSA in the GPM approach. In particular, at the large c.m. energies reached at RHIC, the potentially dominant contribution should come from the gluon Siverson function (GSF). This region is indeed covered by the PHENIX experiment, whose recent data are consistent with a vanishing SSA [66]. This potential gluon dominance, together with the (almost) vanishing of all possible contributions to  $A_N$  other than the Siverson effect, allow to interpret the data – showing tiny values of  $A_N$  – in terms of useful constraints (upper bounds) on the magnitude of the GSF. As  $p_T$  grows, however,  $x_a^{\min}$ , the minimum value of the parton light-cone momentum fraction in the polarized proton, increases and the dominance of the gluonic channels becomes less prominent.

For the same reason, another set of data, for comparable rapidity and  $p_T$  ranges [51] but at much lower energy,  $\sqrt{s} \simeq 20$  GeV, cannot give significant constraints on the GSF. In this case, in fact, even at the smallest  $p_T$  values  $x_a^{\min}$  remains large and a possible mixing with quark initiated contributions cannot be excluded, see Fig. 7 (left panel). Different scenarios have been considered in Ref. [236], where a significant constraint on the GSF has been obtained, see Fig. 7 (right panel). For instance, even allowing for the largest possible cancelations coming from maximized, sea-quark Siverson contributions (still totally unknown), in the small  $x$  region (below 0.05), where the gluon plays a relevant role, the GSF is bounded to be less than 30% in size of its positivity bound (twice the unpolarized gluon distribution).

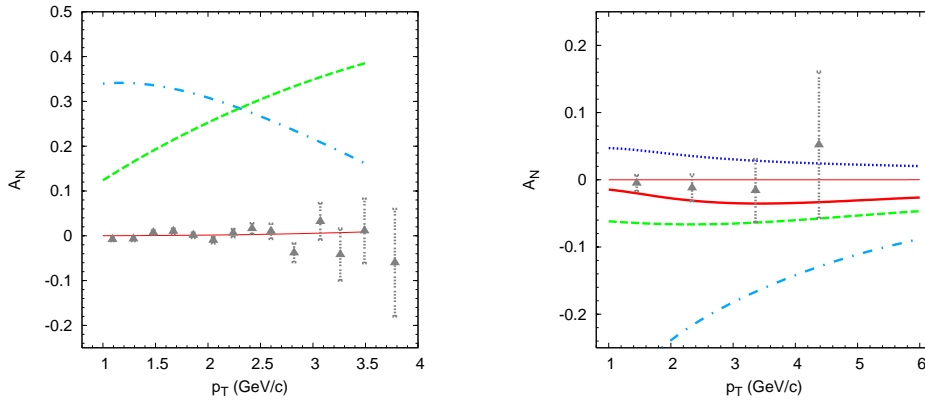


Figure 7:  $A_N(p^\uparrow p \rightarrow \pi^0 + X)$  at mid-rapidity vs.  $p_T$ . Left panel: E704 data [51] at  $\sqrt{s} \simeq 20$  GeV. Maximized contributions, in magnitude, from the quark (dashed line) and gluon (dot-dashed line) Siverson functions. Right panel: PHENIX data [66] at  $\sqrt{s} = 200$  GeV. Contributions of: maximized GSF (dot-dashed line); sea (maximized) + valence quark Siverson functions (dotted line); constrained GSF (dashed line). Overall total Siverson effect (thick, solid line). In both plots the thin, solid lines show the predictions using the  $u$  and  $d$  Siverson functions extracted in Ref. [218]. Unpolarized PDF and FF sets: MRST01-KKP.

As an indirect tool to constrain the gluon Siverson function one could also consider the Burkardt sum rule of Eq. (23) [184]. As discussed in section 3, this rule states that the net transverse momentum due to the Siverson mechanism must vanish. Strict use of the BSR would require integration over the full  $x$  range, including the poorly known low  $x$  region, of each single parton Siverson function, which might even result in divergences. For this reason at the present stage it can be only adopted as a useful cross-check. Similar conclusions on the smallness of a possible GSF have been reached in a different context in Ref. [237]. Let us also mention that in Ref. [238] the BSR, together with the large  $N_c$  limit of QCD, was used to predict a suppression of the gluon Siverson function w.r.t. the non-singlet quark Siverson distribution at not too small  $x$ .

Another interesting process to study is inclusive kaon production in  $p^\uparrow p \rightarrow K + X$ , in particular for charged kaons, where hopefully one could learn more on T-odd mechanisms in the sea-quark sector.

To begin with, one can figure out what SSA's would result in the valence-like picture for the quark Siverson function discussed above. Consider for the sake of clarity the forward region (large positive  $x_F$ ). In this case,  $A_N(K^+)$  should be quite similar to  $A_N(\pi^+)$ : in both cases, a valence  $u$  quark from the incoming proton fragments dominantly into the observed meson. This qualitative expectation of the TMD generalized parton model works, in principle, for the Siverson as well as the Collins effects, and holds true for the twist-three collinear formalism and for the orbiting valence quark model discussed in section 3. However, the  $K^-$  case is more subtle, since the valence  $u, d$ , quarks from the proton are both subleading in the fragmentation process. Therefore, the expected SSA is more sensitive to the details of the approach. We already said in section 3 that in the orbiting valence quark model one would get a zero SSA for  $K^-$ . This would also be the case for the Collins effect in the model of Artru [128], because the specific Lund string model utilized gives a vanishing Collins function for subleading fragmentation. On the other hand the Siverson effect, involving unpolarized TMD fragmentation functions, would give a positive and, depending on the FF set adopted, sizable SSA [125]. This somehow “unexpected” result for  $A_N(K^-)$  comes from a non negligible unfavoured  $u \rightarrow K^-$  fragmentation function and the fact that, at large  $x$ , the (positive)  $u$  quark Siverson function is bigger in size than that for a  $d$  quark. This expectation seems to be confirmed by recent preliminary BRAHMS results (see Fig. 8), although the theoretical predictions still underestimate the data. This discrepancy could be reduced by including the sea-quark Siverson effect, or the non negligible contributions of the Collins effect from favoured and unfavoured FF's.

Similar results have been obtained in the global fit based on the twist-three approach, adopting chiral-even twist-three distributions [192]. See also section 5.5.2 for further discussion on the kaon case.

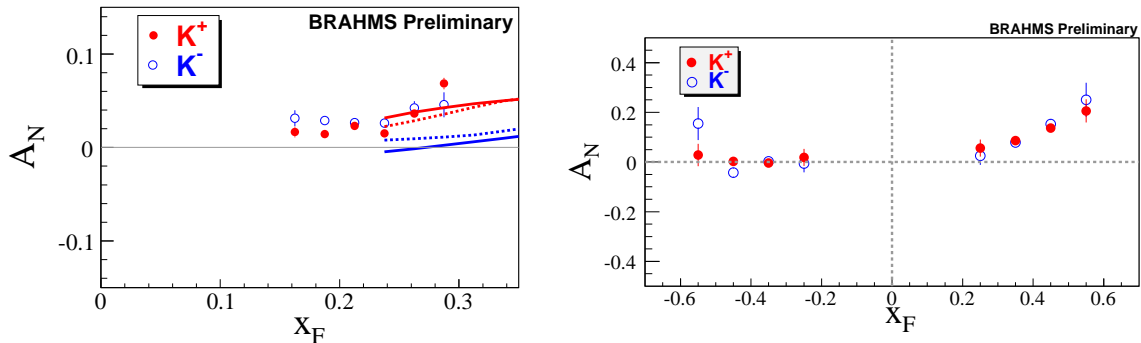


Figure 8:  $A_N$  for inclusive charged kaon production in  $pp$  collisions, at  $\sqrt{s} = 200$  GeV (left) and  $\sqrt{s} = 62$  GeV (right) as a function of  $x_F$ . Dotted line: GPM, Siverson effect; solid line: twist-three approach. Data are from [72].

Another useful tool to access specific spin and TMD effects is the study of heavy meson production in  $pp$  collisions.  $D$  mesons originate predominantly from the fragmentation of  $c$  or  $\bar{c}$  quarks, which at LO can be created either via  $q\bar{q}$  annihilation,  $q\bar{q} \rightarrow c\bar{c}$ , or via the gluon fusion process,  $gg \rightarrow c\bar{c}$ . In this case the heavy quark mass cannot be neglected. This somehow makes the structure of the kernels in the helicity formalism of the GPM more involved. The main difference is that now helicity conservation is broken in the hard scattering amplitudes. Once again, a detailed study including the exact  $\mathbf{k}_\perp$  kinematics shows that upon  $\mathbf{k}_\perp$  integration the azimuthal phase factors suppress all allowed terms but the Siverson contribution.

In Ref. [239] it was shown how at RHIC energies,  $\sqrt{s} = 200$  GeV, and  $p_T$  roughly in the range  $1 \div 3$  GeV/ $c$ , the gluon fusion mechanism gives the dominant contribution to the  $p^\uparrow p \rightarrow D + X$  process, up to  $x_F \simeq 0.6$ , opening the possibility for a direct access to the gluon Siverson function. At lower energies,

like those reachable at the proposed PAX experiment at GSI,  $\sqrt{s} = 14$  GeV, the  $q\bar{q}$  annihilation process becomes dominant, giving the opportunity to access directly the quark Sivers function. For polarized  $p\bar{p}$  collisions at PAX the potential QSF dominance would be even more dramatic [240].

Let us finally mention here that the inclusion of a possible intrinsic charm component in the proton, as originally proposed by Brodsky *et al.* [241] (see e.g. Ref. [242] and references therein), could change drastically this picture. In this case, in fact,  $c$ -quark initiated processes and other TMD effects could play a role. This interesting topic would certainly deserve a more detailed study.

### 5.1.2 Prompt photon production

The inclusive production of direct photons in  $pp$  collisions is certainly another useful tool to access  $\mathbf{k}_\perp$ -dependent PDF's. At LO, only two partonic subprocesses,  $q(\bar{q})g \rightarrow \gamma q(\bar{q})$  and  $q\bar{q} \rightarrow \gamma g$ , contribute. The polarized differential cross section can be obtained from the general case, Eq. (33), by replacing the fragmentation function by a product of two Dirac delta functions,  $\hat{D}_{C/c}(z, \mathbf{k}_\perp) \rightarrow \delta(z)\delta(\mathbf{k}_\perp)$ .

There are in principle three mechanisms that could contribute to the photon SSA: the quark Sivers effect for both subprocesses, the gluon Sivers effect via the Compton-like subprocess, and the Boer-Mulders effect (coupled with the transversity PDF) via  $q\bar{q}$  annihilation. Notice also that electromagnetic couplings will enhance the  $u$ -flavour contributions. For  $x_F > 0$ , and fixed  $p_T$ , the dominant contribution to  $A_N$  should come from the quark Sivers effect. Adopting the QSF parameterizations extracted from the fit to  $A_N(p^\uparrow p \rightarrow \pi + X)$ , in the GPM one gets a positive SSA, rising at larger  $x_F$ , both at  $\sqrt{s} = 20$  GeV and  $\sqrt{s} = 200$  GeV [218]. Notice that the collinear twist-three approach [190, 191, 192], while leading to a similar description of  $A_N$  for pion production, predicts a photon SSA opposite in sign. The reason is just the opposite sign entering the hard scattering part for the dominant channel in the twist-three formalism. In this respect, this process can be considered as a good tool to discriminate between the two approaches.

Concerning the backward rapidity region, in Ref. [243] it was argued that at RHIC energies and large  $p_T$  values (around 20 GeV/ $c$ )  $A_N$  would be directly sensitive to the GSF. In fact, in a more quantitative approach, with proper treatment of the noncollinear kinematics and the relative azimuthal phases, it has been found that the best kinematical region to look for the GSF at RHIC energies is at negative  $x_F$  and  $p_T$  values around 5-8 GeV/ $c$ . In this region the contribution to  $A_N$  from the GSF could be as large as 10%, whereas the other mechanisms would give at most a 1% contribution [240].

An even more interesting case is the photon SSA at lower energies, like for instance at the PAX-GSI experiment. In this case, the QSF gives the main contribution in the forward as well as in the central rapidity region, whereas again the negative  $x_F$  region is potentially dominated by the GSF. Moreover, by colliding polarized protons off unpolarized antiprotons, another effect could become accessible: namely the Boer-Mulders function,  $\Delta^N f_{q^\uparrow/p}$  (or  $h_1^\perp$ ), coupled to the transversity distribution. In this configuration the Compton-like subprocess is suppressed because: *i*) the minimum value of  $x$  reached is still large, being of the order of  $2p_T/\sqrt{s}$ ; *ii*) the  $\bar{q}$  in  $\bar{p}$  has a valence component. As a result, we have a clear dominance of the  $q\bar{q}$  subprocess. Moreover, the integration over the  $\mathbf{k}_\perp$ -dependent phases does not wash out the partonic double spin asymmetry. By using the parameterizations so far extracted for the QSF one gets a photon SSA of the order 5-10% for  $p_T$  around 2-4 GeV/ $c$ , while the (maximized) Boer-Mulders effect might give  $A_N$  values of the order up to 20%. This means that in this kinematical regime a large photon SSA could be a clear signal in favour of the Boer-Mulders effect, then giving another way to access the transversity distribution [240].

### 5.1.3 Transverse $\Lambda$ polarization in unpolarized $pp$ collisions

Another longstanding problem of spin phenomena in particle physics is the transverse polarization of hyperons produced in unpolarized hadronic collisions,  $P_T(Y)$ , that can also be considered as a SSA. A

huge amount of experimental results has been collected, in particular for the  $\Lambda$  particle. These data show that transverse hyperon polarizations can be quite sizable. Their behaviour as a function of  $x_F$  and  $p_T$  is very peculiar and difficult to explain, as well as the differences in size and sign among different hyperons. Several nonperturbative models have been proposed, but none of them is able to give a comprehensive description of all data. We will not address in detail this subject. A quick survey of its experimental and theoretical aspects can be found in Refs. [6], [8] respectively, and a more extensive treatment in the references quoted therein. Most of the experimental data are at fixed target and in the very forward regime. For this reason, a pQCD approach to  $P_T(Y)$  was not seriously considered until recently. In fact, the description of the unpolarized cross section data [2] is difficult in pQCD, even when, as in the GPM approach, full  $\mathbf{k}_\perp$  effects are included (notice that also in this case the leading term in the unpolarized cross section is given by the usual convolution of TMD unpolarized PDF's and FF's). More precisely, data on unpolarized cross sections can be described only partially and in a limited kinematical range, corresponding to not too low  $p_T$  and not too large  $x_F$ . Limiting to the  $\Lambda$  case, for fixed target experiments the kinematical regions where data for the unpolarized cross section and for the  $\Lambda$  polarization are collected overlap only partially. A better agreement is found with the recent STAR data on unpolarized cross sections at larger energies [248].

In the GPM approach, focusing on the  $qq \rightarrow qq$  processes, there are essentially two possible sources for the  $\Lambda$  polarization (see also the end of section 4): the Boer-Mulders function from one of the incoming protons convoluted with a spin transfer partonic factor and the transverse fragmentation function (the analogue, in the fragmentation sector, of the transversity function); the so-called (chiral-even) *polarizing* fragmentation function ( $\Delta^N D_{\Lambda^\uparrow/q}$ ), coupled with unpolarized PDF's and partonic cross sections. This last mechanism is somewhat the analogue of the Sivers effect in the fragmentation process. An ongoing preliminary analysis [217] seems to show that indeed only the polarizing effect can lead to sizable values of  $P_T(\Lambda)$ . This study basically confirms the main findings of Ref. [137] where, adopting a more simplified planar kinematics and a simple parameterization of the polarizing FF, the main features of  $P_T(\Lambda)$  (including its size) were reproduced (see Fig. 9).

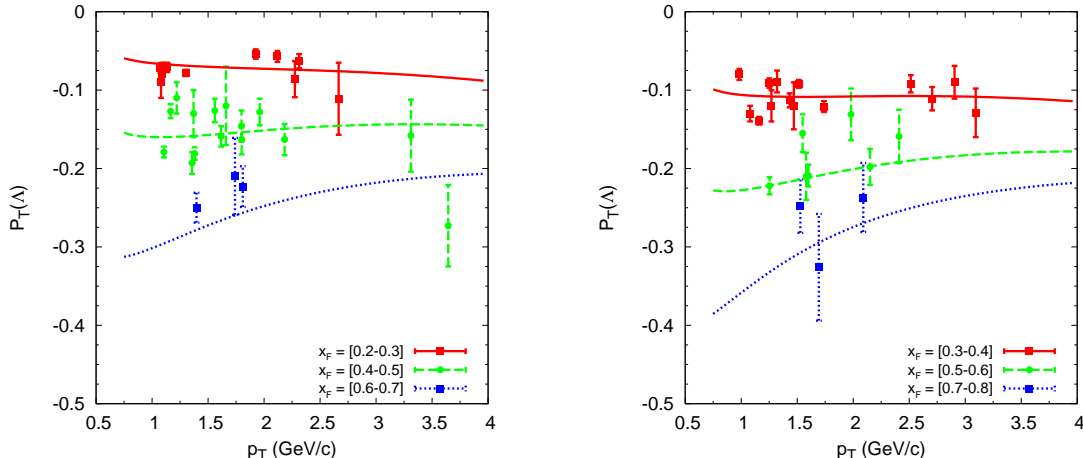


Figure 9: Best fit [137] to  $P_T(\Lambda)$  data from  $p$ - $Be$  reactions vs.  $p_T$  and for different  $x_F$  bins. Data [244, 245, 246] are collected at two different c.m. energies,  $\sqrt{s_{NN}} \simeq 27$  GeV and  $\sqrt{s_{NN}} \simeq 39$  GeV. Theoretical curves are evaluated at the mean  $x_F$  value in the bins, and at  $\sqrt{s_{NN}} = 27$  GeV; the results change very little with the energy. Unpolarized  $\Lambda$  FF set: [247].



## 5.2 SSA's for double inclusive production in $pp$ collisions

Another important source of information on TMD distributions could come from the study of  $pp \rightarrow h_1 h_2 + X$  and  $pp \rightarrow \text{jet jet} + X$  processes. Indeed, by considering specific kinematical configurations they have been advocated as a tool to extract the gluon Sivers function. In Ref. [249] they considered the almost back-to-back asymmetric jet correlation in the mid-rapidity region in the GPM approach and showed that a sizable asymmetry could be observed at RHIC, mainly driven by the gluon Sivers effect. In Refs. [154, 164] a more complete treatment was presented, including gauge-links effects and all possible spin and  $\mathbf{k}_\perp$  dependent distributions at leading twist for double inclusive hadron and jet production in  $pp$  collisions. Recent data on jet-jet correlations have been collected at RHIC showing an almost vanishing asymmetry [62]. A possible explanation of these results could come from the gauge-links effects properly incorporated in the TMD approach [164].

A recent phenomenological study for the SSA in  $pp \rightarrow \gamma \text{jet} + X$  [163] (see also [250]) has addressed the comparison between the approach based on the generalized parton model and the colour-gauge-invariant QCD formalism, where the gauge links are believed to be responsible for initial/final-state interactions (in other words, to be the source of the phase shifts required to generate naively T-odd effects). For hadronic processes different from SIDIS and DY, for instance  $p^\dagger p \rightarrow \text{hadrons}$ , the Wilson line structure becomes more intricate [153]. It is therefore more challenging to derive clear-cut predictions for the sign of the SSA in these processes [164]. Again, in direct photon production the reduced number of channels and the colourless structure of the photon greatly simplify the analysis.

Due to the intrinsic parton motions in the initial hadrons, in the process  $pp \rightarrow \gamma \text{jet} + X$  the photon and the jet are only approximately back-to-back in the plane transverse to the beam collision direction. In other words, the azimuthal angles of the photon and jet transverse momenta,  $\mathbf{K}_{\gamma\perp}$  and  $\mathbf{K}_{j\perp}$ , are related by  $\phi_j - \phi_\gamma = \pi + \delta\phi$ , where  $\delta\phi$  just originates from  $\mathbf{k}_\perp$  effects. By defining suitable weighted azimuthal moments of  $\mathbf{K}_{\gamma\perp}/M$ , sensitive to these effects, in Ref. [163] it has been shown how one could check the role of the gauge-links, that in this simple process should only appear as numerical prefactors for the standard LO partonic cross sections involved.

In a simplified partonic kinematics, keeping only  $\mathcal{O}(k_\perp/K_{\gamma\perp})$  effects, and suitably choosing the kinematical configuration (that is, large positive values of the photon pseudorapidity,  $\eta_\gamma$ , small or negative values for the jet one,  $\eta_j$ ) it has been shown that for RHIC energies the quark-Sivers mechanism dominates. Moreover, the weighted moment of interest could reach values of 4-5% in size. Notice that fixing the sign of the valence quark Sivers functions from SIDIS, the GPM approach would predict an opposite sign w.r.t. the colour-gauge-invariant QCD formalism.

The experimental investigation of the sign of the weighted moment, discriminating among these predictions, seems to be accessible at RHIC and could have the same significance as the measurement of the relative sign of the Sivers effect in SIDIS and DY processes. However, a word of caution is needed here and for the double inclusive processes discussed above, being the validity of factorization for these processes still under debate, see Refs. [160, 161, 162] and section 3.1.1.

## 5.3 Azimuthal asymmetries and SSA's in Drell-Yan processes

The Drell-Yan process is definitely another valuable tool to access naively T-odd TMD effects in the PDF sector and discriminate among them. Starting already from the unpolarized cross section, we can learn on  $\mathbf{k}_\perp$  effects in PDF's by studying the  $q_T$  spectrum of the final lepton pair [218]. But there is much more to learn from the DY process. Indeed the unpolarized differential cross section, as measured in the so-called Collins-Soper frame [120] for the process  $\pi^- N \rightarrow \mu^+ \mu^- + X$ , where  $N$  is either deuterium or tungsten, using a  $\pi^-$  beam with various energies in the range of 150-300 GeV [102, 103, 106],

$$\frac{1}{\sigma} \frac{d\sigma}{d\Omega} = \frac{3}{4\pi} \frac{1}{\lambda + 3} \left( 1 + \lambda \cos^2 \theta + \mu \sin 2\theta \cos \phi + \frac{\nu}{2} \sin^2 \theta \cos 2\phi \right), \quad (72)$$

shows remarkably large values of  $\nu$  (see Fig. 10 for the proper definition of the angles).

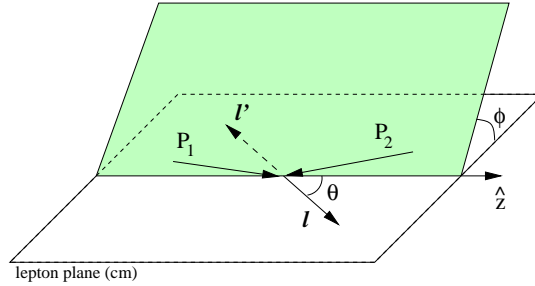


Figure 10: Kinematics of the Drell-Yan process in the lepton center of mass frame.

Leading and next-to-leading order perturbative QCD corrections cannot explain these results. Several explanations have been proposed, e.g. higher twist effects [251, 252] and the role of QCD-vacuum structure in hadron-hadron scattering [253, 254, 255].

In the context of a pQCD approach with TMD distribution functions, such a large  $\cos 2\phi$  azimuthal dependence can arise at *leading order* only from a convolution of two Boer-Mulders functions,  $\Delta^N f_{s_y/A}$  or  $h_1^\perp$ . In Ref. [136] it was shown how by a suitable parametrization of this naively T-odd function, under some simple but reasonable assumptions a description of the  $\cos 2\phi$  asymmetry could be obtained, see Fig. 11 (left panel). More recently, the  $\cos 2\phi$  asymmetry in the unpolarized DY process  $p\bar{p} \rightarrow \mu^+\mu^- X$  at  $s = 50 \text{ GeV}^2$ , has been studied in detail in the same framework but using a more realistic model for the Boer-Mulders function in the quark-diquark spectator approach [256]. Notice that the negligible  $\cos 2\phi$  dependence observed recently for DY dimuons in  $pD$  collisions [107] could imply an almost vanishing sea-quark Boer-Mulders function.

Considering the transverse SSA in the Drell-Yan process  $p^\uparrow p \rightarrow \ell^+\ell^- + X$ , again two TMD mechanisms could play a role: the Sivers effect and the Boer-Mulders effect, which involves also the transversity distribution. The main difference with respect to the inclusive processes considered above, like  $pp \rightarrow h + X$ , is that in this case the measurement of the lepton-pair angular distribution automatically allows to select one specific effect. In Ref. [136] the full structure of the polarized cross section, at  $\mathcal{O}(k_\perp/M_h)$ , has been presented. From there, one can easily see that integrating over the lepton-plane angular variables, only the Sivers effect survives in the kinematical regime where  $k_\perp \simeq q_T \ll M$  ( $M$  here is the invariant mass of the lepton pair). Notice that other mechanisms that could also generate SSA's in the Drell-Yan process [257, 258, 259, 260], based on higher twist quark-gluon correlation functions in a generalized pQCD factorization theorem [191], lead to expressions of  $A_N$  which, being dependent on the angle between the proton polarization direction and the plane containing the final lepton pair [120], vanish upon corresponding angular integrations. In Ref. [261], considering in the hadronic c.m. frame the polarized differential cross section  $d\sigma/dM^2 dy d^2\mathbf{q}_T$ , where  $y$  is the rapidity of the lepton pair, a phenomenological analysis of the Sivers asymmetry has been performed in great detail. By adopting the Sivers functions as extracted from pion production data (with the reversed sign, see below) preliminary predictions for  $A_N$  at RHIC were given, see Fig. 11 (right panel). A factorized Gaussian ansatz for the  $\mathbf{k}_\perp$ -dependent PDF's, with some reasonable approximations, allowed to perform analytically the integration over the transverse parton momenta, resulting in a simple factorized expression for  $A_N$ .

Let us comment on the sign of the SSA originating from the Sivers effect in the Drell-Yan process. As already discussed in section 3, if the Sivers effect is due to initial/final state interactions and colour-gauge invariance (Wilson lines) the corresponding asymmetry should have opposite sign in Drell-Yan and SIDIS processes, respectively because of past and future-pointing gauge-links, related, somehow, to  $s$ -channel and  $t$ -channel elementary reactions. On the other hand, the SSA in the  $p^\uparrow p \rightarrow \pi + X$  process at large positive  $x_F$  and moderately large  $p_T$  is dominated by  $t$ -channel, quark initiated processes. Therefore, one can tentatively assume that the Sivers function as extracted from pion SSA data should

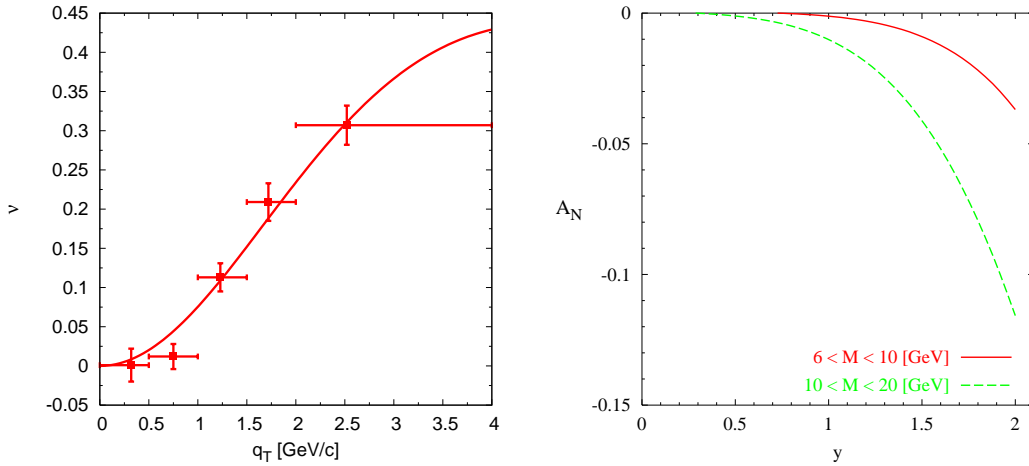


Figure 11: Left panel: Data on the  $\nu$  coefficient in Eq. (72) [102, 103] at 194 GeV, vs.  $q_T$ , compared with the fit of Ref. [136]. Right panel: Maximized  $A_N$  for the DY process, at RHIC energies,  $\sqrt{s} = 200$  GeV, as a function of the rapidity  $y$  and for two ranges of the invariant mass. The asymmetry is practically negligible in the range  $y < 0$ . PDF set: MRST01.

contribute with opposite sign to DY processes. Notice that this assumption is *not* a prediction of the GPM approach, which would consider the Siverson function as universal, but rather an attempt to incorporate in it additional information coming from different approaches not yet directly applicable to the  $p^\uparrow p \rightarrow \pi + X$  process. Given these considerations, even a simple comparison of the sign of these estimates with data might be highly significant.

Notice also that, as we will see below, the valence-quark Siverson functions as extracted by SIDIS data have the same sign as those extracted from  $pp \rightarrow \pi + X$ : this somehow supports the sign change adopted for DY in this preliminary study.

Predictions for SSA's in DY processes based on the extraction of the Siverson effect from SIDIS [262] (see also section 5.5.2) have been discussed in Refs. [238, 250, 263, 264]. As pointed out in Ref. [264], the Siverson asymmetry at RHIC should be strongly sensitive to the sea-quark Siverson distributions.

We finally stress that the study of Ref. [261] included a combined description, in the GPM approach, of the unpolarized Drell-Yan cross sections.

Another promising idea in the study of SSA's has been proposed in Ref. [265], where they considered electroweak Drell-Yan processes. In this case by looking at a  $\nu_\ell - \ell$  lepton pair one selects a  $W$ -exchange channel and therefore only one parton helicity state contributes. The transversity function that could couple to the Boer-Mulders effect is therefore absent. This process would then give another way to directly access the Siverson effect.

## 5.4 $e^+e^-$ annihilation in two nearly back-to-back hadrons

Hadron production in  $e^+e^-$  collisions would be in principle the most valuable and clean process for the study of TMD polarized fragmentation functions, like the Collins function, thanks to the lack of corresponding TMD effects in the initial state. Unfortunately, there is not in the process  $e^+e^- \rightarrow q\bar{q}$  any transverse polarization transfer to a single, on-shell massless quark. Therefore, it is not possible to observe the Collins effect individually by measuring, e.g., the asymmetry in the distribution around the jet trust axis (i.e. the fragmenting quark direction) of a hadron species (typically pions) produced in the quark fragmentation. Indeed, in hadron production in  $e^+e^- \rightarrow q\bar{q} \rightarrow 2$  jets events, the Collins effect

can only be observed when the quark and the antiquark are considered *simultaneously*. As reported in section 2.3.3, the Belle Collaboration at the KEK-B asymmetric-energy  $e^+e^-$  storage rings has in fact performed a measurement of azimuthal asymmetries in hadron-hadron correlations for inclusive charged dihadron production,  $e^+e^- \rightarrow \pi^+\pi^- + X$  [109]. This asymmetry has been interpreted as a direct measure of the Collins effect, involving however (and unavoidably) the convolution of two Collins functions. Two experimental methods have been used to extract the azimuthal asymmetry from raw data: 1) The first method, requiring the knowledge of the two-jet thrust axis, corresponds to the kinematical setup shown in the left plot of Fig. 12 and gives rise to a  $\cos(\phi_1 + \phi_2)$  modulation in the dihadron yields, the  $A_{12}$  asymmetry discussed below and shown in Fig. 13 ( $\phi_1, \phi_2$  are the azimuthal angles of the two hadron momenta); 2) The second method, leading to the asymmetry  $A_0$  (see Fig. 13), does not rely on the knowledge of the thrust axis and corresponds to the setup shown in the right plot of Fig. 12.

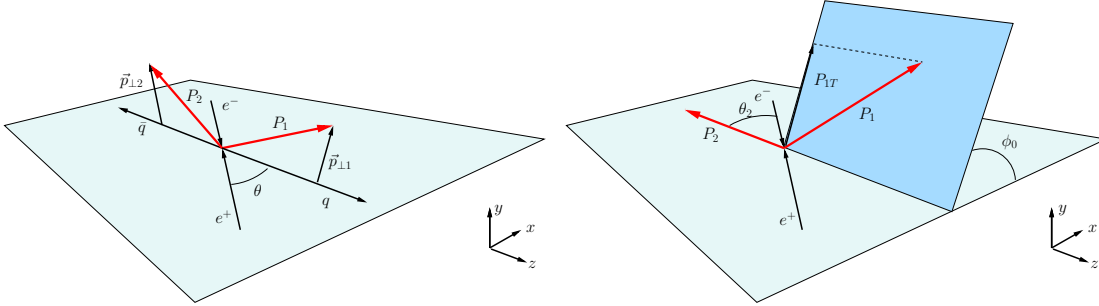


Figure 12: Kinematics for the  $e^+e^- \rightarrow h_1h_2 + X$  process, according to two different configurations considered by Belle and discussed in the text: setup 1 (left) and setup 2 (right).

On the theoretical side this azimuthal asymmetries have been studied in Ref. [266], where their phenomenological interest was pointed out, and more recently in Refs. [267, 268], where Belle results were used to extract additional information on the Collins function. Both Refs. [266, 267] have used in their analysis the setup 2. In Ref. [267], utilizing the formalism of Ref. [266] and a quark soliton model for the transversity distribution, the Collins function was extracted by fitting the HERMES and COMPASS data on azimuthal spin asymmetries in the SIDIS process  $\ell p^\dagger \rightarrow \ell' h + X$  (see next section). The parameterization extracted for the Collins function was shown to be compatible with Belle results on  $e^+e^- \rightarrow \pi^+\pi^- + X$ . In Ref. [268] both kinematical setups were considered, and SIDIS and  $e^+e^-$  data were combined to get a simultaneous fit of the Collins and the transversity distribution functions.

As an illustration, let us briefly summarize the case of setup 1, which is more simple to figure out. Within the GPM approach and the helicity formalism, the differential cross section for dihadron production can be written as (see Fig. 12 for notation):

$$\frac{d\sigma^{e^+e^- \rightarrow h_1h_2+X}}{dz_1 dz_2 d^2\mathbf{p}_{\perp 1} d^2\mathbf{p}_{\perp 2} d\cos\theta} = \frac{3\pi\alpha^2}{2s} \sum_q e_q^2 \left\{ (1 + \cos^2\theta) D_{h_1/q}(z_1, p_{\perp 1}) D_{h_2/\bar{q}}(z_2, p_{\perp 2}) + \frac{1}{4} \sin^2\theta \Delta^N D_{h_1/q^\dagger}(z_1, p_{\perp 1}) \Delta^N D_{h_2/\bar{q}^\dagger}(z_2, p_{\perp 2}) \cos\phi_1 \cos\phi_2 \right\}. \quad (73)$$

The azimuthal asymmetry, as defined by the Belle collaboration (setup 1), can be obtained from here by the following steps: *i*) Performing a change of angular variables from  $(\phi_1, \phi_2)$  to  $(\phi_1, \phi_1 + \phi_2)$  and then integrating over the moduli of the intrinsic transverse momenta,  $p_{\perp 1}, p_{\perp 2}$ , and over the azimuthal angle  $\phi_1$ ; *ii*) Normalizing the result to the azimuthally averaged cross section; *iii*) Taking the ratio  $R$

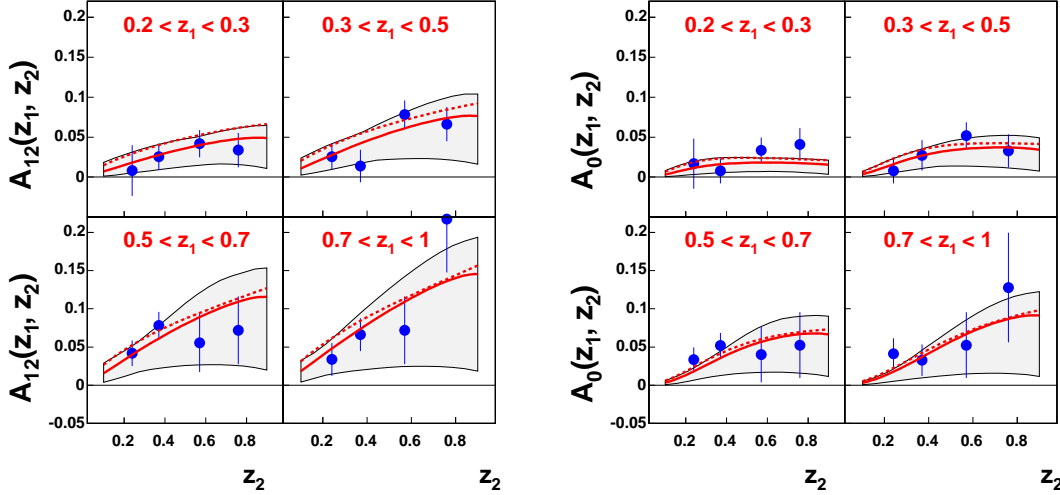


Figure 13: Belle data on two azimuthal correlations in  $e^+e^- \rightarrow \pi\pi + X$  processes [109]. Solid lines: results obtained by fitting the  $A_{12}$  asymmetry [268]; dashed lines: results obtained by fitting the  $A_0$  asymmetry, according to the setup of Fig. 12 (right panel) [268]. The shaded area corresponds to the theoretical uncertainty on the parameters. FF set: K.

of unlike-sign (U) to like-sign (L) pion-pair production, in order to eliminate false asymmetries:

$$R \simeq 1 + \cos(\phi_1 + \phi_2) A_{12}(z_1, z_2), \quad \text{where} \quad A_{12}(z_1, z_2) = \frac{1}{4} \frac{\langle \sin^2 \theta \rangle}{\langle 1 + \cos^2 \theta \rangle} (P_U - P_L), \quad (74)$$

the angle  $\theta$  is averaged over a range of values given by the detector acceptance,

$$P_{U(L)} = \frac{\sum_q e_q^2 \Delta^N D_{\pi^+/q^\dagger}(z_1) \Delta^N D_{\pi^{-(+)}/\bar{q}^\dagger}(z_2)}{\sum_q e_q^2 D_{\pi^+/q}(z_1) D_{\pi^{-(+)}/\bar{q}}(z_2)}, \quad (75)$$

and

$$\Delta^N D_{h/q^\dagger}(z) = \int d^2 \mathbf{p}_\perp \Delta^N D_{h/q^\dagger}(z, p_\perp) = \int d^2 \mathbf{p}_\perp \frac{2p_\perp}{zm_h} H_1^{+q}(z, p_\perp) = 4 H_1^{\perp(1/2)q}(z). \quad (76)$$

In this last equation, the relationship among the involved moments of the Collins function, as defined in Refs. [267, 268], has been also given. As an example, in Fig. 13 we show the quality of the fit to the asymmetry, as defined by the Belle Collaboration for the two experimental setups, according to Ref. [268]. This allowed to extract the first independent parameterization of the Collins function, that was then used to extract, in combination with HERMES and COMPASS results on azimuthal asymmetries, the  $u$  and  $d$  quark transversity distribution function (see also section 5.5).

Let us finally remind that preliminary Belle data using the unlike-sign over the all charged (C) pion-pair ratio [110] have been found in agreement with the predictions of Ref. [267].

## 5.5 Semi-inclusive deeply inelastic scattering

Semi-inclusive particle production in deeply inelastic lepton proton scattering,  $\ell p \rightarrow \ell' h + X$ , is a rich case of study over many points of view. By focusing once again on the role of intrinsic parton motion, both in the unpolarized and in the single polarized case, we will show how a consistent picture of various asymmetries observed experimentally can be given.



At variance with inclusive particle production in proton-proton collisions, the standard reference frame adopted to deal with SIDIS scattering is not the lepton-proton c.m. frame, but rather the virtual boson-proton c.m. one, for the process  $\gamma^*p \rightarrow h + X$ . Therefore, one cannot adapt in a straightforward way the kernel structure discussed in section 4 to this case. Indeed, a complete treatment of full  $k_\perp$  effects in SIDIS within the generalized parton model and the helicity formalism is still in progress [269]. What is currently adopted by many groups, using also different approaches, is a first order approximation in a  $(k_\perp/Q)$  power expansion, where  $Q$  is the virtuality of the exchanged boson. In this context, a complete classification for SIDIS cross sections in the TMD approach has recently appeared [87].

As in Drell-Yan processes, in SIDIS the intrinsic parton motions result in azimuthally dependent terms in the unpolarized and single polarized cross sections for hadron production [270, 271, 272, 93, 92].

Let us first of all set the kinematics that we will adopt in the rest of this section. As already said above we work in the  $\gamma^*p$  c.m. frame, shown in Fig. 14. We take the photon and the proton colliding along the  $z$  axis with momenta  $\mathbf{q}$  and  $\mathbf{P}$  respectively; following the so-called ‘‘Trento conventions’’ [73], the leptonic plane coincides with the  $x$ - $z$  plane. We consider the kinematic regime in which  $P_T \simeq \Lambda_{\text{QCD}} \simeq k_\perp$ , where  $P_T = |\mathbf{P}_T|$  is the final hadron transverse momentum. In this region QCD factorization holds [122] and leading order elementary processes,  $\ell q \rightarrow \ell q$ , are dominating: the soft  $P_T$  of the detected hadron is mainly originating from quark intrinsic motion rather than from higher order pQCD interactions, which, instead, would dominantly produce large  $P_T$  hadrons [273, 274, 275].

### 5.5.1 Azimuthal dependence in unpolarized SIDIS

In the QCD factorization scheme the SIDIS cross section for hadron production reads

$$\frac{d^5\sigma^{\ell p \rightarrow \ell h + X}}{dx_B dQ^2 dz_h d^2\mathbf{P}_T} = \sum_q e_q^2 \int d^2\mathbf{k}_\perp f_{q/p}(x, k_\perp) \frac{2\pi\alpha^2}{x_B^2 s^2} \frac{\hat{s}^2 + \hat{u}^2}{Q^4} D_{h/q}(z, p_\perp) \frac{z}{z_h} \frac{x_B}{x} \left(1 + \frac{x_B^2 k_\perp^2}{x^2 Q^2}\right)^{-1}, \quad (77)$$

where the elementary Mandelstam variables are given by ( $\ell$  being the incoming lepton three-momentum)

$$\hat{s} = xs - 2\ell \cdot \mathbf{k}_\perp - k_\perp^2 \frac{x_B}{x} \left(1 - \frac{x_B s}{Q^2}\right) \quad \hat{u} = -x \left(s - \frac{Q^2}{x_B}\right) + 2\ell \cdot \mathbf{k}_\perp - k_\perp^2 \frac{x_B s}{x Q^2}. \quad (78)$$

The on-shell condition for the final quark implies  $x = x_B \left[1 + \sqrt{1 + 4k_\perp^2/Q^2}\right]/2$ .

Notice that  $\mathbf{p}_\perp$  is the transverse momentum of the hadron  $h$  w.r.t. the direction of motion of the fragmenting quark, and  $z$  is the light-cone momentum fraction carried by the produced hadron. After some algebra one can find an exact expression, at all orders in  $(k_\perp/Q)$ , for the light-cone fragmentation variables  $z$  and  $\mathbf{p}_\perp$ , in terms of the usual SIDIS and hadronic variables  $x_B$ ,  $Q^2$ ,  $\mathbf{P}_T$ ,  $z_h = (P \cdot P_h)/(P \cdot q)$ .

Due to these relations among the kinematical variables, momentum conservation and the integration over intrinsic  $\mathbf{k}_\perp$  at fixed  $\mathbf{P}_T = P_T(\cos\phi_h, \sin\phi_h, 0)$  result in a dependence on the azimuthal angle of the produced hadron,  $\phi_h$ , that is the angle between the leptonic and the hadronic planes, see Fig. 14. This azimuthal dependence also appears in the SIDIS cross section. To see this, we will adopt for the  $k_\perp$  dependent PDF's and FF's the usual factorized, flavour independent Gaussian forms (this helps in finding analytical expressions), that is:

$$f_{q/p}(x, k_\perp) = f_{q/p}(x) \frac{1}{\pi\langle k_\perp^2 \rangle} e^{-k_\perp^2/\langle k_\perp^2 \rangle}, \quad D_{h/q}(z, p_\perp) = D_{h/q}(z) \frac{1}{\pi\langle p_\perp^2 \rangle} e^{-p_\perp^2/\langle p_\perp^2 \rangle}. \quad (79)$$

To have a closer look at the azimuthal dependence of the cross section it is instructive, and often quite accurate, to consider Eq. (77) at the order  $\mathcal{O}(k_\perp/Q)$ . In such a case  $x \simeq x_B$ ,  $z \simeq z_h$  and

$$\begin{aligned} \frac{d^5\sigma^{\ell p \rightarrow \ell h + X}}{dx_B dQ^2 dz_h d^2\mathbf{P}_T} &\simeq \sum_q \frac{2\pi\alpha^2 e_q^2}{Q^4} f_q(x_B) D_{h/q}(z_h) \\ &\times \left[1 + (1-y)^2 - 4 \frac{(2-y)\sqrt{1-y} \langle k_\perp^2 \rangle z_h P_T}{\langle p_\perp^2 \rangle Q} \cos\phi_h\right] \frac{1}{\pi\langle p_\perp^2 \rangle} e^{-P_T^2/\langle p_\perp^2 \rangle}, \quad (80) \end{aligned}$$

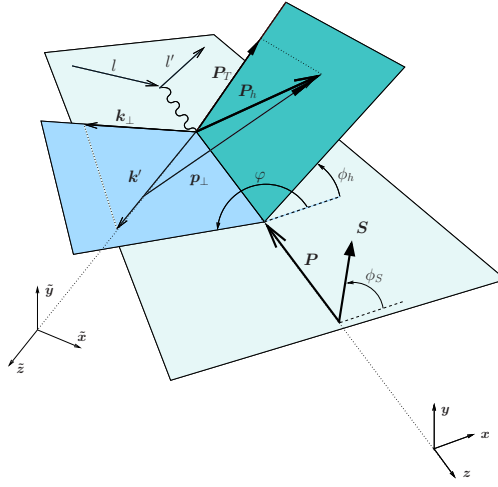


Figure 14: Kinematics of the SIDIS process in the  $\gamma^* - p$  c.m. frame.

where

$$\langle P_T^2 \rangle = \langle p_\perp^2 \rangle + z_h^2 \langle k_\perp^2 \rangle. \quad (81)$$

This approximate result illustrates very clearly the origin of the dependence of the unpolarized SIDIS cross section on the azimuthal angle  $\phi_h$ . As first observed by Cahn [270], such a dependence is directly related to the parton intrinsic motion and vanishes when  $k_\perp = 0$ .

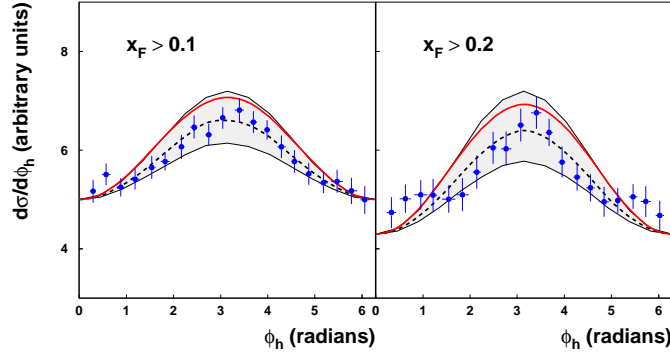


Figure 15: Fits to data [92] on the  $\cos \phi_h$  dependence of the unpolarized SIDIS cross section for charged hadron production. Dashed line: exact kinematics; solid bold line:  $\mathcal{O}(k_\perp/Q)$  calculation. The shadowed region corresponds to varying the parameters  $\langle k_\perp^2 \rangle$  and  $\langle p_\perp^2 \rangle$ , given in Eq. (82) of the text, by 20%. Unpolarized PDF and FF sets: MRST01-K.

Indeed, this effect (also known as *Cahn effect*) has been measured in different SIDIS experiments [92, 93, 94]. In the TMD approach the available data can be used to extract information on the Gaussian widths entering the PDF's and FF's. A systematic analysis, using several sets of experimental data (see Fig. 15 as an example) has been carried out in Ref. [276], leading to the following best values of the parameters:

$$\langle k_\perp^2 \rangle = 0.25 \text{ (GeV}/c)^2 \quad \langle p_\perp^2 \rangle = 0.20 \text{ (GeV}/c)^2. \quad (82)$$

This study leads to an excellent agreement with data for small values of the final hadron transverse momentum,  $P_T$ . However, as somehow expected, it fails in reproducing data at higher  $P_T$ , the turning

point being around  $P_T \sim 1 \text{ GeV}/c$ . A similar conclusion was drawn in Ref. [273]. As discussed in Ref. [277], by including also NLO corrections (like hard gluonic radiation and gluon-initiated elementary scatterings) the agreement with data can be extended at much larger  $P_T$  values. This analysis also confirms that the transition between the regime dominated by nonperturbative, intrinsic transverse momentum effects and the one mainly governed by NLO radiative effects sits around  $P_T \simeq 1 \text{ GeV}/c$ .

We also mention that preliminary results [278] in lattice QCD for the first  $x$ -moment of the unpolarized TMD distribution are compatible with a Gaussian  $k_\perp$  dependence with  $\langle k_\perp^2 \rangle \simeq 0.3 \text{ (GeV}/c)^2$ .

In the context of azimuthal asymmetries in unpolarized SIDIS there could be also a  $\cos 2\phi_h$  dependence. Indeed a contribution to this term is already present in Eq. (77), due to kinematical  $(k_\perp/Q)^2$  effects. Moreover, in the TMD approach including spin effects, an additional contribution appears, coming from the convolution of the Boer-Mulders and the Collins functions [108, 168, 279, 87].

### 5.5.2 Transverse SSA's in SIDIS

Let us now consider the single-transverse polarized cross section  $d\sigma(\ell p^\uparrow \rightarrow \ell' h + X)$ , or  $d\sigma_{UT}$ . Retaining only leading terms in  $\mathcal{O}(k_\perp/Q)$ , in the TMD approach at leading twist the differential cross section can be formally expressed as

$$\frac{d^6 \sigma^{\ell p^\uparrow \rightarrow \ell' h + X}}{dx_B dQ^2 dz_h d^2 \mathbf{P}_T d\phi_S} = A_0 + \frac{1}{2} [A_{\text{Sivers}} + A_{\text{Collins}} + A'_{\text{Collins}}]. \quad (83)$$

The  $\phi_S$  dependence originates from the cross section dependence on the angle between the proton (transverse) polarization vector and the leptonic plane; in the configuration of Fig. 14 this angle is simply  $\phi_S - \phi_{\ell'} \equiv \phi_S$ , having chosen  $\phi_{\ell'}$  to be zero, with  $\phi_S$  varying event by event.

The  $A_0$  term in Eq. (83) is, apart from a factor of  $2\pi$  coming from the  $\phi_S$  integration, the unpolarized cross section given in Eq. (77) and, in the consistent  $\mathcal{O}(k_\perp/Q)$  approximation, in Eq. (80). The terms  $A_{\text{Sivers}}$  and  $A_{\text{Collins}}$  in Eq. (83) correspond respectively to the Sivers effect and to the Collins effect (involving the  $k_\perp$  dependent transversity distribution,  $\Delta_T q(x, k_\perp)$ ) and are related to the  $A_{UT}^{\sin(\phi_h \pm \phi_S)}$  asymmetries discussed in detail below. The fourth term,  $A'_{\text{Collins}}$ , involving again the Collins function coupled with the  $h_{1T}^\perp$  distribution (in the notation of the Amsterdam group) provides eventually a  $\sin(3\phi_h - \phi_S)$  azimuthal modulation. Only recent preliminary results from COMPASS are available on this observable [86]. The measured asymmetry is compatible with zero within the statistical errors. We will not consider this contribution in the following phenomenological analysis.

Exploiting the helicity formalism, the two interesting additional terms,  $A_{\text{Sivers}}$  and  $A_{\text{Collins}}$ , read

$$A_{\text{Sivers}} \equiv \sum_q e_q^2 \int d^2 \mathbf{k}_\perp \Delta^N f_{q/p^\uparrow}(x, k_\perp) \sin(\varphi - \phi_S) \frac{d\hat{\sigma}}{dQ^2} D_{h/q}(z, p_\perp), \quad (84)$$

$$A_{\text{Collins}} \equiv \sum_q e_q^2 \int d^2 \mathbf{k}_\perp \Delta_T q(x, k_\perp) \frac{d(\Delta\hat{\sigma})}{dQ^2} \Delta^N D_{h/q^\uparrow}(z, p_\perp) \sin(\phi_S + \varphi + \phi_q^h). \quad (85)$$

Let us explain in more detail the above equations.  $\phi_S$  and  $\varphi$  identify the directions of the proton spin,  $\mathbf{S}$ , and of the quark intrinsic transverse momentum,  $\mathbf{k}_\perp$ , see Fig. 14;  $\phi_q^h$  is the azimuthal angle of the final hadron  $h$ , as defined in the helicity frame of the fragmenting quark.  $d\hat{\sigma}/dQ^2$  is the usual unpolarized elementary cross section for the  $\ell q \rightarrow \ell q$  process, see also Eq. (77), while  $(y = Q^2/x_B s)$

$$\frac{d(\Delta\hat{\sigma})}{dQ^2} = \frac{d\hat{\sigma}^{\ell q^\uparrow \rightarrow \ell q^\uparrow}}{dQ^2} - \frac{d\hat{\sigma}^{\ell q^\uparrow \rightarrow \ell q^\downarrow}}{dQ^2} = \frac{4\pi\alpha^2}{Q^4} (1 - y). \quad (86)$$

The Sivers effect comes directly from the possible azimuthal dependence of the number density for unpolarized quarks inside a transversely polarized proton (generically denoted by  $p^\uparrow$ , with  $p^\downarrow$  denoting

the opposite polarization state), that can be written as (see also section 3.1):

$$\hat{f}_{q/p^\uparrow}(x, \mathbf{k}_\perp) = f_{q/p}(x, k_\perp) + \frac{1}{2} \Delta^N f_{q/p^\uparrow}(x, k_\perp) \mathbf{S} \cdot (\hat{\mathbf{P}} \times \hat{\mathbf{k}}_\perp), \quad (87)$$

where the triple product gives in our kinematical configuration the  $\sin(\varphi - \phi_S)$  factor entering Eq. (84). Upon integration over  $\mathbf{k}_\perp$ ,  $A_{\text{Sivers}}$  gets the well known  $\sin(\phi_h - \phi_S)$  azimuthal dependence.

Because of the kinematics, the Collins case is a bit more involved. Here is the transverse spin polarization of the fragmenting quark (as inherited by the initial polarized quark) that originates the possible azimuthal asymmetry in the  $\mathbf{k}_\perp$ -dependent fragmentation process. Namely, for a transversely polarized quark with spin polarization  $\hat{\mathbf{s}}$  and three-momentum  $\mathbf{p}_q$ ,

$$\hat{D}_{h/q,s}(z, \mathbf{p}_\perp) = D_{h/q}(z, p_\perp) + \frac{1}{2} \Delta^N D_{h/q^\uparrow}(z, p_\perp) \hat{\mathbf{s}} \cdot (\hat{\mathbf{p}}_q \times \hat{\mathbf{p}}_\perp). \quad (88)$$

The  $\sin(\phi_S + \varphi + \phi_q^h)$  azimuthal dependence in Eq. (85) arises from the combination of the phase factors appearing in the transversity distribution function, in the non-planar  $\ell q \rightarrow \ell q$  elementary scattering amplitudes, and in the Collins fragmentation function. Neglecting  $\mathcal{O}(k_\perp^2/Q^2)$  terms, one finds

$$\cos \phi_q^h = \frac{P_T}{p_\perp} \cos(\phi_h - \varphi) - z \frac{k_\perp}{p_\perp}, \quad \sin \phi_q^h = \frac{P_T}{p_\perp} \sin(\phi_h - \varphi). \quad (89)$$

The integration upon  $\mathbf{k}_\perp$  results, among other factors, in the well known  $\sin(\phi_h + \phi_S)$  dependence of the Collins effect in SIDIS.

The different azimuthal dependence of the Sivers and the Collins contributions in SIDIS offers indeed a clear separation technique and the possibility to gain valuable information on both of them. This is particularly true for the Sivers mechanism, since the other terms in Eq. (84) are well known. On the other hand, the Collins contribution involves also the still unknown transversity distribution function. We have seen in section 5.4 how a combined analysis of SIDIS results with data on azimuthal asymmetries in  $e^+e^- \rightarrow \pi\pi + X$  processes is of great help in this respect.

To separate the contributions in the polarized cross section coming from the two naively T-odd effects, one defines the moments of the azimuthal asymmetry  $A_{UT}^{\sin(\phi_h \pm \phi_S)}$ , given in Eq. (2), where in this case  $d\sigma(\phi_S)$  corresponds to  $(d^6\sigma^{\ell p^\uparrow \rightarrow \ell' h + X})/(dx_B dy dz_h d^2\mathbf{P}_T d\phi_S)$ , see Eq. (83).

In order to perform analytically all  $k_\perp$  integrations one can choose suitable Gaussian parameterizations for the TMD distributions appearing in the above equations, see Ref. [268]:

$$\Delta_T q(x, k_\perp) = \frac{1}{2} \mathcal{N}_q^T(x) [f_{q/p}(x) + \Delta_L q(x)] \frac{e^{-k_\perp^2/\langle k_\perp^2 \rangle}}{\pi \langle k_\perp^2 \rangle} \quad (90)$$

$$\Delta^N f_{q/p^\uparrow}(z, k_\perp) = 2 \mathcal{N}_q^S(x) f_{q/p}(x) \sqrt{2e} \frac{k_\perp}{M'} \frac{e^{-k_\perp^2/\langle k_\perp^2 \rangle_S}}{\pi \langle k_\perp^2 \rangle} \quad (91)$$

$$\Delta^N D_{h/q^\uparrow}(z, p_\perp) = 2 \mathcal{N}_q^C(z) D_{h/q}(z) \sqrt{2e} \frac{p_\perp}{M} \frac{e^{-p_\perp^2/\langle p_\perp^2 \rangle_C}}{\pi \langle p_\perp^2 \rangle}, \quad (92)$$

where  $\Delta_L q(x)$  is the usual collinear helicity distribution, and

$$\langle k_\perp^2 \rangle_S = \frac{M'^2 \langle k_\perp^2 \rangle}{M'^2 + \langle k_\perp^2 \rangle}, \quad \langle p_\perp^2 \rangle_C = \frac{M^2 \langle p_\perp^2 \rangle}{M^2 + \langle p_\perp^2 \rangle}, \quad (93)$$

with  $|\mathcal{N}_q^{T,S,C}| \leq 1$  to automatically fulfill proper bounds. With these choices one gets

$$A_{UT}^{\sin(\phi_h - \phi_S)}(x, y, z, P_T) \simeq \frac{\Delta\sigma_{\text{Sivers}}}{\sigma_0}, \quad A_{UT}^{\sin(\phi_h + \phi_S)}(x, y, z, P_T) \simeq \frac{\Delta\sigma_{\text{Collins}}}{\sigma_0}, \quad (94)$$

where, omitting a common overall factor,  $2\pi\alpha^2/xy^2s$ , [recall that  $x \simeq x_B$  and  $z \simeq z_h$  at  $\mathcal{O}(k_\perp/Q)$ ],

$$\Delta\sigma_{\text{Sivers}} = \frac{z P_T}{M'} \frac{\sqrt{2e} \langle k_\perp^2 \rangle_S^2}{\langle k_\perp^2 \rangle} \frac{e^{-P_T^2/(P_T^2)_S}}{\langle P_T^2 \rangle_S^2} \left[ 1 + (1-y)^2 \right] \sum_q e_q^2 2\mathcal{N}_q^S(x) f_{q/p}(x) D_{h/q}(z) \quad (95)$$

$$\Delta\sigma_{\text{Collins}} = \frac{P_T}{M} \frac{\sqrt{2e} \langle p_\perp^2 \rangle_C^2}{\langle p_\perp^2 \rangle} \frac{e^{-P_T^2/(P_T^2)_C}}{\langle P_T^2 \rangle_C^2} (1-y) \sum_q e_q^2 \mathcal{N}_q^T(x) \left[ f_{q/p}(x) + \Delta_L q(x) \right] \mathcal{N}_q^C(z) D_{h/q}(z) \quad (96)$$

$$\sigma_0 = 2\pi \frac{1}{\pi \langle P_T^2 \rangle} e^{-P_T^2/(P_T^2)} \left[ 1 + (1-y)^2 \right] \sum_q e_q^2 f_{q/p}(x) D_{h/q}(z), \quad (97)$$

with

$$\langle P_T^2 \rangle_S = \langle k_\perp^2 \rangle_S + z^2 \langle k_\perp^2 \rangle, \quad \langle P_T^2 \rangle_C = \langle p_\perp^2 \rangle_C + z^2 \langle k_\perp^2 \rangle, \quad (98)$$

and  $\langle P_T^2 \rangle$  given in Eq. (81). Eq. (95) shows that  $A_{UT}^{\sin(\phi_h - \phi_S)} = 0$  when  $z = 0$  or  $P_T = 0$ . Analogously, Eq. (96) shows that  $A_{UT}^{\sin(\phi_h + \phi_S)} = 0$  for  $P_T = 0$ .

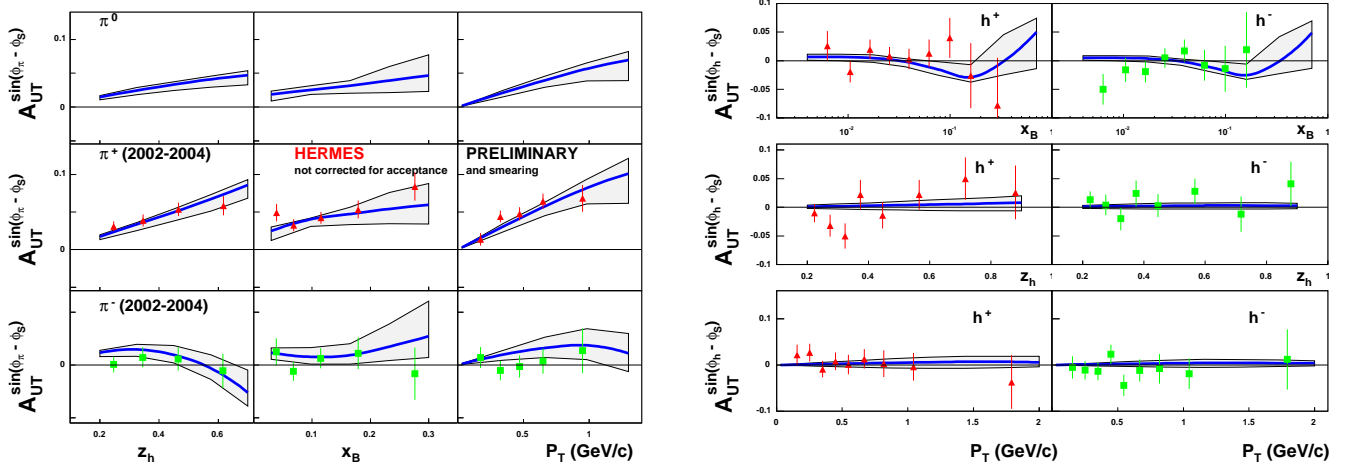


Figure 16: Left panel: HERMES data on  $A_{UT}^{\sin(\phi_\pi - \phi_S)}$  [78] for  $e^+p^\uparrow \rightarrow e^+\pi^\pm + X$ . Right panel: COMPASS data [82] on  $A_{UT}^{\sin(\phi_h - \phi_S)}$  for  $\mu D^\uparrow \rightarrow \mu h^\pm + X$ . Curves are the results of the fit in Ref. [263]. Predictions for  $\pi^0$  asymmetries (left panel, upper plot) are also shown. The shaded areas span a region corresponding to one-sigma deviation at 90% CL. Unpolarized PDF and FF sets: MRST01-K.

Concerning the unknown functions,  $\mathcal{N}_q$ , in Refs. [263, 268] forms like

$$\mathcal{N}_q(x) = N_q x^{a_q} (1-x)^{b_q} (a_q + b_q)^{a_q + b_q} / a_q^{a_q} b_q^{b_q} \quad (99)$$

have been adopted. In particular, for the Sivers function only  $u$  and  $d$  quarks were considered, with a total of 7 free parameters (including  $M'$ ); for the  $u$  and  $d$  quark transversity distributions,  $a_u = a_d$  and  $b_u = b_d$  have been adopted, keeping the flavour distinction only in  $N_q$ , besides the one coming from the flavour structure in Eq. (90) (4 free parameters). Finally, for the Collins function, in the pion case both favoured and unfavoured fragmentation functions have been considered, with the same  $a, b$  but different  $N_{\text{fav}}$  and  $N_{\text{unf}}$  for a total of 5 parameters (including  $M$ ).

The curves obtained by fitting HERMES (COMPASS) data on  $A_{UT}^{\sin(\phi_h - \phi_S)}$  for pion (charged hadron) production are shown in Fig. 16. Preliminary data from HERMES [81] and COMPASS [84, 85] on kaon asymmetries are also available. The corresponding theoretical estimates, adopting the Sivers functions



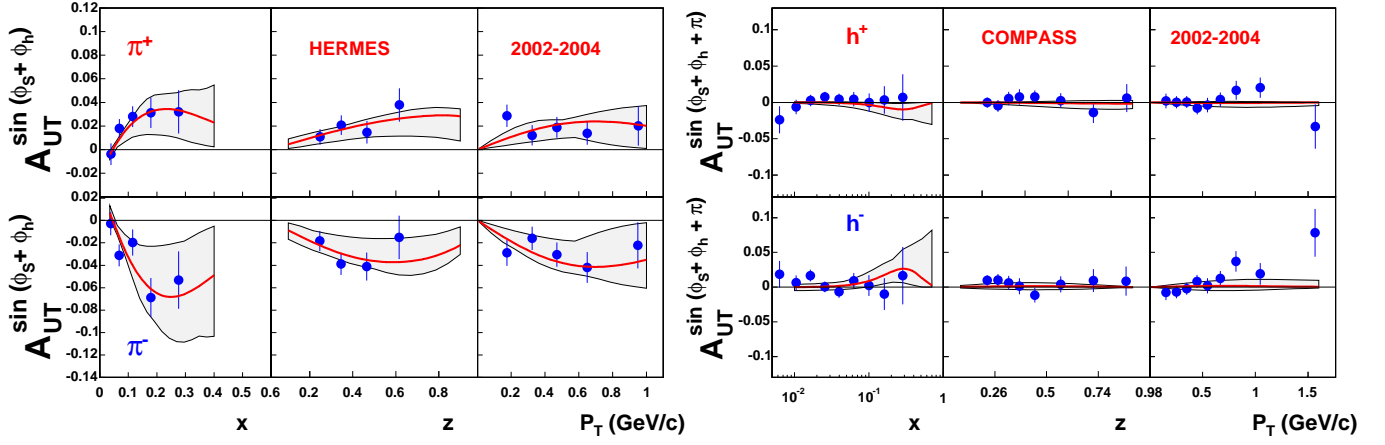


Figure 17: Left panel: HERMES data [78] on the azimuthal asymmetry  $A_{UT}^{\sin(\phi_S+\phi_h)}$  for  $\pi^\pm$  production. Right panel: COMPASS data [83] on  $A_{UT}^{\sin(\phi_S+\phi_h)}$ , for charged hadron production in  $\mu D^\dagger \rightarrow \mu h^\pm + X$ . The extra  $\pi$  phase in the figure label keeps into account the different choice w.r.t. Trento conventions [73]. The curves are obtained from Eq. (96) with the parameterizations of Ref. [268]. The shaded areas correspond to the theoretical uncertainty on the parameters. (Un)polarized PDF and FF sets: (GRV98)GRSV2000-K.

so extracted, are in fair agreement with HERMES data, even if the  $K^+$  results are underestimated in the low  $x$  region. Further work is needed, in particular concerning the study of the sea-quark Sivers functions and flavour decomposition in the fragmentation sector.

For the Collins asymmetry a global fit on HERMES, COMPASS and Belle data in SIDIS and  $e^+e^-$  annihilation has been performed (9 free parameters) allowing the first extraction of the transversity distribution. The results for the SIDIS case and a comparison with the HERMES and COMPASS data are presented in Fig. 17.

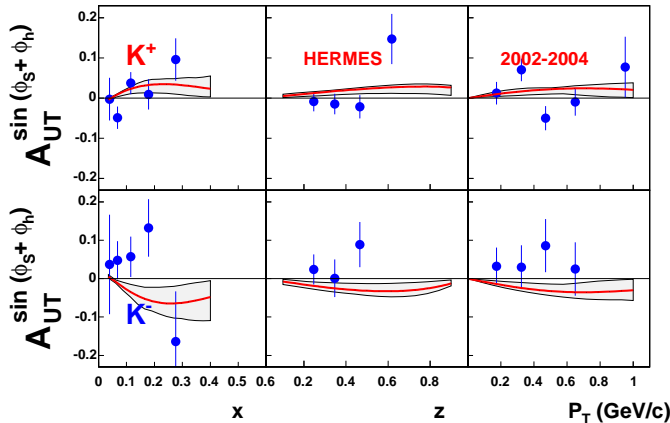


Figure 18: HERMES data [81] on  $A_{UT}^{\sin(\phi_S+\phi_h)}$  for  $K^\pm$ , compared with the results of Ref. [268]. (Un)polarized PDF and FF sets: (GRV98)GRSV2000-K.

Finally, we compare the azimuthal asymmetry  $A_{UT}^{\sin(\phi_S+\phi_h)}$  for the production of  $K$  mesons with existing HERMES results [77]. Preliminary results are also available from COMPASS [84, 85]. These data have not been included in the best fit of Ref. [263], as they might involve the transversity distribution

of strange quarks in the nucleon, which have been neglected for SIDIS data on  $\pi$  production. We show in Fig. 18 the results obtained using the extracted  $u$  and  $d$  transversity distributions of Fig. 20 (a, b panels). For the Collins function the same  $\mathcal{N}_q^C$  and  $M$  as extracted for the pion case were tentatively used, with the appropriate unpolarized FF's,  $D_{K^\pm/q}$ .

We notice that the above computations are in fair agreement with data concerning the  $K^+$  production, which is presumably dominated by  $u$  quarks; instead, there seem to be discrepancies for the  $K^-$  asymmetry, for which the role of  $s$  quarks might be relevant. New data on the azimuthal asymmetry for  $K$  production, possible from COMPASS and JLab experiments, might be very helpful in sorting out the eventual importance of the sea quark transversity distributions in the nucleon.

### 5.5.3 Phenomenological extractions of Sivers and Collins functions

The phenomenological analysis of HERMES and COMPASS data on moments of the azimuthal asymmetries in the SIDIS process, with the aim of extracting information on the Sivers and Collins functions, has been performed independently by three different theoretical groups [238, 280, 276, 263, 250, 267, 268]. Although the three groups have used different theoretical approaches, at the level of accuracy considered (calculations are performed within LO pQCD, using leading twist TMD parton distribution and fragmentation functions and keeping only the leading term in a  $(k_\perp/Q)$  power expansion) the results are quite similar and easily comparable. Several other simplifying approximations were common between these groups, namely the neglect of the so-called soft-factors [122, 146] and of Sudakov suppression factors [149] (see also section 3). However, slightly different approaches were followed concerning the dependence of the distributions on the transverse parton momenta. As an example, different functional forms were used. Also, possible constraints coming from general bounds (e.g. positivity bounds, the Soffer bound) were imposed and used in different ways. Regarding the Collins function, in Ref. [267] a quark soliton model was used for the transversity distribution, while in Ref. [250] the Soffer bound was tentatively adopted. As we have already discussed, in Ref. [268] Belle  $e^+e^-$  data on azimuthal asymmetries in dihadron production were used to independently extract the Collins function. From there and HERMES and COMPASS data, the first extraction of the transversity distribution for  $u$  and  $d$  quarks was performed, see Fig. 20 ((a), (b) panels). Also, different sets for the usual  $\mathbf{k}_\perp$ -integrated PDF's and FF's, in different combinations, were adopted. A useful summary and more detailed comparisons may be found, in the case of the Sivers function, in Ref. [262].

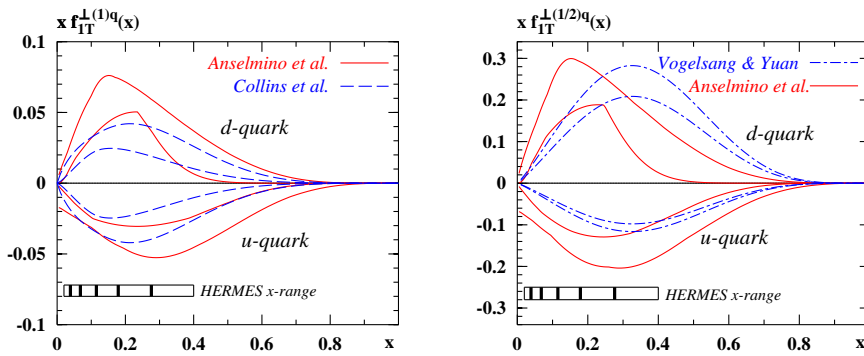


Figure 19: The first and 1/2-transverse moments of the quark Sivers functions, see Eq. (17), as extracted in Refs. [280, 263, 250]. The curves indicate the 1- $\sigma$  regions of the various parameterizations.

In Fig. 19 the first two moments (in  $\mathbf{k}_\perp$ ) of the Sivers function (multiplied by  $x$ ), as extracted by the three theoretical groups, are shown for comparison (see also Eqs. (16), (17)). Notice that for each

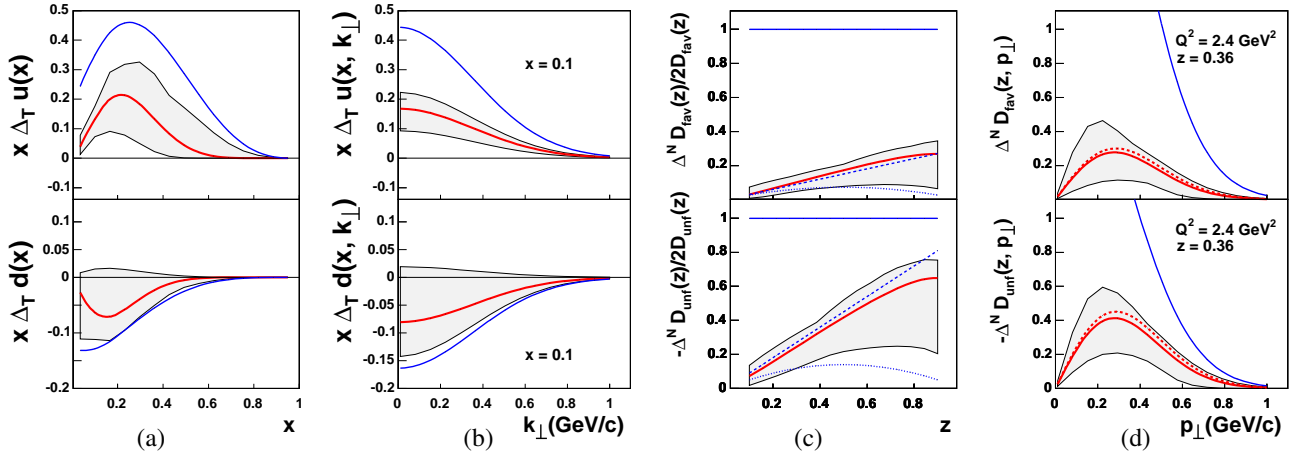


Figure 20: The transversity distribution for  $u$  and  $d$  quarks and the favoured and unfavoured Collins FF's from Ref. [268]. (a):  $x \Delta_T u(x)$  (upper plot) and  $x \Delta_T d(x)$  (lower plot), as functions of  $x$  at  $Q^2 = 2.4$  (GeV/c) $^2$ . The Soffer bound [182] is also shown (solid blue lines). (b): unintegrated transversity distributions,  $x \Delta_T u(x, k_\perp)$  (upper plot) and  $x \Delta_T d(x, k_\perp)$  (lower plot), as defined in Eq. (90), as functions of  $k_\perp$  at  $x = 0.1$ . PDF sets: GRV98-GRSV2000. (c): the  $p_\perp$  integrated Collins functions, Eq. (76), normalized to twice the corresponding unpolarized FF's, vs.  $z$ ; results of Refs. [267] (dashed line) and [250] (dotted line) are also shown. (d): the Collins function from the fits of Ref. [268] vs.  $p_\perp$  at  $z = 0.36$  and  $Q^2 = 2.4$  (GeV/c) $^2$  (lower lines). The positivity bound is also shown (upper blue lines). FF set: K. The shaded areas correspond to the theoretical uncertainty on the parameters.

parameterization the two curves delimiting the one-sigma deviation region are shown. The range of  $x$  values spanned by HERMES experiment is also depicted. Clearly, the parameterizations extracted suffer of larger uncertainties in the large  $x$  sector, which is not well covered by data. Roughly speaking, all parameterizations are in favour of a negative(positive) Sivers function ( $f_{1T}^\perp$ ) for  $u(d)$  quarks, with shapes and magnitudes comparable. This behaviour reasonably complies with the prediction [281, 282]  $f_{1T}^{\perp d} = -f_{1T}^{\perp u}$ , also derived in the large  $N_C$  limit of QCD in Ref. [283]. See also the discussion on the theoretical models in section 3.1.3.

Fig. 20 ((c), (d) panels) shows the first moment of the favoured and unfavoured Collins fragmentation functions for pions, normalized to twice the corresponding unpolarized FF, as a function of  $z$  ((c) panel) and  $p_\perp$  ((d) panel) at fixed  $Q^2$ . The three theoretical extractions are compared: Ref. [263] (solid lines and the shaded, one-sigma deviation, area); Ref. [267] (dashed line); Ref. [250] (dotted line). For comparison, we also show the positivity bound (upper solid line). The  $p_\perp$  dependence in panel (d) is not a prediction but has been imposed to the parameterization. Notice also that there is no curve from Ref. [250] here: this is because of some additional simplifying assumptions performed there.

## 6 Conclusions and outlook

In this paper we have presented a thorough review of our present theoretical understanding of azimuthal and transverse single spin asymmetries in high-energy hadronic processes in the framework of perturbative QCD. The basic features of the main theoretical approaches to SSA's and an overview of the available experimental information have been given. An in-depth treatment of the generalized parton model, including spin and transverse momentum effects within the helicity formalism, and a detailed discussion of the phenomenology concerning azimuthal and SSA's complete this analysis. Hopefully, this work will provide the reader with a useful overview of the present status of this field of research and

with a fresh feeling of its ever-growing development. In fact, in the past few years several important results have been reached, both from the experimental and theoretical points of view. These results have confirmed earlier indications that spin and intrinsic transverse momentum effects can be relevant even at high energies and large  $p_T$  and led to a profusion of interesting physical consequences. In the last years, a wide dedicated experimental activity has definitely confirmed previous pioneering results, refining their quality and statistical significance and enlarging the kinematical regime explored and the number of experimental observables investigated. From the theoretical side, significant progress has been reached in the understanding of new spin and TMD functions, like the Sivers distribution and the Collins function. The crucial role of initial and final state interactions, of a proper account of gauge links and QCD colour gauge invariance and of their consequences has been clarified. Related to this, the universality of the new TMD functions both in the distribution and in the fragmentation sector has been investigated. QCD factorization theorems and collinear twist-three approaches have been extended to cover several processes and new kinematical regimes. The theoretical formulation of the generalized parton model has been refined and its phenomenological applications extended to include most of the new experimental data. The interplay between twist-three approaches and QCD-improved parton models with inclusion of intrinsic parton motion has been extensively studied. The large amount of activity devoted to SSA's and its significant but partial successes have also naturally raised new theoretical problems and experimental challenges. They will hopefully set up the stage for new developments in the forthcoming years.

From the theoretical side, some of the most relevant open points are: 1) The formal properties of spin and  $\mathbf{k}_\perp$  dependent functions, their universality and evolution with scale; 2) The systematic comparison among different theoretical approaches and a deeper understanding of their interplay and complementarity; 3) The role of Sudakov and soft factors, and of parton off-shellness and doubly unintegrated parton distributions; 4) A better understanding of the physical mechanisms involved, according to their twist classification and their behaviour with the relevant scales; 5) A comprehensive phenomenological analysis of all experimental data available as a test of universality and of the effectiveness of the proposed parameterizations for all the new unknown soft functions involved; 6) An improvement of nonperturbative models and approaches, including lattice calculations, for the same functions; 7) An improved understanding of the connections among TMD functions, generalized parton distributions and the orbital angular momentum of partons and its role for hadronic structure.

From the experimental side, interesting developments are awaited in the near future: 1) The BRAHMS, PHENIX and STAR collaborations at RHIC-BNL will provide us with new results at 62, 200, and 500 GeV c.m. energies, with larger statistics, an improved kinematical coverage and including new interesting physical observables; 2) Hopefully, the COMPASS Collaboration will soon measure azimuthal single spin asymmetries for several charged hadrons with a transversely polarized proton target; on a more extended time scale they will also study the polarized Drell-Yan process with a pion beam colliding on transversely polarized proton and deuteron targets; 3) The proposed JLAB 12 GeV upgrade, with polarized proton, neutron and deuteron targets and a large-acceptance detector will provide a detailed kinematical coverage in both longitudinal and transverse momentum, with a large  $x_B$  experimental reach; 4) The foreseen fixed-target experiments at  $\sqrt{s} \sim 10$  GeV at the JPARC facility will help in testing spin asymmetries and TMD distributions in the valence region ( $x_B > 0.1$ ); 5) The proposed 70 GeV upgrade of the transversely polarized proton beam at the IHEP-Protvino accelerator will provide further information on the moderate energy regime; 6) On a longer time scale, the PAX experiment at GSI will improve our knowledge of the transversity distribution and the other spin and TMD functions, provided the capability of efficiently polarizing antiprotons will be confirmed.

Hopefully, the new forthcoming experimental results and the prosecution of active theoretical investigation will lead in the near future to significant improvements in our understanding of SSA's, the spin structure of hadrons and related issues.

# References

- [1] C. Bourrely, J. Soffer, and E. Leader, *Phys. Rep.* 59 (1980) 95
- [2] L. G. Pondrom, *Phys. Rep.* 122 (1985) 57
- [3] M. Anselmino, A. Efremov, and E. Leader, *Phys. Rep.* 261 (1995) 1, [hep-ph/9501369](#)
- [4] S. M. Troshin and N. E. Tyurin, *Spin phenomena in particle interactions*, World Scientific, Singapore (1994).
- [5] U. Stiegler, *Phys. Rep.* 277 (1996) 1
- [6] K. J. Heller, *Spin96 Proceedings*, World Scientific, Singapore (1997), p. 23.
- [7] S. B. Nurushev, *Int. J. Mod. Phys. A* 12 (1997) 3433
- [8] J. Felix, *Mod. Phys. Lett. A* 14 (1999) 827
- [9] Z.-t. Liang and C. Boros, *Int. J. Mod. Phys. A* 15 (2000) 927, [hep-ph/0001330](#)
- [10] B. Lampe and E. Reya, *Phys. Rep.* 332 (2000) 1, [hep-ph/9810270](#)
- [11] G. Bunce, N. Saito, J. Soffer, and W. Vogelsang, *Ann. Rev. Nucl. Part. Sci.* 50 (2000) 525, [hep-ph/0007218](#)
- [12] V. Barone, A. Drago, and P. G. Ratcliffe, *Phys. Rep.* 359 (2002) 1, [hep-ph/0104283](#)
- [13] E. Leader, *Spin in particle physics*, Cambridge University Press, Cambridge (2001).
- [14] B. W. Filippone and X.-D. Ji, *Adv. Nucl. Phys.* 26 (2001) 1, [hep-ph/0101224](#)
- [15] V. Barone and P. G. Ratcliffe, *Transverse spin physics*, World Scientific, River Edge (2003).
- [16] S. D. Bass, *Rev. Mod. Phys.* 77 (2005) 1257, [hep-ph/0411005](#)
- [17] W. Vogelsang, *J. Phys. G* 34 (2007) S149
- [18] D. W. Sivers, *Phys. Rev. D* 41 (1990) 83
- [19] D. W. Sivers, *Phys. Rev. D* 43 (1991) 261
- [20] J. C. Collins, *Nucl. Phys. B* 396 (1993) 161, [hep-ph/9208213](#)
- [21] J. C. Collins, S. F. Heppelmann, and G. A. Ladinsky, *Nucl. Phys. B* 420 (1994) 565, [hep-ph/9305309](#)
- [22] D. Mueller, D. Robaschik, B. Geyer, F. M. Dittes, and J. Horejsi, *Fortschr. Phys.* 42 (1994) 101, [hep-ph/9812448](#)
- [23] X.-D. Ji, *Phys. Rev. Lett.* 78 (1997) 610, [hep-ph/9603249](#)
- [24] X.-D. Ji, *Phys. Rev. D* 55 (1997) 7114, [hep-ph/9609381](#)
- [25] A. V. Radyushkin, *Phys. Rev. D* 56 (1997) 5524, [hep-ph/9704207](#)
- [26] X.-D. Ji, *J. Phys. G* 24 (1998) 1181, [hep-ph/9807358](#)
- [27] M. Diehl, *Phys. Rep.* 388 (2003) 41, [hep-ph/0307382](#)
- [28] A. V. Belitsky and A. V. Radyushkin, *Phys. Rep.* 418 (2005) 1, [hep-ph/0504030](#)
- [29] M. Diehl, A. Manashov, and A. Schafer, *Eur. Phys. J. A* 31 (2007) 335, [hep-ph/0611101](#)
- [30] M. Burkardt, *Int. J. Mod. Phys. A* 18 (2003) 173, [hep-ph/0207047](#)
- [31] M. Burkardt, *Phys. Rev. D* 66 (2002) 114005, [hep-ph/0209179](#)
- [32] M. Burkardt and D. S. Hwang, *Phys. Rev. D* 69 (2004) 074032, [hep-ph/0309072](#)
- [33] M. Burkardt, *Phys. Rev. D* 72 (2005) 094020, [hep-ph/0505189](#)
- [34] M. Diehl and P. Hagler, *Eur. Phys. J. C* 44 (2005) 87, [hep-ph/0504175](#)
- [35] S. Meissner, A. Metz, and K. Goeke, *Phys. Rev. D* 76 (2007) 034002, [hep-ph/0703176](#)



- [36] HERMES Collaboration, P. B. van der Nat, *Transversity 2005*, World Scientific, Singapore (2006), [hep-ph/0512019](#)
- [37] COMPASS Collaboration, C. Schill, *DIS 2007*, [arXiv:0706.1459](#) [hep-ex]
- [38] A. V. Efremov, L. Mankiewicz, and N. A. Tornqvist, *Phys. Lett. B* 284 (1992) 394
- [39] J. C. Collins and G. A. Ladinsky, [hep-ph/9411444](#)
- [40] X. Artru and J. C. Collins, *Z. Phys. C* 69 (1996) 277, [hep-ph/9504220](#)
- [41] R. L. Jaffe, X.-m. Jin, and J. Tang, *Phys. Rev. Lett.* 80 (1998) 1166, [hep-ph/9709322](#)
- [42] A. Bianconi, S. Boffi, R. Jakob, and M. Radici, *Phys. Rev. D* 62 (2000) 034008, [hep-ph/9907475](#)
- [43] A. Bacchetta and M. Radici, *Phys. Rev. D* 69 (2004) 074026, [hep-ph/0311173](#)
- [44] F. A. Ceccopieri, M. Radici, and A. Bacchetta, *Phys. Lett. B* 650 (2007) 81, [hep-ph/0703265](#)
- [45] G. Bunce *et al.*, *Phys. Rev. Lett.* 36 (1976) 1113
- [46] G. L. Kane, J. Pumplin, and W. Repko, *Phys. Rev. Lett.* 41 (1978) 1689
- [47] E581 Collaboration, D. L. Adams *et al.*, *Phys. Lett. B* 261 (1991) 201
- [48] E704 Collaboration, D. L. Adams *et al.*, *Phys. Lett. B* 264 (1991) 462
- [49] E581 Collaboration, D. L. Adams *et al.*, *Z. Phys. C* 56 (1992) 181
- [50] E704 Collaboration, A. Bravar *et al.*, *Phys. Rev. Lett.* 77 (1996) 2626
- [51] E704 Collaboration, D. L. Adams *et al.*, *Phys. Rev. D* 53 (1996) 4747
- [52] E704 Collaboration, D. L. Adams *et al.*, *Phys. Lett. B* 345 (1995) 569
- [53] E704 Collaboration, A. Bravar *et al.*, *Phys. Rev. Lett.* 75 (1995) 3073
- [54] E704 Collaboration, D. L. Adams *et al.*, *Nucl. Phys. B* 510 (1998) 3
- [55] V. D. Apokin *et al.*, *Phys. Lett. B* 243 (1990) 461
- [56] V. V. Abramov *et al.*, *Nucl. Phys. B* 492 (1997) 3, [hep-ex/0110011](#)
- [57] K. Krueger *et al.*, *Phys. Lett. B* 459 (1999) 412
- [58] C. E. Allgower *et al.*, *Phys. Rev. D* 65 (2002) 092008
- [59] STAR Collaboration, J. Adams *et al.*, *Phys. Rev. Lett.* 92 (2004) 171801, [hep-ex/0310058](#)
- [60] STAR Collaboration, J. Adams *et al.*, *Phys. Rev. Lett.* 97 (2006) 152302, [nucl-ex/0602011](#)
- [61] D. de Florian, R. Sassot, and M. Stratmann, *Phys. Rev. D* 75 (2007) 114010, [hep-ph/0703242](#)
- [62] STAR Collaboration, B. I. Abelev *et al.*, *Phys. Rev. Lett.* 99 (2007) 142003, [arXiv:0705.4629](#) [hep-ex]
- [63] STAR Collaboration, L. Nogach, *AIP Conf. Proc.* 915 (2007) 543, [hep-ex/0612030](#)
- [64] STAR Collaboration, F. Simon, *AIP Conf. Proc.* 870 (2006) 428, [hep-ex/0608050](#)
- [65] PHENIX Collaboration, S. S. Adler *et al.*, *Phys. Rev. Lett.* 91 (2003) 241803, [hep-ex/0304038](#)
- [66] PHENIX Collaboration, S. S. Adler *et al.*, *Phys. Rev. Lett.* 95 (2005) 202001, [hep-ex/0507073](#)
- [67] PHENIX Collaboration, A. Adare *et al.*, [arXiv:0704.3599](#) [hep-ex]
- [68] PHENIX Collaboration, S. S. Adler *et al.*, *Phys. Rev. D* 71 (2005) 071102, [hep-ex/0502006](#)
- [69] PHENIX Collaboration, S. S. Adler *et al.*, *Phys. Rev. Lett.* 98 (2007) 012002, [hep-ex/0609031](#)
- [70] PHENIX Collaboration, C. Aidala, *DNP Spin Workshop 2006*, unpublished
- [71] BRAHMS Collaboration, I. Arsene *et al.*, *Phys. Rev. Lett.* 98 (2007) 252001, [hep-ex/0701041](#)
- [72] BRAHMS Collaboration, J. H. Lee and F. Videbaek, *AIP Conf. Proc.* 915 (2007) 533
- [73] A. Bacchetta, U. D'Alesio, M. Diehl, and C. A. Miller, *Phys. Rev. D* 70 (2004) 117504, [hep-ph/0410050](#)

- [74] HERMES Collaboration, A. Airapetian *et al.*, *Phys. Rev. Lett.* 84 (2000) 4047, hep-ex/9910062
- [75] HERMES Collaboration, A. Airapetian *et al.*, *Phys. Rev.* D 64 (2001) 097101, hep-ex/0104005
- [76] HERMES Collaboration, A. Airapetian *et al.*, *Phys. Lett.* B 562 (2003) 182, hep-ex/0212039
- [77] HERMES Collaboration, A. Airapetian *et al.*, *Phys. Rev. Lett.* 94 (2005) 012002, hep-ex/0408013
- [78] HERMES Collaboration, M. Diefenthaler, *AIP Conf. Proc.* 792 (2005) 933, hep-ex/0507013
- [79] HERMES Collaboration, A. Airapetian *et al.*, *Phys. Lett.* B 622 (2005) 14, hep-ex/0505042
- [80] HERMES Collaboration, A. Airapetian *et al.*, *Phys. Lett.* B 648 (2007) 164, hep-ex/0612059
- [81] HERMES Collaboration, M. Diefenthaler, *AIP Conf. Proc.* 915 (2007) 509, hep-ex/0612010
- [82] COMPASS Collaboration, V. Y. Alexakhin *et al.*, *Phys. Rev. Lett.* 94 (2005) 202002, hep-ex/0503002
- [83] COMPASS Collaboration, E. S. Ageev *et al.*, *Nucl. Phys.* B 765 (2007) 31, hep-ex/0610068
- [84] COMPASS Collaboration, A. Martin, *Czech. J. Phys.* 56 (2006) F33, hep-ex/0702002
- [85] COMPASS Collaboration, F. Bradamante, *AIP Conf. Proc.* 915 (2007) 513, hep-ex/0702007
- [86] COMPASS Collaboration, A. Kotzinian, *DIS 2007*, arXiv:0705.2402[hep-ex]
- [87] A. Bacchetta *et al.*, *JHEP* 02 (2007) 093, hep-ph/0611265
- [88] CLAS Collaboration, H. Avakian *et al.*, *Phys. Rev.* D 69 (2004) 112004, hep-ex/0301005
- [89] CLAS Collaboration, H. Avakian, P. Bosted, V. Burkert, and L. Elouadrhiri, *Transversity 2005*, World Scientific, Singapore (2006), p. 88.
- [90] CLAS Collaboration, H. Avakian, P. E. Bosted, V. Burkert, and L. Elouadrhiri, *AIP Conf. Proc.* 792 (2005) 945, nucl-ex/0509032
- [91] M. Ahmed and T. Gehrman, *Phys. Lett.* B 465 (1999) 297, hep-ph/9906503
- [92] European Muon Collaboration, M. Arneodo *et al.*, *Z. Phys.* C 34 (1987) 277
- [93] European Muon Collaboration, J. J. Aubert *et al.*, *Phys. Lett.* B 130 (1983) 118
- [94] E665 Collaboration, M. R. Adams *et al.*, *Phys. Rev.* D 48 (1993) 5057
- [95] ZEUS Collaboration, J. Breitweg *et al.*, *Phys. Lett.* B 481 (2000) 199, hep-ex/0003017
- [96] ZEUS Collaboration, S. Chekanov *et al.*, *Phys. Lett.* B 551 (2003) 226, hep-ex/0210064
- [97] ZEUS Collaboration, S. Chekanov *et al.*, *Eur. Phys. J.* C 51 (2007) 289, hep-ex/0608053
- [98] C. S. Lam and W.-K. Tung, *Phys. Rev.* D 18 (1978) 2447
- [99] C. S. Lam and W.-K. Tung, *Phys. Lett.* B 80 (1979) 228
- [100] C. S. Lam and W.-K. Tung, *Phys. Rev.* D 21 (1980) 2712
- [101] NA3 Collaboration, J. Badier *et al.*, *Z. Phys.* C 11 (1981) 195
- [102] NA10 Collaboration, S. Falciano *et al.*, *Z. Phys.* C 31 (1986) 513
- [103] NA10 Collaboration, M. Guanziroli *et al.*, *Z. Phys.* C 37 (1988) 545
- [104] E. L. Berger and S. J. Brodsky, *Phys. Rev. Lett.* 42 (1979) 940
- [105] E. L. Berger, *Z. Phys.* C 4 (1980) 289
- [106] J. S. Conway *et al.*, *Phys. Rev.* D 39 (1989) 92
- [107] E866/NuSea Collaboration, L. Y. Zhu *et al.*, *Phys. Rev. Lett.* 99 (2007) 082301, hep-ex/0609005
- [108] D. Boer and P. J. Mulders, *Phys. Rev.* D 57 (1998) 5780, hep-ph/9711485
- [109] Belle Collaboration, K. Abe *et al.*, *Phys. Rev. Lett.* 96 (2006) 232002, hep-ex/0507063
- [110] A. Ogawa, M. Grosse-Perdekamp, R. Seidl, and K. Hasuko, *DIS 2006*, hep-ex/0607014

- [111] Belle Collaboration, A. Ogawa, M. Grosse Perdekamp, R.-C. Seidl, and K. Hasuko, *AIP Conf. Proc.* 915 (2007) 575
- [112] N. I. Kochelev, *JETP Lett.* 72 (2000) 481, hep-ph/9905497
- [113] D. Ostrovsky and E. Shuryak, *Phys. Rev. D* 71 (2005) 014037, hep-ph/0409253
- [114] P. Hoyer and M. Jarvinen, *JHEP* 10 (2005) 080, hep-ph/0509058
- [115] P. Hoyer and M. Jarvinen, *JHEP* 02 (2007) 039, hep-ph/0611293
- [116] C. Bourrely and J. Soffer, *Eur. Phys. J. C* 36 (2004) 371, hep-ph/0311110
- [117] D. de Florian and W. Vogelsang, *Phys. Rev. D* 71 (2005) 114004, hep-ph/0501258
- [118] R. D. Field and R. P. Feynman, *Phys. Rev. D* 15 (1977) 2590
- [119] R. P. Feynman, R. D. Field, and G. C. Fox, *Phys. Rev. D* 18 (1978) 3320
- [120] J. C. Collins and D. E. Soper, *Phys. Rev. D* 16 (1977) 2219
- [121] J. C. Collins and D. E. Soper, *Nucl. Phys. B* 193 (1981) 381
- [122] X.-d. Ji, J.-p. Ma, and F. Yuan, *Phys. Rev. D* 71 (2005) 034005, hep-ph/0404183
- [123] X.-d. Ji, J.-P. Ma, and F. Yuan, *Phys. Lett. B* 597 (2004) 299, hep-ph/0405085
- [124] M. Anselmino, M. Boglione, and F. Murgia, *Phys. Lett. B* 362 (1995) 164, hep-ph/9503290
- [125] M. Anselmino and F. Murgia, *Phys. Lett. B* 442 (1998) 470, hep-ph/9808426
- [126] P. Mulders and R. Tangerman, *Nucl. Phys. B* 461 (1996) 197, hep-ph/9510301
- [127] J. P. Ralston and D. E. Soper, *Nucl. Phys. B* 152 (1979) 109
- [128] X. Artru, J. Czyzewski, and H. Yabuki, *Z. Phys. C* 73 (1997) 527, hep-ph/9508239
- [129] B. Andersson, G. Gustafson, G. Ingelman, and T. Sjostrand, *Phys. Rep.* 97 (1983) 31
- [130] J. Czyzewski, *Acta Phys. Polon.* 27 (1996) 1759, hep-ph/9606390
- [131] M. Anselmino, M. Boglione, and F. Murgia, *Phys. Rev. D* 60 (1999) 054027, hep-ph/9901442
- [132] A. Metz and M. Schlegel, *Eur. Phys. J. A* 22 (2004) 489, hep-ph/0403182
- [133] A. Bacchetta, P. J. Mulders, and F. Pijlman, *Phys. Lett. B* 595 (2004) 309, hep-ph/0405154
- [134] K. Goeke, A. Metz, and M. Schlegel, *Phys. Lett. B* 618 (2005) 90, hep-ph/0504130
- [135] M. Anselmino *et al.*, *Phys. Rev. D* 73 (2006) 014020, hep-ph/0509035
- [136] D. Boer, *Phys. Rev. D* 60 (1999) 014012, hep-ph/9902255
- [137] M. Anselmino, D. Boer, U. D'Alesio, and F. Murgia, *Phys. Rev. D* 63 (2001) 054029, hep-ph/0008186
- [138] S. J. Brodsky, D. S. Hwang, and I. Schmidt, *Phys. Lett. B* 530 (2002) 99, hep-ph/0201296
- [139] J. C. Collins, *Phys. Lett. B* 536 (2002) 43, hep-ph/0204004
- [140] X.-d. Ji and F. Yuan, *Phys. Lett. B* 543 (2002) 66, hep-ph/0206057
- [141] A. V. Belitsky, X. Ji, and F. Yuan, *Nucl. Phys. B* 656 (2003) 165, hep-ph/0208038
- [142] J. C. Collins, *Acta Phys. Polon.* B 34 (2003) 3103, hep-ph/0304122
- [143] J. C. Collins, D. E. Soper, and G. Sterman, in *Perturbative Quantum Chromodynamics*, World Scientific, Singapore (1989), 1-92.
- [144] S. J. Brodsky, D. S. Hwang, and I. Schmidt, *Nucl. Phys. B* 642 (2002) 344, hep-ph/0206259
- [145] A. Metz, *Phys. Lett. B* 549 (2002) 139
- [146] J. C. Collins and A. Metz, *Phys. Rev. Lett.* 93 (2004) 252001, hep-ph/0408249
- [147] A. Idilbi, X.-d. Ji, J.-P. Ma, and F. Yuan, *Phys. Rev. D* 70 (2004) 074021, hep-ph/0406302
- [148] A. Idilbi, X.-d. Ji, and F. Yuan, *Phys. Lett. B* 625 (2005) 253, hep-ph/0507196

- [149] D. Boer, *Nucl. Phys.* B 603 (2001) 195, [hep-ph/0102071](#)
- [150] A. A. Henneman, D. Boer, and P. J. Mulders, *Nucl. Phys.* B 620 (2002) 331, [hep-ph/0104271](#)
- [151] F. A. Ceccopieri and L. Trentadue, *Phys. Lett.* B 636 (2006) 310, [hep-ph/0512372](#)
- [152] F. A. Ceccopieri and L. Trentadue, [arXiv:0706.4242 \[hep-ph\]](#)
- [153] C. J. Bomhof, P. J. Mulders, and F. Pijlman, *Phys. Lett.* B 596 (2004) 277, [hep-ph/0406099](#)
- [154] A. Bacchetta, C. J. Bomhof, P. J. Mulders, and F. Pijlman, *Phys. Rev.* D 72 (2005) 034030, [hep-ph/0505268](#)
- [155] C. J. Bomhof, P. J. Mulders, and F. Pijlman, *Eur. Phys. J.* C 47 (2006) 147, [hep-ph/0601171](#)
- [156] C. J. Bomhof and P. J. Mulders, *JHEP* 02 (2007) 029, [hep-ph/0609206](#)
- [157] J. Collins and J.-W. Qiu, *Phys. Rev.* D 75 (2007) 114014, [arXiv:0705.2141 \[hep-ph\]](#)
- [158] J.-W. Qiu, W. Vogelsang, and F. Yuan, *Phys. Lett.* B 650 (2007) 373, [arXiv:0704.1153 \[hep-ph\]](#)
- [159] J.-W. Qiu, W. Vogelsang, and F. Yuan, *Phys. Rev.* D 76 (2007) 074029, [arXiv:0706.1196 \[hep-ph\]](#)
- [160] J. Collins, [arXiv:0708.4410 \[hep-ph\]](#)
- [161] W. Vogelsang and F. Yuan, *Phys. Rev.* D 76 (2007) 094013, [arXiv:0708.4398 \[hep-ph\]](#)
- [162] C. J. Bomhof and P. J. Mulders, [arXiv:0709.1390 \[hep-ph\]](#)
- [163] A. Bacchetta, C. Bomhof, U. D'Alesio, P. J. Mulders, and F. Murgia, *Phys. Rev. Lett.* 99 (2007) 212002, [hep-ph/0703153](#)
- [164] C. J. Bomhof, P. J. Mulders, W. Vogelsang, and F. Yuan, *Phys. Rev.* D 75 (2007) 074019, [hep-ph/0701277](#)
- [165] M. Burkardt, *Phys. Rev.* D 69 (2004) 057501, [hep-ph/0311013](#)
- [166] D. Boer, S. J. Brodsky, and D. S. Hwang, *Phys. Rev.* D 67 (2003) 054003, [hep-ph/0211110](#)
- [167] G. R. Goldstein and L. Gamberg, [hep-ph/0209085](#)
- [168] L. P. Gamberg, G. R. Goldstein, and K. A. Oganessyan, *Phys. Rev.* D 67 (2003) 071504, [hep-ph/0301018](#)
- [169] F. Yuan, *Phys. Lett.* B 575 (2003) 45, [hep-ph/0308157](#)
- [170] A. Bacchetta, A. Schaefer, and J.-J. Yang, *Phys. Lett.* B 578 (2004) 109, [hep-ph/0309246](#)
- [171] Z. Lu and B.-Q. Ma, *Nucl. Phys.* A 741 (2004) 200, [hep-ph/0406171](#)
- [172] I. O. Cherednikov, U. D'Alesio, N. I. Kochelev, and F. Murgia, *Phys. Lett.* B 642 (2006) 39, [hep-ph/0606238](#)
- [173] S. J. Brodsky and F. Yuan, *Phys. Rev.* D 74 (2006) 094018, [hep-ph/0610236](#)
- [174] D. Amrath, A. Bacchetta, and A. Metz, *Phys. Rev.* D 71 (2005) 114018, [hep-ph/0504124](#)
- [175] L. Gamberg, G. Goldstein, and M. Schlegel, [arXiv:0708.0324 \[hep-ph\]](#)
- [176] M. Burkardt and B. Hannafious, [arXiv:0705.1573 \[hep-ph\]](#)
- [177] A. Bacchetta, R. Kundu, A. Metz, and P. J. Mulders, *Phys. Lett.* B 506 (2001) 155, [hep-ph/0102278](#)
- [178] A. Bacchetta, R. Kundu, A. Metz, and P. J. Mulders, *Phys. Rev.* D 65 (2002) 094021, [hep-ph/0201091](#)
- [179] L. P. Gamberg, G. R. Goldstein, and K. A. Oganessyan, *Phys. Rev.* D 68 (2003) 051501, [hep-ph/0307139](#)
- [180] A. Bacchetta, A. Metz, and J.-J. Yang, *Phys. Lett.* B 574 (2003) 225, [hep-ph/0307282](#)



- [181] A. Bacchetta, M. Boglione, A. Henneman, and P. J. Mulders, *Phys. Rev. Lett.* 85 (2000) 712, hep-ph/9912490
- [182] J. Soffer, *Phys. Rev. Lett.* 74 (1995) 1292, hep-ph/9409254
- [183] A. Schafer and O. V. Teryaev, *Phys. Rev. D* 61 (2000) 077903, hep-ph/9908412
- [184] M. Burkardt, *Phys. Rev. D* 69 (2004) 091501, hep-ph/0402014
- [185] K. Goeke, S. Meissner, A. Metz, and M. Schlegel, *Phys. Lett. B* 637 (2006) 241, hep-ph/0601133
- [186] A. V. Efremov and O. V. Teryaev, *Sov. J. Nucl. Phys.* 36 (1982) 140
- [187] A. V. Efremov and O. V. Teryaev, *Sov. J. Nucl. Phys.* 39 (1984) 962
- [188] A. V. Efremov and O. V. Teryaev, *Phys. Lett. B* 150 (1985) 383
- [189] J.-w. Qiu and G. Sterman, *Phys. Rev. Lett.* 67 (1991) 2264
- [190] J.-w. Qiu and G. Sterman, *Nucl. Phys. B* 378 (1992) 52
- [191] J.-w. Qiu and G. Sterman, *Phys. Rev. D* 59 (1998) 014004, hep-ph/9806356
- [192] C. Kouvaris, J.-W. Qiu, W. Vogelsang, and F. Yuan, *Phys. Rev. D* 74 (2006) 114013, hep-ph/0609238
- [193] Y. Koike and K. Tanaka, *Phys. Rev. D* 76 (2007) 011502, hep-ph/0703169
- [194] Y. Kanazawa and Y. Koike, *Phys. Lett. B* 478 (2000) 121, hep-ph/0001021
- [195] Y. Kanazawa and Y. Koike, *Phys. Lett. B* 490 (2000) 99, hep-ph/0007272
- [196] Y. Koike, *Nucl. Phys. A* 721 (2003) 364, hep-ph/0211400
- [197] Y. Kanazawa and Y. Koike, *Phys. Rev. D* 64 (2001) 034019, hep-ph/0012225
- [198] H. Eguchi, Y. Koike, and K. Tanaka, *Nucl. Phys. B* 752 (2006) 1, hep-ph/0604003
- [199] H. Eguchi, Y. Koike, and K. Tanaka, *Nucl. Phys. B* 763 (2007) 198, hep-ph/0610314
- [200] D. Boer, P. J. Mulders, and F. Pijlman, *Nucl. Phys. B* 667 (2003) 201, hep-ph/0303034
- [201] J. P. Ma and Q. Wang, *Eur. Phys. J. C* 37 (2004) 293, hep-ph/0310245
- [202] X. Ji, J.-W. Qiu, W. Vogelsang, and F. Yuan, *Phys. Rev. Lett.* 97 (2006) 082002, hep-ph/0602239
- [203] X. Ji, J.-w. Qiu, W. Vogelsang, and F. Yuan, *Phys. Rev. D* 73 (2006) 094017, hep-ph/0604023
- [204] X. Ji, J.-W. Qiu, W. Vogelsang, and F. Yuan, *Phys. Lett. B* 638 (2006) 178, hep-ph/0604128
- [205] Y. Koike, W. Vogelsang, and F. Yuan, arXiv:0711.0636 [hep-ph]
- [206] G. Watt, A. D. Martin, and M. G. Ryskin, *Phys. Rev. D* 70 (2004) 014012, hep-ph/0309096
- [207] O. Linnyk, S. Leupold, and U. Mosel, *Phys. Rev. D* 75 (2007) 014016, hep-ph/0607305
- [208] J. C. Collins, T. C. Rogers, and A. M. Stasto, arXiv:0708.2833 [hep-ph]
- [209] Z.-T. Liang and T.-C. Meng, *Z. Phys. A* 344 (1992) 171
- [210] C. Boros, Z. T. Liang, and T. C. Meng, *Phys. Rev. Lett.* 70 (1993) 1751
- [211] Z.-t. Liang and T.-c. Meng, *Phys. Rev. D* 49 (1994) 3759
- [212] C. Boros, Z. T. Liang, and T. C. Meng, *Phys. Rev. D* 51 (1995) 4867
- [213] C. Boros, Z.-t. Liang, and T.-c. Meng, *Phys. Rev. D* 54 (1996) 4680, hep-ph/9603232
- [214] H. Dong, F.-z. Li, and Z.-t. Liang, *Phys. Rev. D* 69 (2004) 017501, hep-ph/0311121
- [215] C. Boros and Z.-t. Liang, *Phys. Rev. D* 53 (1996) 2279, hep-ph/9510319
- [216] Z.-t. Liang and C. Boros, *Phys. Rev. Lett.* 79 (1997) 3608, hep-ph/9708488
- [217] U. D'Alesio, S. Melis, and F. Murgia, unpublished, 2007.
- [218] U. D'Alesio and F. Murgia, *Phys. Rev. D* 70 (2004) 074009, hep-ph/0408092



- [219] M. Anselmino, M. Boglione, U. D’Alesio, E. Leader, and F. Murgia, *Phys. Rev. D* 71 (2005) 014002, [hep-ph/0408356](#)
- [220] P. J. Mulders and J. Rodrigues, *Phys. Rev. D* 63 (2001) 094021, [hep-ph/0009343](#)
- [221] A. D. Martin, R. G. Roberts, W. J. Stirling, and R. S. Thorne, *Phys. Lett. B* 531 (2002) 216, [hep-ph/0201127](#)
- [222] M. Glück, E. Reya, and A. Vogt, *Eur. Phys. J. C* 5 (1998) 461, [hep-ph/9806404](#)
- [223] M. Glück, E. Reya, M. Stratmann, and W. Vogelsang, *Phys. Rev. D* 63 (2001) 094005, [hep-ph/0011215](#)
- [224] E. Leader, A. V. Sidorov, and D. B. Stamenov, *Eur. Phys. J. C* 23 (2002) 479, [hep-ph/0111267](#)
- [225] B. A. Kniehl, G. Kramer, and B. Potter, *Nucl. Phys. B* 582 (2000) 514, [hep-ph/0010289](#)
- [226] S. Kretzer, *Phys. Rev. D* 62 (2000) 054001, [hep-ph/0003177](#)
- [227] A. P. Contogouris, R. Gaskell, and S. Papadopoulos, *Phys. Rev. D* 17 (1978) 2314
- [228] C.-Y. Wong and H. Wang, *Phys. Rev. C* 58 (1998) 376, [hep-ph/9802378](#)
- [229] X.-N. Wang, *Phys. Rev. C* 61 (2000) 064910, [nucl-th/9812021](#)
- [230] Y. Zhang, G. I. Fai, G. Papp, G. G. Barnafoldi, and P. Levai, *Phys. Rev. C* 65 (2002) 034903, [hep-ph/0109233](#)
- [231] G. Donaldson *et al.*, *Phys. Lett. B* 73 (1978) 375
- [232] F. Yuan, [arXiv:0709.3272 \[hep-ph\]](#)
- [233] U. D’Alesio, Talk delivered at the ECT\* workshop “Transverse momentum, spin, and position distributions of partons in hadrons” Trento, June 11-15, 2007.
- [234] PAX Collaboration, V. Barone *et al.*, [hep-ex/0505054](#)
- [235] STAR Collaboration, C. A. Gagliardi, *DIS 2006*, [hep-ex/0607003](#)
- [236] M. Anselmino, U. D’Alesio, S. Melis, and F. Murgia, *Phys. Rev. D* 74 (2006) 094011, [hep-ph/0608211](#)
- [237] S. J. Brodsky and S. Gardner, *Phys. Lett. B* 643 (2006) 22, [hep-ph/0608219](#)
- [238] A. V. Efremov, K. Goeke, S. Menzel, A. Metz, and P. Schweitzer, *Phys. Lett. B* 612 (2005) 233, [hep-ph/0412353](#)
- [239] M. Anselmino, M. Boglione, U. D’Alesio, E. Leader, and F. Murgia, *Phys. Rev. D* 70 (2004) 074025, [hep-ph/0407100](#)
- [240] U. D’Alesio and F. Murgia, *AIP Conf. Proc.* 915 (2007) 559, [hep-ph/0612208](#)
- [241] S. J. Brodsky, P. Hoyer, C. Peterson, and N. Sakai, *Phys. Lett. B* 93 (1980) 451
- [242] J. Pumplin, *Phys. Rev. D* 73 (2006) 114015, [hep-ph/0508184](#)
- [243] I. Schmidt, J. Soffer, and J.-J. Yang, *Phys. Lett. B* 612 (2005) 258, [hep-ph/0503127](#)
- [244] K. J. Heller *et al.*, *Phys. Rev. Lett.* 51 (1983) 2025
- [245] B. Lundberg *et al.*, *Phys. Rev. D* 40 (1989) 3557
- [246] E. J. Ramberg *et al.*, *Phys. Lett. B* 338 (1994) 403
- [247] D. Indumathi, H. S. Mani, and A. Rastogi, *Phys. Rev. D* 58 (1998) 094014, [hep-ph/9802324](#)
- [248] STAR Collaboration, B. I. Abelev *et al.*, *Phys. Rev. C* 75 (2007) 064901, [nucl-ex/0607033](#)
- [249] D. Boer and W. Vogelsang, *Phys. Rev. D* 69 (2004) 094025, [hep-ph/0312320](#)
- [250] W. Vogelsang and F. Yuan, *Phys. Rev. D* 72 (2005) 054028, [hep-ph/0507266](#)
- [251] A. Brandenburg, S. J. Brodsky, V. V. Khoze, and D. Mueller, *Phys. Rev. Lett.* 73 (1994) 939, [hep-ph/9403361](#)

- [252] K. J. Eskola, P. Hoyer, M. Vanttinen, and R. Vogt, *Phys. Lett.* B333 (1994) 526, hep-ph/9404322
- [253] O. Nachtmann and A. Reiter, *Z. Phys.* C 24 (1984) 283
- [254] A. Brandenburg, O. Nachtmann, and E. Mirkes, *Z. Phys.* C 60 (1993) 697
- [255] D. Boer, A. Brandenburg, O. Nachtmann, and A. Utermann, *Eur. Phys. J.* C 40 (2005) 55, hep-ph/0411068
- [256] L. P. Gamberg and G. R. Goldstein, *Phys. Lett.* B 650 (2007) 362, hep-ph/0506127
- [257] N. Hammon, O. Teryaev, and A. Schafer, *Phys. Lett.* B 390 (1997) 409, hep-ph/9611359
- [258] D. Boer, P. J. Mulders, and O. V. Teryaev, *Phys. Rev.* D 57 (1998) 3057, hep-ph/9710223
- [259] D. Boer and P. J. Mulders, *Nucl. Phys.* B 569 (2000) 505, hep-ph/9906223
- [260] D. Boer and J.-w. Qiu, *Phys. Rev.* D 65 (2002) 034008, hep-ph/0108179
- [261] M. Anselmino, U. D'Alesio, and F. Murgia, *Phys. Rev.* D 67 (2003) 074010, hep-ph/0210371
- [262] M. Anselmino *et al.*, *Transversity 2005*, World Scientific, Singapore (2006), hep-ph/0511017
- [263] M. Anselmino *et al.*, *Phys. Rev.* D 72 (2005) 094007, hep-ph/0507181
- [264] J. C. Collins *et al.*, *Phys. Rev.* D 73 (2006) 094023, hep-ph/0511272
- [265] S. J. Brodsky, D. S. Hwang, and I. Schmidt, *Phys. Lett.* B 553 (2003) 223, hep-ph/0211212
- [266] D. Boer, R. Jakob, and P. J. Mulders, *Nucl. Phys.* B 504 (1997) 345, hep-ph/9702281
- [267] A. V. Efremov, K. Goeke, and P. Schweitzer, *Phys. Rev.* D 73 (2006) 094025, hep-ph/0603054
- [268] M. Anselmino *et al.*, *Phys. Rev.* D 75 (2007) 054032, hep-ph/0701006
- [269] M. Anselmino, M. Boglione, U. D'Alesio, F. Murgia, and A. Prokudin, unpublished, 2007.
- [270] R. N. Cahn, *Phys. Lett.* B 78 (1978) 269
- [271] R. N. Cahn, *Phys. Rev.* D 40 (1989) 3107
- [272] A. Konig and P. Kroll, *Z. Phys.* C 16 (1982) 89
- [273] J.-g. Chay, S. D. Ellis, and W. J. Stirling, *Phys. Rev.* D 45 (1992) 46
- [274] H. Georgi and H. D. Politzer, *Phys. Rev. Lett.* 40 (1978) 3
- [275] A. Daleo, D. de Florian, and R. Sassot, *Phys. Rev.* D 71 (2005) 034013, hep-ph/0411212
- [276] M. Anselmino *et al.*, *Phys. Rev.* D 71 (2005) 074006, hep-ph/0501196
- [277] M. Anselmino, M. Boglione, A. Prokudin, and C. Türk, *Eur. Phys. J.* A 31 (2007) 373, hep-ph/0606286
- [278] LHC Collaboration, B. U. Musch *et al.*, arXiv:0710.4423 [hep-lat]
- [279] V. Barone, Z. Lu, and B.-Q. Ma, *Phys. Lett.* B 632 (2006) 277, hep-ph/0512145
- [280] J. C. Collins *et al.*, *Phys. Rev.* D 73 (2006) 014021, hep-ph/0509076
- [281] M. Anselmino, V. Barone, A. Drago, and F. Murgia, hep-ph/0209073
- [282] A. Drago, *Phys. Rev.* D 71 (2005) 057501, hep-ph/0501282
- [283] P. V. Pobylitsa, hep-ph/0301236